Department of Mechanical and Aerospace Engineering

Testing and validation of an enhancement to photovoltaic electrical model applied to the source code of ESP-r.

Author: Bartosz Jakub Nowak

Supervisor: Dr Nicolas James Kelly

A thesis submitted in partial fulfilment for the requirement of the degree

Master of Science

Sustainable Engineering: Renewable Energy Systems and the Environment

2015

Copyright Declaration

Signed: Nowak Bartosz Date: 04.09.2015

ABSTRACT

Photovoltaic panels are one of the devices where the phenomenon of radiation absorption plays a key role in power output estimation. Due to the multiple layer construction of an array, radiation beams passing through those layers experience several reflections, which cause losses in magnitudes of their intensity. In order to improve accuracy of photovoltaic calculations in ESP-r, this phenomenon has to be included in the algorithm. This thesis will provide validation for proposed source code change that is supposed to deal with radiation absorption by the PV layer.

Multiple simulations have been performed in order to validate the new code. Simulations considered two different climate zones: Aberdeen and Guantanamo Bay. Three different time periods has been investigated for each climate zone: one year, one month for each season (December, March, June and September) and two singular days for each season – one cloudy and the other one with clear sky in order to examine differences between the codes during periods of low direct beam radiation magnitudes and how it affects the large scale outcomes.

Final conclusion led to the statement that the new code deals well with reflection losses and includes them at every case. This can be noticed in each daily trend during sunrises and sunsets. Moreover for poorly adjusted tilt angles in Guantanamo climate the differences between the codes due to reflection losses reached values around 14,6%. The simulations have also shown that for colder periods enhanced code provided higher outputs during times of major operation, which for Aberdeen climate overgrown reflection losses for most of the time.

ACKNOWLEDGEMENTS

First of all I wish to express my sincere gratitude to my supervisor, Dr Nicolas James Kelly, for immense patience and valuable guidelines that led me to completion of this thesis. His continuous support and faith in my skills, kept me on track the whole time. It was a pleasure to work under his supervision for the second time.

I would also like to thank Dr Paul Strachan for teaching all of us (MSc RESE students) how to use ESP-r and also for advices regarding academic papers available on the issue I investigated in this thesis.

Many thanks to my family for spiritual and financial support, without them I wouldn't be able to study at the Strathclyde University.

Gratitude to all my friends, the old ones and those who I met in Glasgow, for mental support and faith they've put in my proceedings.

Finally I would like to thank all the teachers, university staff and all the people I've had chance to meet here that made this year a fantastic adventure.

TABLE OF CONTENTS

LIST OF FIGURES

LIST OF TABLES

1. INTRODUCTION

ESP-r is a modelling tool used for assessing performance of energy systems applied to buildings. The range of applications within the software is immense. ESP-r allows importing or creating CAD geometry, and applying multiple energy systems and their combinations to evaluate hypothetical performance of proposed design. Due to the large amount of possible configurations and variety of energy systems that can be used in ESP-r, the software has to provide multiple algorithms to calculate each case with an acceptable accuracy. Covering so many phenomenon and equations related to them, ESP-r developers have to constantly work on improving these algorithms, so they reflect the reality in more accurate way giving better predictions for proposed designs. This project will focus on one of the issues related to photovoltaic electrical model.

Chapter 2 presents review of academic sources related to the examined topic. It will cover a quick introduction to PV technology, flash test description, factors that affect PV performance and exemplar electrical models

Chapter 3 describes the electrical model currently used in ESP-r, algorithm to PV power output calculations and description of the issue connected with the current model.

Chapter 4 allows the reader to familiarize with the chosen methodology to approach the project, with applied simulation methods. Simulation design details are also pointed in this chapter.

Chapter 5 covers the results obtained from simulations and their preliminary analysis. Simulations present differences between the old and the new enhanced code.

Chapter 6 concludes the work done in previous chapters and presents the outcomes in general. Conclusions taken from each simulated period will be reviewed and merged further in final statements on the differences between the codes, the causes of differences and their magnitudes. This will be followed by further work recommendations.

1.1 Aim

The aim of the project is to apply the modification to the electrical model of ESP-r by replacing incident radiation ratio with ratio of absorbed radiation by PV layer to absorbed radiation at standard reference conditions, and then test and validate the changes by comparing simulated outcomes with the old version of the electrical model.

1.2 Objectives

- Access and understand the electrical model algorithm of ESP-r
- Gather and investigate relevant information about electrical models, general issues influencing PV output and associate some of them with the investigated problem.
- Try out different versions of enhancements and apply the most appropriate one.
- Choose the methodology of simulations, to clearly define the differences between codes.
- Perform set of simulations, gather the results, present them in a clear way and identify the flaws of the design.
- Describe differences between the codes, their causes and trends, and cover those in a commentary followed with recommendations based on gathered knowledge.

2. LITERATURE REVIEW

This chapter will present all the relevant information that has been found on the investigated topic. First part of literature review will focus on nature and technical issues of photovoltaic devices, presenting working principles and technical structure. Further on the reader will be familiarized with more specific information related to the thesis itself. The way of PV testing will be briefly described and values obtained during the test. Afterwards the factors influencing PV performance will be put into analysis and finally different commonly accepted electrical models of photovoltaics will be presented.

2.1 Working principles and types of photovoltaic cells

Photovoltaic technology is fairly new, constantly investigated and improved branch of power generation devices. Development of quantum mechanics allowed scientists to approach radiation conversion into electrical power. Solar cells are built of semi-conductors which react on quanta (photons) that possess enough energy to enter the PN (positive-negative) junction. Once photons get to the PN junction, they force electrons of similar energy values to "move" towards semiconductor N. When it happens, a hole appears in semiconductor P forming a pair with the knocked off electron. Once electron-holes pairs are formed, potential difference appears in the junction, which results in electrical current generation if the circuit is formed. (Wenham, 2007)

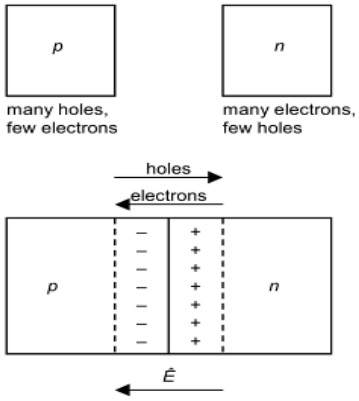

Figure 1 PN junction with electron-hole movement (Wenham, 2007)

Currently the most common types of PV modules are crystalline modules. So called crystal based modules has proven to be preferred economic choice for grid-connected applications. This is due to relatively high efficiencies achieved by manufacturers (some may reach 20% (Swanson, 2007)) and comparatively long lifespan (around 30 years (Tiwari, Mishra, & Solanki, 2011)). Mono-crystalline PV modules are more efficient and stable in their output than multi-crystalline devices. This is because mono-crystalline modules don't have grain

boundaries. Production process of mono-crystalline PV is slower, more expensive and requires more energy, therefore multi-crystalline PV modules became more suitable economical solution for grid connected and building integrated systems. (Tiwari, Mishra, & Solanki, 2011)

Thin film is an alternative to crystalline technology used in photovoltaics that is quite promising but not very developed so far. First thin film PV modules were made of very thin layer of silicon called amorphous silicon. Production process requires less temperature than in crystalline PV modules production, moreover PV film could be applied to a variety of materials including glass, steel and different plastics. Their main drawbacks are relatively low efficiency (6%-7%, (Roedern & Ullal, 2008)), vulnerability to outdoor environmental factors that vastly reduces their performance. Amorphous cells have better response to spectral distribution and their thinner built may result in cheaper cell costs. Much research is currently made to design and produce commercially viable thin film PV cells and apart from amorphous silicon, different materials are considered. (Tiwari, Mishra, & Solanki, 2011).

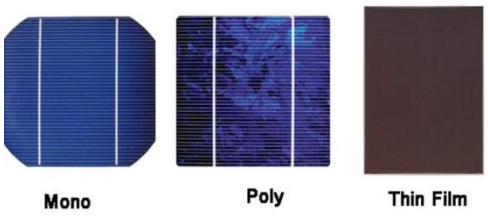

Figure 2 Visual differences in PV technology

It is worth to mention that there are alternative developing PV technologies such as concentrator silicon cells, where instead of large areas of cells, radiation beams are concentrated on the panel (20% efficient concentrator cell produces same amount of power under the same conditions as 17% efficient flat plate system (Markvart & Castaner, 2003)). Photo electrochemical cells, fairly new technology with 10,4% efficiency and 70,41% fill factor achieved (Markvart & Castaner, 2003).

2.2 Photovoltaics structure

Photovoltaic cell is quite small device due to very fragile materials a cell can be constructed of. A typical cell might have dimensions of 125 x 125 mm with an open circuit voltage around 0,6 V (Labouret & Villoz, 2010). Device with such dimensions wouldn't be able to produce large power outputs that could be efficiently exported to the grid. In order to make PV

Figure 3 Assembly parts of PV Array

technology useful it is common to merge cells into a module, which usually may consist of various numbers of cells (48, 54, 72, 96, usually formed in a rectangle). Afterwards solar panels or modules are connected in series and parallel into PV arrays. Photovoltaic modules submit to the primal laws of electric circuits, which mean that panels connected in series have the same current, but the voltage is increased, while connected in parallel voltage remains the same and current increases. Therefore it is necessarily to connect in series modules operating at similar current and in parallel modules operating at similar voltage. (Ideally it'd be same current in series connection and same voltage for parallel connection. Nevertheless in reality it's impossible to obtain exactly the same operating conditions.) (Luque & Hegedus, 2003)

In order to provide as safe and efficient as possible energy output of a PV module over the years of its operation, the layer of cells is enclosed within a structure basically made of glass, encapsulant (most popular EVA – ethylene-vinyl-acetate) and a back layer or another glass layer depending on a design. (Luque & Hegedus, 2003)

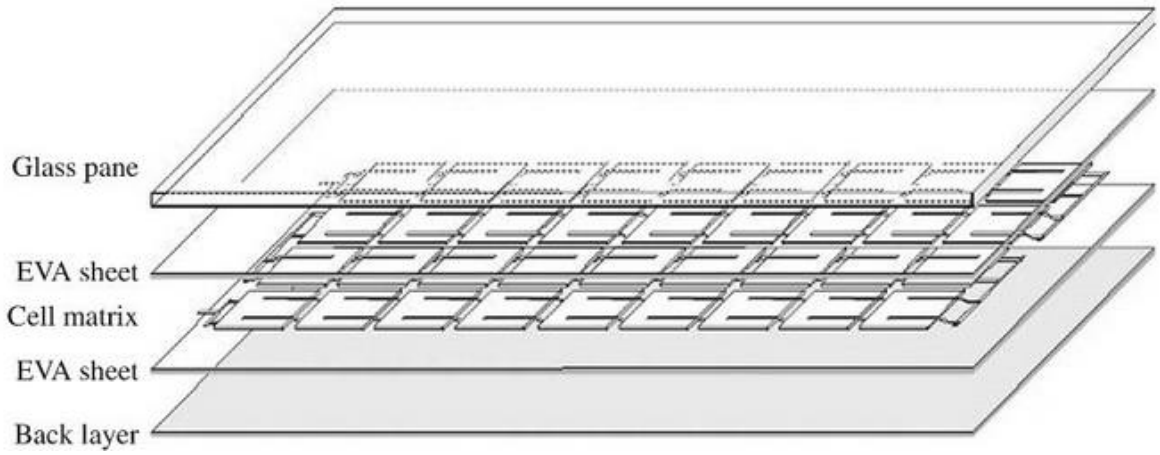

Figure 4 Basic structure of a PV module (Luque & Hegedus, 2003)

It is very common to add anti-reflective coating layer between the upper layer of encapsulant and cell matrix. Anti-reflective coating ensures more radiation absorption inside the actual cells eliminating additional reflection of solar radiation from cell matrix.

2.3 Flash test

Every device can be described by commonly agreed values that characterize it. For photovoltaic modules the usual data provided by the manufacturers are presented in table 1.

Table 1 Manufacturer's data usually available for any commercial photovoltaic array.

Values obtained at Standard Reference Conditions						
I_{sc} [A]	**I_{mp} [A]**	**V_{mp} [V]**	**V_{oc} [V]**	**μ_{Voc} [-]**	**μ_{Isc} [-]**	**NOCT [K]**
Short circuit current	Current at maximum power point	Voltage at maximum power point	Open circuit voltage	Temperature coefficient of open circuit voltage	Temperature coefficient of short circuit current	Nominal operational cell temperature

These data provided by manufacturers are the results of a laboratory flash test at Standard Reference Conditions (SRC) where the incident radiation equals 1000 W/m^2 and the cell temperature is maintained at 25 °C. The only exception is NOCT value, which is obtained at incident radiation of 800 W/m^2 and cell temperature of 20 °C. (Beckman, De Soto, & Klein, 2005)

To obtain current-voltage characteristics of a power generator, it is necessarily to obtain points of various magnitudes of power. In order to do so, power generator is connected to the variable load, which resistance can be adjusted and the response of the system recorded. To draw characteristic of a PV array it is important to submit the tested array to a radiation intensity and spectrum similar to the one of the sun. Performing the test outdoors with natural sun's radiation would not be effective because it would cause an increase of the cells temperature which would affect the current voltage characteristic. (Sturcbecher & Larue, 1994)

Basic requirements for radiation source during the test of PV electrical performance are:

- Spectrum – source must have relatively close electromagnetic wave spectrum to the spectrum of the sun.
- Uniformity – it is important that the irradiance is uniform, this is a critical factor for accurate measurements of PV arrays.
- Stability – the radiation values and spectrum has to be stable during the test.

The above requirements are compulsory for continuous solar simulators (artificially emitted radiation remains constant over the test duration). For cells or small sets of cells usually xenon short arc lamps are used, because the beams they emit satisfy the above conditions. For larger areas (modules/arrays) argon discharged lamps are commonly used. (Markvart & Castaner, 2003)

Different method of simulating the sun's radiation is done using pulsed solar simulators, usually xenon large arc lamps. The beam usually does not submit to the above conditions on the test plane. Both cells and large panels can be tested this way. The advantage of this method is that because of short pulses it doesn't heat the panel at any point. (Markvart & Castaner, 2003)

2.4 Photovoltaic modeling

Modeling of energy systems has become a main tool to forecast energy yield for any scale of investment. It allows testing variable scenarios and applying multiple changes in order to satisfy the customer or the idea itself. Now days many softwares are using predefined mathematical models for simulation. Some of the softwares are used more for commercial purposes, where one of the main outputs are financial benefits, while other may present more depth in terms of technical and physical relations between the system and the environment. Despite the purpose, each modeling tool should mimic the reality as good as possible for the most accurate forecasts. The overall model of photovoltaic generation system usually consists of following parts. (Navabi, Abedi, Pal, & Hosseinian, 2014)

- Geometry – Dimensions, mounting of the system (façade-integrated, roof installed, free standing), influencing environment (trees, buildings, shading devices) and number of devices included in the system.

- System devices – physical properties and geometry linked with materials that a given device is consist of. Manufacturer's data available for model calculations.
- Climate – Database of relevant climate variables related to photovoltaics (Solar radiation, temperature). For higher accuracy the climate data should be provided in dense time-steps.
- Sky model – Assumptions and descriptions regarding radiation distribution (both diffuse and direct beam) in relation to the sky conditions.
- Electrical model – set of equations that represent physical phenomena that are occurring within the photovoltaic panel's equivalent circuit, which sets the main trend to overall electrical output.
- Thermal model – set of equations that determine thermal phenomena that are occurring within the photovoltaic panel. Predicts cell temperature and helps in more accurate estimation of electrical power output based on the total heat and radiation flows within the panel.

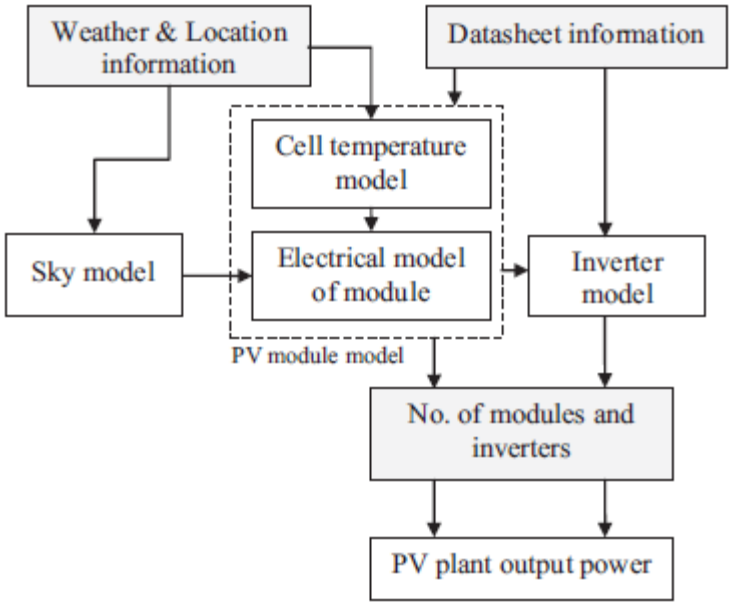

Figure 5 Block representation of main components of a photovoltaic generator model. (Navabi, Abedi, Pal, & Hosseinian, 2014)

This thesis will focus on improving the accuracy of the photovoltaic output in ESP-r, which relates to enhancement of electrical model used by ESP-r software.

2.5 Factors affecting photovoltaic panels performance

Performance of PV panels relies on many factors. It is very common for renewable energy devices that their outputs are highly dependent on weather and environmental conditions. In this section each of most common and influential factors will be presented along with their effect on the output accuracy. Knowing these factors is extremely important in order to understand and find the flaws of electrical and thermal models. Main parameters affecting PV output that will be described in this section are listed below:

- Solar Radiation
- Temperature
- Angle of Incidence
- Spectral distribution
- Ageing (with induced ageing factors)

2.5.1 Solar radiation effects on PV performance

Solar Radiation is described to be the main factor influencing photovoltaics performance. (Thevenard, 2005) Due to the fact that photovoltaic technology is based on photoelectric effect, radiation absorbed by the cells triggers power production in the PV circuit. Therefore the intensity of the incident radiation mainly determines PV power output range.

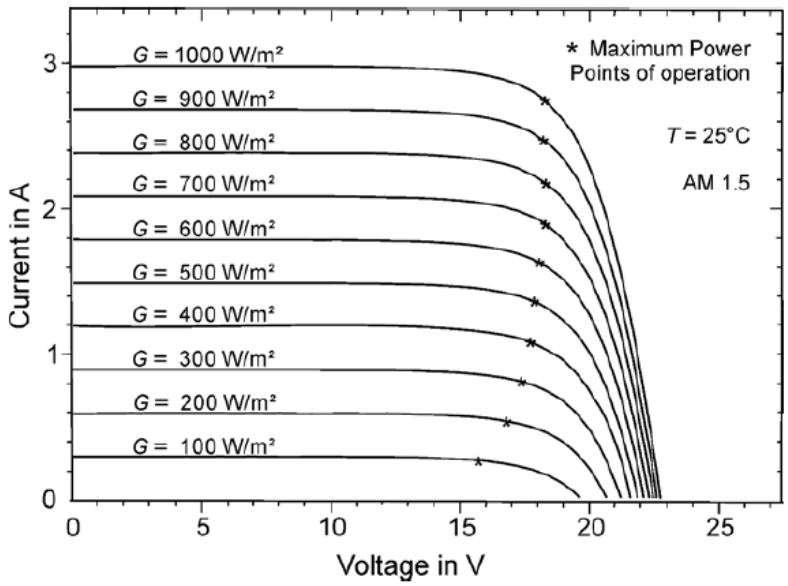

Figure 6 I-V curve for different incident radiation values at constant temperature. (Krauter, 2006)

Above figure shows linear proportion between solar radiation and short circuit current. Open circuit voltage doesn't change much in the range of 350W/m^2 to 1000W/m^2, which implies constant conversion efficiency for this frame. For lower incident radiation, energy conversion drops which is because of larger voltage drops. (Krauter, 2006) This is due to larger impact of shunt resistance, which can be linked with imperfection of the device. It can be noticed that for higher radiation values maximum power point corresponds to approximately same voltage. First significant drop in the corresponding voltage can be seen for radiation value of 500 W/m^2. Further drop in radiation values results in lower values of maximum power point voltage.

According to (Islam, Rahman, & Mominuzzaman, 2014) for lower values of incident solar radiation (100W/m^2-600W/m^2) at monocrystalline photovoltaic panels non-linear effects take charge which implies larger drops in monocrystalline PV performance. The explanation for that are in both shunt and series resistances. The impact of shunt resistance has been described in the previous paragraph. Series resistance has equal or even stronger impact on PV power output in the low radiation region. Large increase of series resistance (from 14.35 Ω at 602 W/m^2 to 128.15 Ω at 105 W/m^2) affects fill factor, causing it to drop. Solar irradiance highly impacts on series resistance, which according to (Islam, Rahman, & Mominuzzaman, 2014) isn't included by any generally accepted models. In the conducted experiment the efficiency varied from 7.7% to 13.6% for 128.15 Ω and 14.35 Ω consecutive.

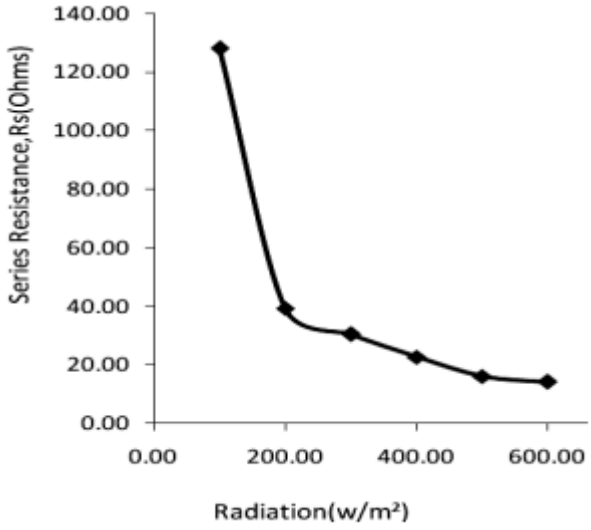

Figure 7 Series Resistance vs incident radiation for monocrystalline PV panel. (Islam, Rahman, & Mominuzzaman, 2014)

2.5.2 Temperature effects on PV performance.

Temperature is one of the core secondary effects on PV performance. Both voltage and current of the photovoltaic device are independently influenced by the cell temperature. Increase of the module's operating temperature implies drop in voltage and slight increase in current. Voltage drops have larger influence on the PV output than rise of current, therefore the overall performance of the device decreases. There are many factors that influence operation temperature. Among the most important are: module design, mounting technique, irradiance level, ambient temperature, wind speed and direction. (King, Kratochvil, & Boyson, 2002).

According to (Labouret & Villoz, 2010) in crystalline PV cells approximatelly voltage drops are in range of 2mV per °C, which gives -0,4% per °C for 500mV cell. The difference of 50°C in operating temperature makes a voltage drop of 100mV per cell, multiplying the drop times number of cells in a module gives a total voltage drop in a PV module.

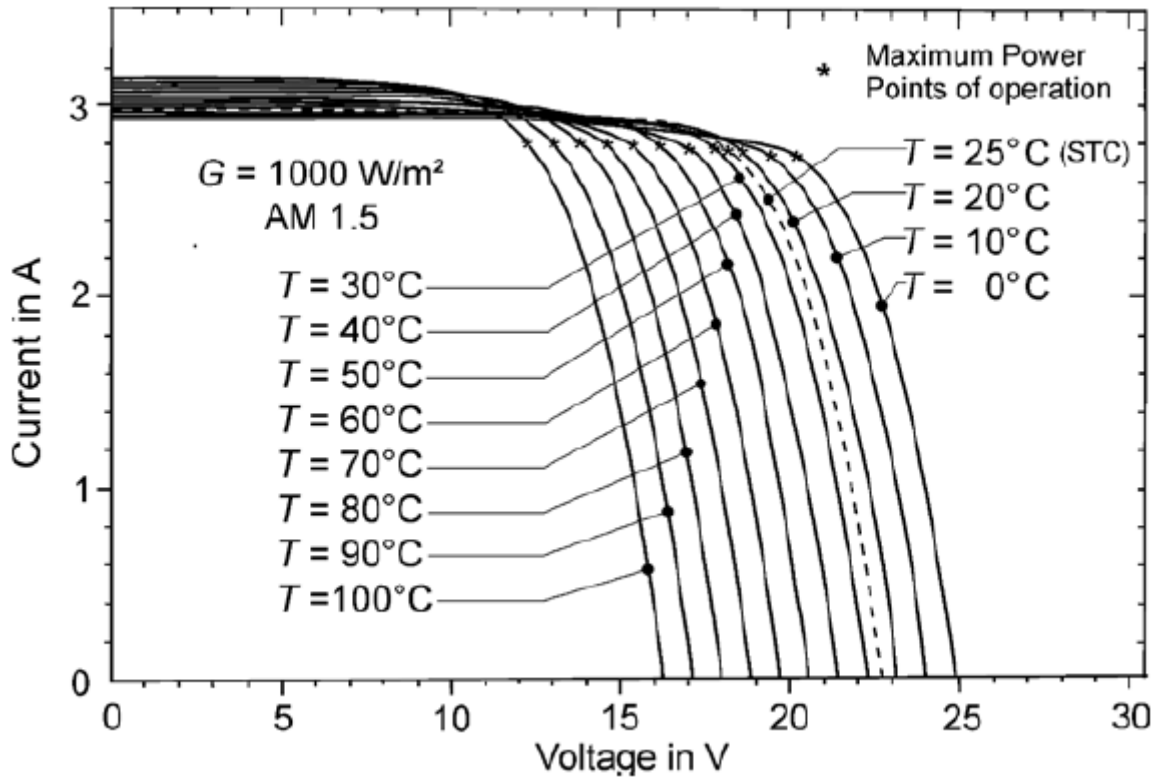

Figure 8 I-V curves for different operating temperatures of a PV cell at constant solar radiation. (Krauter, 2006)

The above figure confirms findings on temperature effects on PV cells. Short circuit current increases slightly as the temperature increases. According to (Markvart & Castaner, 2003) an

increase of current per °C for the BP 585 module equals 0,065%/°C. Comparing this result to previously mentioned voltage drops (0,4%/°C) it proves that voltage has more significant effect on the module's performance. Maximum Power points of operation marked on the figure seem to remain at the same current, which in fact is slightly higher for higher temperature. Voltage drops can be easily noticed, for each 10 °C of temperature rise, voltage difference seems to be the same, which implies the assumption that temperature has almost linear influence on the power output for a given radiation level. (Dubey, Sarvaiya, & Seshadri, 2012)

Estimation of the cell temperature can be done with equation that requires NOCT value (Nominal Operating Cell Temperature). The equation uses also irradiance value and the ambient temperature.

$$T_c = T_a + \frac{NOCT-20}{800} G \qquad (1)$$

$T_c - cell\ operating\ temperature\ [K]$

$T_a - ambient\ temperature\ [K]$

$G - Irradiance\ [W/m^2]$

$NOCT - nominal\ operating\ cell\ temperature\ [K]$

If NOCT value is not available, usually the value of 48°C is recommended and works fine for most of the commonly used PV panels. (Markvart & Castaner, 2003)

2.5.3 Angle of Incidence effects on PV performance

Wrong designed fixed PV module for a given location can suffer large output losses through the period of operation. Optical losses connected with Angle of Incidence (AOI) are related to the direct beam radiation, while diffuse is independent on the modules angle. (King, Kratochvil, & Boyson, 2002) For well designed angles of PV arrays the losses aren't very significant

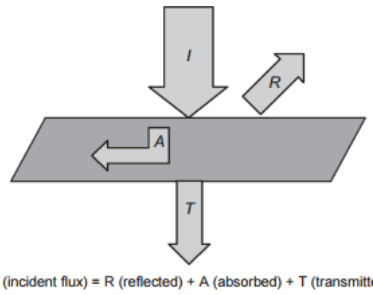

Figure 9 Solar radiation incident on a surface. (Labouret & Villoz, 2010)

(around 1% yearly loss for latitude-tilt angle and 4% for vertical angle (King, Kratochvil, & Boyson, 2002)) due to the low amount of reflected direct beam radiation, nevertheless for fixed PV modules, seasonal or monthly losses could become significant as the relative angle between solar radiation and PV array may become large enough, which will be discussed later in this subchapter.

First of all reflection losses occur when an electromagnetic wave such as sun's radiation enters different environment, which can be different material or medium (i.e. water). Some materials transmit radiation better than others, nevertheless for large AOI, transmittance of many materials can drop even to 0 (for case when AOI= 90°). Figure 9 shows how exemplar beam behaves when it contacts different medium. A part of it which is dependent on reflection angle is reflected (R), some of the radiation is absorbed (A), while remain gets through the medium at a different angle (T), which is determined by refractive index n. It is worth to mention that reflected radiation becomes partially polarized which can be treated as two separate components (parallel and perpendicular) which are included in determining the transmittance of the PV module cover. (Sjerps-Koomen, Alsema, & Turkenburg, 1997)

In a typical PV panel there are several stages of reflection and transmission, which is because of PV physics and different materials that PV panel is consist of. Before radiation reaches the actual PV cell it has to transmit from air to glass, from glass to EVA (Ethylene-Vinyl-Acetate) layer, from EVA layer to Anti-Reflective coating and once it gets past AR coating radiation reaches the cell itself.

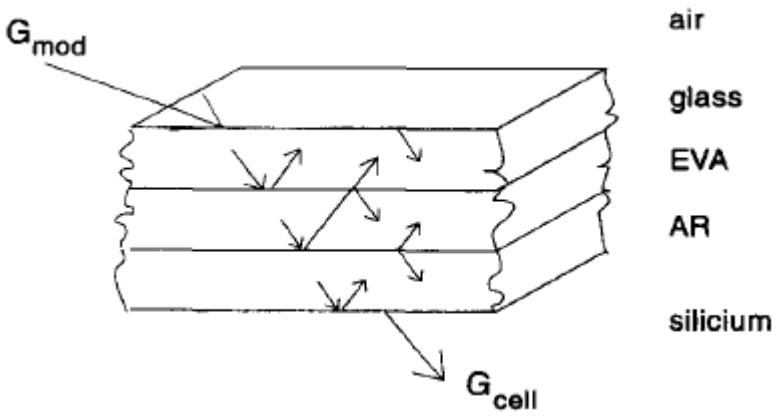

Figure 10 Three layers model of PV panel with paths of reflected and transmitted beams between the layers. (Sjerps-Koomen, Alsema, & Turkenburg, 1997)

According to (Martin & Ruiz, 2001) for three different PV technologies (monocrystalline, polycrystalline and amorphous) and for several tested configurations of the panel (variation of materials and their amount within the panel) reflectance values start to rapidly increase from AOI 60° and higher which can be seen on the figure. Reflectance is the opposite of transmittance.

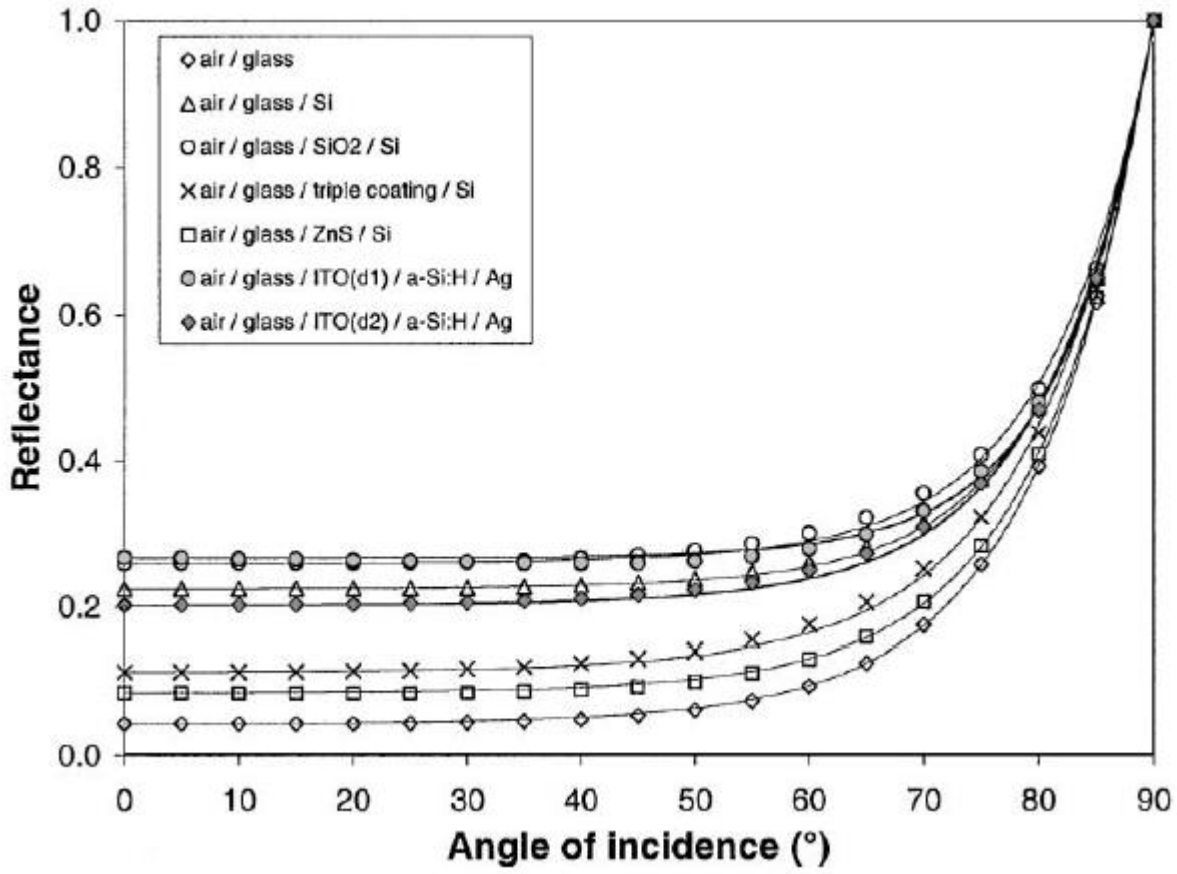

Figure 11Reflectange vs AoI for different set of materials within PV panel. (Martin & Ruiz, 2001)

Investigations described in (Martin & Ruiz, 2001) have proven that for Southern Europe the highest angular losses are in June-July for vertical positioned modules. For northern Europe the highest losses occurred in December for horizontal panel position. Minimum values were obtained for all the investigated sites in winter season (December-January) at around 80° tilt angle for northern Europe and 70° for southern Europe. Anaylsis of yearly angular losses has shown that for each location the most appropriate tilt angle would be close enough to the latitude angle of the location.

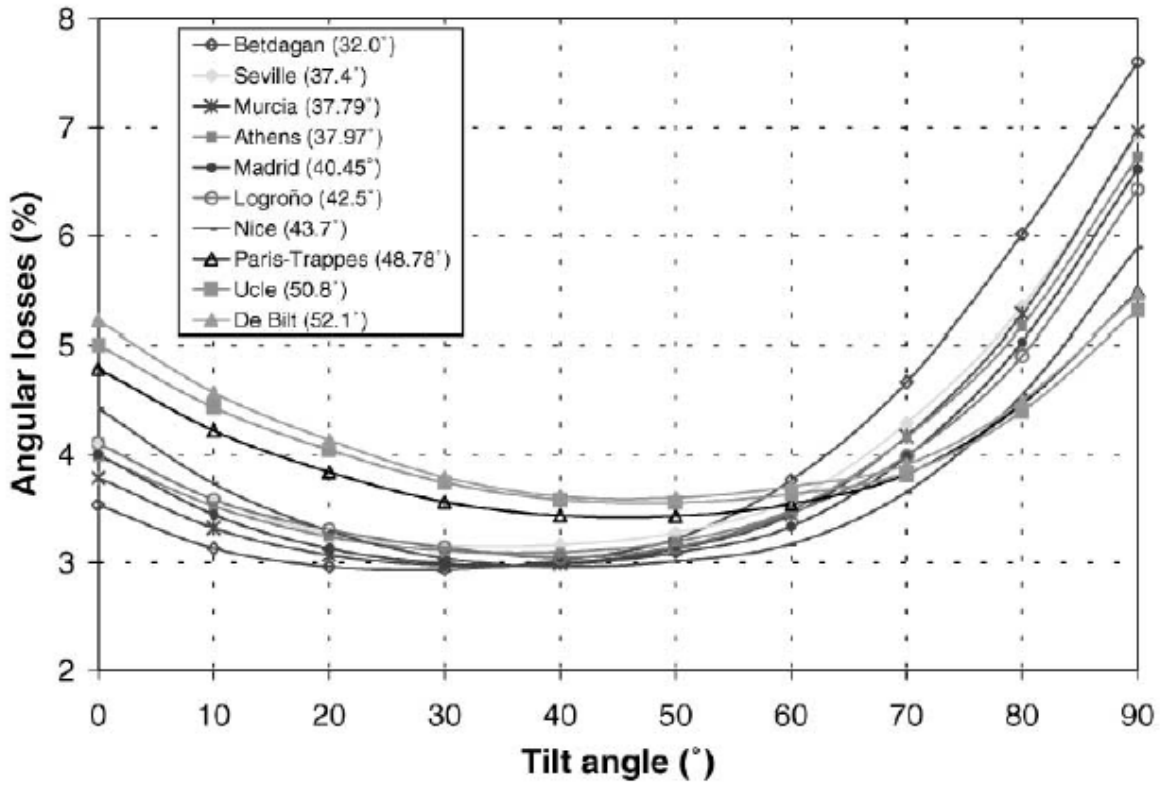

Figure 12 Yearly angular losses for several locations vs tilt angle of the PV panel. (Martin & Ruiz, 2001)

The analysis presented in (Sjerps-Koomen, Alsema, & Turkenburg, 1997) has proven that angular losses can vary a lot depending on tilt angle, location or month. For a façade integrated PV in the Netherlands, angular losses varied from 2% to 10% through the year. For Zimbabwe the range was even higher 2% to 20%. This proves that AOI factor cannot be neglected and has to be very seriously considered in the PV system design process.

2.5.4 Spectral distribution effects on PV performance

Spectral distribution changes over the year constantly. There are minor changes during each day and significant differences when comparing days of different seasons. Spectral response is a characteristic of a PV device which describes what kind of electromagnetic waves are preferably absorbed by PV cell. Considering spectral distribution crystalline PV cells differ a lot in comparison to amorphous PV cells. Crystalline panels have better response to longer wavelengths (red and near infrared 700nm-1100nm) while amorphous for shorter blue-green wavelengths (350nm-550nm). (Labouret & Villoz, 2010)

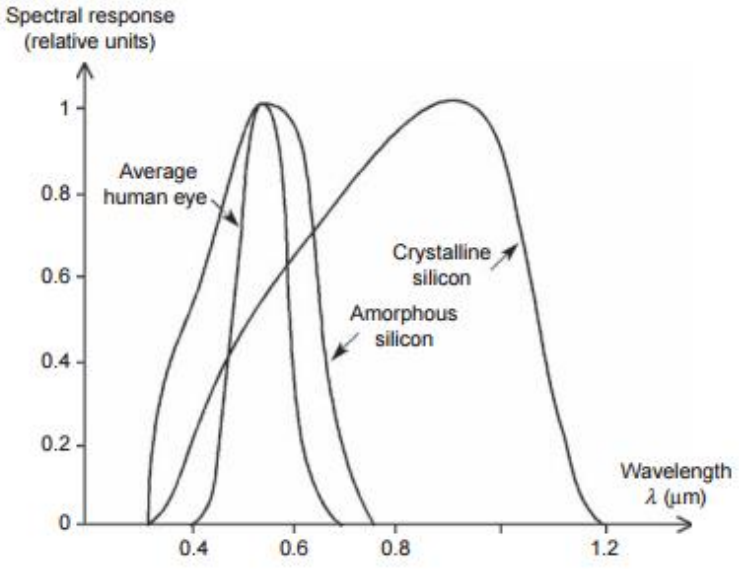

Figure 13 Spectral response of Crystalline and Amorphous silicon PV cells. (Labouret & Villoz, 2010)

According to (King, Kratochvil, & Boyson, 2002) there isn't any significant impact of spectral distribution on PV output. The influence is visible each day and is different during different season, although they average out on yearly basis.

Visible light, especially blue light region has the biggest impact on power production. For the same radiation values at two different time steps in the same day PV output is slightly different. This is because electromagnetic wave spectrum is different in the morning than the one in the afternoon. Investigations presented in (Ghitas, 2012) have shown that for a spectrum with more visible radiation, short circuit current increases.

The difference in spectral distribution effects between crystalline and amorphous PV cells was investigated in (Ishii, Otani, Itagaki, & Utsunomiya, 2013). Measurements were done in four different stations (Sapporo, Tosu, Gifu and Okinoerabu). For crystalline cells the outputs were consecuitve +0,4%; +0,6%; +0,5%; +1,0%. For amorphous cells outputs were +1,9%; +3,9%; +3,9%; +7,6%. Crystalline panels weren't significantly influenced by the spectral distribution, amorphous cells on the other hand have proven to be more sensitive on that factor. Tosu and Gifu are approximatelly at the same latitude, Sapporo is further north and Okinoerabu south. It can be noticed that PV performance increase for places closer to equator.

2.5.5 Performance drop with ageing of photovoltaic cells

The influence of ageing of the PV panels on performance depends on several factors. First of all it has to be said that different PV technologies would perform in different way with time.

Despite ageing and fatigue of the materials that PV panels are built of, behavior of the environment can speed up ageing process. Main environmental factors that may shorten the lifespan of a PV panel are: bird droppings, seeds, pollen, leaves, branches, dirt and dust, human constructions of all kind and localized increase of temperature. Moreover strong winds, hail or any mechanical impacts may damage the glass cover of a panel, which makes it vulnerable to rapid decomposition. (Krauter, 2006)

Experiment described in (Kaplani, 2012) has shown the ageing effects of monocrystalline PV panels. Six PV modules were examined in terms of their condition after 18 to 22 years of operation. Four of them were exposed to different scale environmental factors that speed up ageing process, while the remaining two were ageing in natural way without any catalyst. Researchers looked carefully on optical degradation effects due to partial or total shading, degradation of AR coating and thermal degradation incurred by local temperature variations.

Table 2 Relative degradation in power output and fill factor for six tested PV modules.

PV module	RD_{Pm} [%]	RD_{FF} [%]
I1	23,8	16,9
I2	27,6	20,4
I3	32,6	26,7
I4	42,2	37,8
N1	18,3	11,9
N2	23,6	12,0

Table 2 presents ageing effects. Consecutive modules I (1-4) were exposed to induced ageing effects from mild (1) to very severe (4). Modules N (1-2) were exposed only to natural ageing process. Values in the table were calculated for 18 years old of operation.

In comparison with recently used technologies crystalline PV modules have the largest lifespan. According to (Tiwari, Mishra, & Solanki, 2011) crystalline modules can operate for 30 years, amorphous (a-si) cells for 20 years, thin silicon cell 25 years and Cadmium telluride for around 15 years.

2.6 Photovoltaic electrical models

The main purpose of photovoltaics modeling is to evaluate its overall performance during an influence of occurring weather factors (Irradiance and temperature). Performance can be measured in current, voltage and power. These three variables can be formed in I-V and P-V characteristics, which are non-linear functions based on manufacturers data, constant variables and variables that have to be simulated. (Habbati Bellia, 2014) Current-Voltage and Power-Voltage characteristics can be obtained through varying the load applied to the circuit for specific conditions at constant temperature and radiation level. (Krauter, 2006)

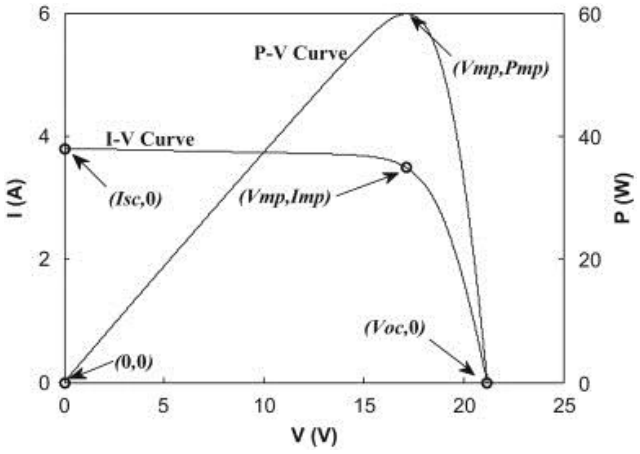

Figure 14 Exemplar I-V and P-V curves with characteristic points. (Ishaque, Salam, & Taheri, 2010)

These characteristics can be obtained for constant incident radiation and constant cell temperature, thus it would be impossible to use them in order to determine energy yield of a power generation system in natural conditions. In this case it is essential to choose an electrical model, which is able to predict energy output for various periods with a use of variables determined for a given radiation and temperature.

In this chapter, the main idea of two most commonly used electrical models will be described.

- One diode photovoltaic generator model (including description of few variants)
- Sandia model.

2.6.1 General one diode photovoltaic generator model.

Generally common and accepted equivalent circuit for photovoltaic generator is the one-diode model, which is presented at the figure 15.

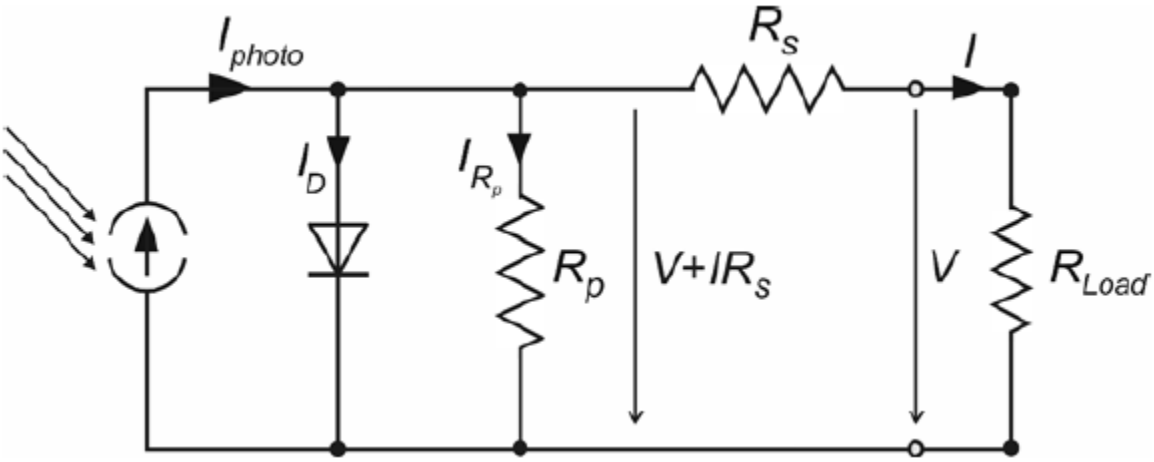

Figure 15 General equivalent circuit for a photovoltaic generator. (Krauter, 2006)

The first Kirchhoff law for the above circuit:

$$I = I_L - I_D - I_{R_p} = I_L - I_0 \left[\exp\left(\frac{V+IR_s}{a}\right) - 1\right] - \frac{V+IR_s}{R_p} \qquad (2)$$

$I - output\ current\ at\ the\ load\ [A]$

$I_L(I_{photo}) - Light\ generated\ current\ [A]$

$I_D - diode\ current\ [A]$

$I_{R_p} - current\ flowing\ through\ parallel\ resistance\ [A]$

$I_0 - diode\ reverse\ saturation\ current\ [A]$

$V - output\ voltage\ at\ the\ load\ [V]$

$R_s - series\ resistance\ [\Omega]$

$R_p - parallel\ resistance\ (shunt\ resistance)\ [\Omega]$

$a - modified\ ideality\ factor\ [-]$

In the presented model values I and V are the outputs that draw the I-V characteristics through R_{Load} variation. Radiation absorbed by the photovoltaic panel invokes light generated current, which splits further in the circuit on three components presented in the equation (2). (Krauter, 2006)

Resistances parallel and series are in form of correction factors used to obtain higher accuracy of the model output and are related with hardly to measure phenomenon, which occur within photovoltaic modules that affect output values. (Habbati Bellia, 2014)

Parallel resistance, also known as shunt resistance R_{sh} is the equivalent of high-conductivity paths within the p-n junction, it is mainly connected with manufacturing defects. It has significant impact on short circuit current and also improves the accuracy during occurrence of low radiation levels. (Alamri & Benghanem, 2008) (Honsberg & Bowden)

The series resistance R_s represents the sum of contact resistance between the metal and the silicon, the resistance of the front and back surfaces. Series resistances help determine more accurately the fill factor of the photovoltaic module, high values may reduce short-circuit current. (Alamri & Benghanem, 2008) (Honsberg & Bowden)

The modified ideality factor is related to physical constants and properties of a diode, which is represented by symbol n=1 for ideal diode and n ϵ (1,2). (Duffie & Beckman, 2013)

$$a = \frac{nkTN_S}{q} \quad (3)$$

$n - diode\ ideality\ factor\ [-]$

$k - Boltzmann\ constant, 1.381 * 10^{-23}[\frac{J}{K}]$

$T - cell\ temperature\ [℃], N_s - number\ of\ cells\ in\ series\ [-]$

$q - electronic\ charge, 1.602 * 10^{-19}[C]$

According to (Duffie & Beckman, 2013) the general one diode equivalent circuit is dependent on five parameters. In order to obtain them, it is necessarily to know manufacturers data presented in table 1.

Apart from the general model, many researchers or softwares are using simplified versions of the general one diode photovoltaic electrical model. Simplified models are less accurate, although are easier to simulate. There are two simplifications from the general one diode photovoltaic model.

Ideal one diode model, according to (Wagner, 2000) is described as low accurate model. The exemplar circuit is presented below at figure 16.

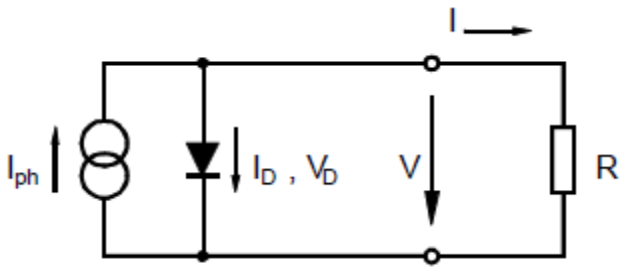

Figure 16 Ideal one diode model circuit. (Wagner, 2000)

The difference between the general model and the ideal one is lack of series and shunt resistance within the ideal pattern. Model assumes that there aren't any losses due to imperfection of the device and interaction between its internal parts.

The first Kirchhoffs's law for the ideal model circuit:

$$I = I_L - I_D = I_L - I_0 \left[exp\left(\frac{V}{a}\right) - 1 \right] \qquad (4)$$

Another simplified model with accuracy approximation described as good (Wagner, 2000) is the one diode model with series resistance. It is more accurate than the ideal model because it includes resistance of cell and connection between cells (Donsion & Skocil).

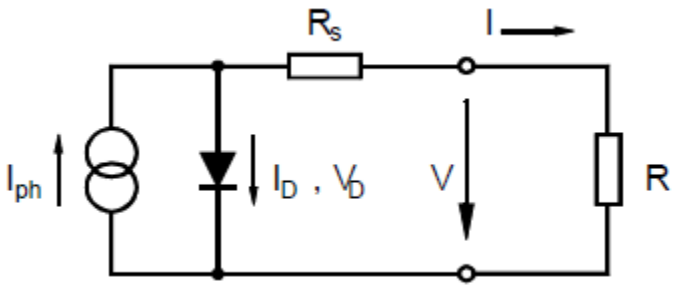

Figure 17 Simple model with series resistance. (Wagner, 2000)

The drawback of this model is that it doesn't include shunt losses related with imperfection of the device. Nevertheless some researchers are still using this simplification as enough accurate (Habbati Bellia, 2014).

The first Kirchhoffs's law for the series resistance model circuit:

$$I = I_L - I_D = I_L - I_0 \left[exp\left(\frac{V+IR_s}{a}\right) - 1 \right] \qquad (5)$$

The general one-diode model and its simplifications have been described. The difference within their algorithms and accuracy levels are beyond the scope of this thesis. Output calculations algorithm itself will be presented further for the ESP-r electrical model.

2.6.2 Two diode photovoltaic generator model

Two diode model is a more complex, but also proven to be more accurate than any one diode model. (Ishaque, Salam, & Taheri, 2010). The equivalent circuit is presented below.

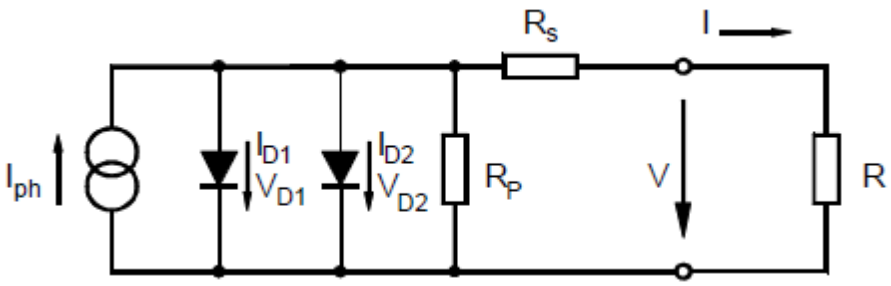

Figure 18 Two diode photovoltaic generator model. (Wagner, 2000)

Addition of the second diode creates more complex algorithm, which strongly affects simulation time. It is considered to be the main drawback of this model. (Salam & Ishaque) Researchers are looking for ways to simplify the model in order to speed up the simulation time while staying with very accurate approximation.

According to (Ishaque, Salam, & Taheri, 2010) relative errors of two diode models were smaller than for all the one diode models for every PV device technology. Three models (one diode with R_s, one diode with R_s and R_p, two diode model) were compared with measured data for three different PV technology (poly-crystalline, mono-crystalline, thin film) at 4 different temperatures (-25°C, 0°C, 25°C, 50°C).

Simple one diode model with R_s had significantly higher relative error for every single configuration. The difference between two diode and the enhanced one diode models were varying slightly, without any trend. Nevertheless for every single configuration two diode model appeared to be more accurate than enhanced one diode model. (Ishaque, Salam, & Taheri, 2010), (Benghanem & Alamri, 2008)

2.6.3 Sandia model

Sandia PV Array Performance Model was created at Sandia National Laboratories (SNL). The model was prepared from 1991 until 2004 and described in (King, Boyson, & Kratochvill, 2004). SNL has prepared large database of parameters used in the model. In order to do that, SNL had to test variety of PV modules coming from different manufacturers. Archived data is used in electrical model to calculate the PV system power rating based on original PV module-specific derived formulas discovered at SNL. (Klise & Stein, 2009)

The model uses an algorithm of 10 equations, which if supplied with reference values, solar resource and performance coefficients, can predict power output of a solar photovoltaics array. (King, Boyson, & Kratochvill, 2004).

The algorithm calculates values of I_{sc}, I_{mp}, V_{oc}, V_{mp}, P_{mp}, FF, I_x and I_{xx}, and based on these values the I-V curve for occurring solar radiation conditions can be sketched with a very good approximation. First four values were described earlier in the paper as characteristic points of I-V curve. To achieve higher accuracy, Sandia model involves two additional currents:

I_x – current occurring at voltage equal to half value of the open circuit voltage. $\left(I_x, \frac{V_{oc}}{2}\right)$

I_{xx} – current occurring at the voltage in the middle between V_{oc} and V_{mp} $\left(I_{xx}, \frac{V_{oc}+V_{mp}}{2}\right)$

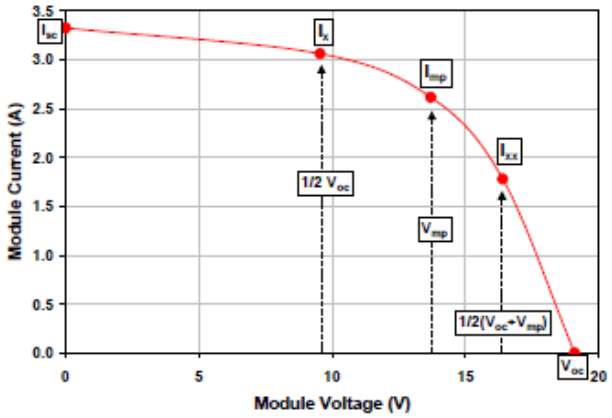

Figure 19 I-V curve with characteristic points calculated in Sandia model. (King, Boyson, & Kratochvill, 2004)

Fill factor (FF [-]) is determined in order to analyse the performance of the cell. It represents how large are losses within the cell (ohmic, optical, recombination). High fill factor implies low series resistance values and high shunt resistance values or low optical losses related to radiation absorption by the photovoltaic cell. (Krauter, 2006)

One of the most important values within the model is the effective solar irradiance E_e. It shows the proportion of solar irradiance on which photovoltaic panel reacts to the total solar irradiance incident on the module. Performance coefficients which are laboratory determined values relate I-V curve characteristic points with the effective solar irradiance, which solves the problem of optical issues with the radiation. (King, Boyson, & Kratochvill, 2004)

Sandia model uses pre-determined performance coefficients and empirical functions for over 50 tested crystalline silicon modules and 300 crystalline silicon modules estimated values. (King & Pratt) These coefficients and other constants determined at SNL are necessary to perform electrical model analysis. This is the main drawback of Sandia model. Despite its very good accuracy (according to Fanney, around 1% error in yearly output prediction for various geographical locations) the need for pre-determined data makes the model difficult to apply without the access to the database or without coefficients determined for investigated PV panel. Some softwares have access to Sandia database which allows them to use the model. In case there aren't any data for a given PV module, the software can use one diode electrical model.

3. MODEL DESCRIPTION

This section will cover the explanation of current photovoltaic model of ESP-r and suggested changes. First of all the theoretical base of ESP-r's model will be introduced, with general equations and equivalent circuit. Later in this chapter, the part of code that ESP-r uses to calculate power output will be presented. Finally, the problem with the code will be described and the solution for it.

3.1 Photovoltaic electrical model used in ESP-r

Electrical model used in ESP-r is a simplified model of single diode model case. The model doesn't include parallel and series resistances. Thus on the first sight it can be noticed that the model lacks accuracy. ESP-r electrical model has a few more drawbacks that may question the output calculated by the software. Before describing the issue investigated in this thesis, the model will be presented as it is for now.

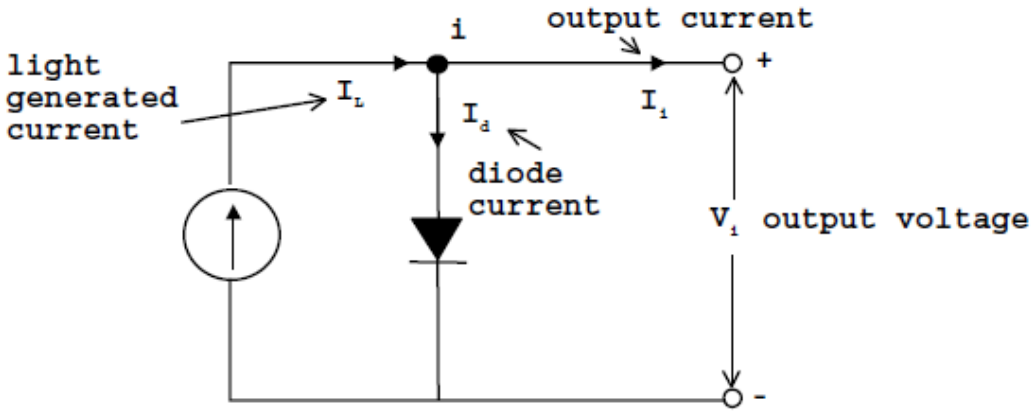

Figure 20 Equivalent circuit of the photovoltaic electrical model in ESP-r. (Kelly, 1998)

Figure 20 presents an equivalent circuit of the model. As it was mentioned before, neither shunt nor series resistances are included. Kirchhoff's first law for this circuit for node i:

$$I_i = I_L - I_D \qquad (6)$$

To obtain output current I_i the values of I_L and I_D have to be defined. Light generated current (I_L) is a linear function of the solar radiation absorbed by the PV layer. Nevertheless in the current electrical model, the software links light generated current with shortwave incident radiation. This will be discussed later in this chapter. Originally the equation looks as follow:

$$I_L = \frac{q_{isw}}{a} \quad (7)$$

$q_{isw} - nodal\ incident\ short\ wave\ radiation\ flux\ [W]$

$a - ratio\ of\ radiation\ absorbed\ at\ the\ node\ (a_{pnl})$

$to\ the\ radiation\ absorbed\ at\ SRC(a_{ref})\ [-]$

$$a = \frac{a_{pnl}}{a_{ref}} \quad (8)$$

Diode current is represented with the equation 9 :

$$I_D = I_0 \left(1 - exp\left[\frac{eV_i}{DF*k*T_i}\right]\right) \quad (9)$$

$I_0 - diffuse\ current\ [A]$

$V_i - nodal\ voltage\ [V]$

$DF - diode\ factor\ [-]$

$,k - boltzmann'sconstant\ [-]$

$,T_i - nodal\ temperature\ [K]$

Once light generated and diode currents are defined, equation 10 takes form:

$$I_i = I_0 \left(1 - exp\left[\frac{eV_i}{DFkT_i}\right]\right) - \frac{q_{isw}}{a} \quad (10)$$

Multiplying the equation with the nodal voltage, power output can be obtained:

$$P_i = V_i I_i = V_i I_0 \left(1 - exp\left[\frac{eV_i}{DFkT_i}\right]\right) - V_i \frac{q_{isw}}{a} \qquad (11)$$

In order to obtain power output from a layer it is necessarily to multiply nodal value by the number of cells in the layer. (Kelly, 1998)

The algorithm presented through equations (6-11) gives the basic idea and base for the practical algorithm where manufacturer's data can be used, thus the model can be universal for every PV panel. In fact ESP-r in its electrical model uses modified equations for the mentioned purpose of known inputs. The algorithm submits to the above laws and equations. Presentation of the current ESP-r algorithm and a short commentary will come next in this chapter.

3.2 ESP-r electrical model's algorithm

The electrical model, equations and values related to the previously described general model are within the special materials section of ESP-r source code. To start with the description of the model's logic, the inputs will be introduced. Input values are presented in table 3.

Table 1 Inputs to the photovoltaic electrical model of ESP-r.

Value's symbol and unit	Description
V_{oc} $[V]$	Voltage obtained in open circuit conditions. (I=0, no load applied)
I_{sc} $[A]$	Short circuit current (closed circuit at minimum resistance)
V_{mp} $[V]$	Voltage at maximum power point.
I_{mp} $[A]$	Current at maximum power point.

Q_{ref} $[\frac{W}{m^2}]$	Incident radiation at SRC (1000 $\frac{W}{m^2}$)
T_{ref} $[°C]$	Temperature at SRC (25°C)
n [-]	Number of cells in series.
m [-]	Number of parallel branches.
np [-]	Number of panels in the surface.
EMPV [-]	Empirical constant related to the characteristics of PV material.

Once the inputs are recorded, next step is the description of the load type of the panel and shading treatment. There are three types of load type: maximum power point tracking (which is a default setting), fixed resistance and fixed voltage. For shading treatment the default option is that shading impacts proportional percentage losses to the percent of shaded area, other conditions are: total power loss, power output at shaded insolation level. For all the further analysis in the result chapter these settings have been set to default because they were not necessarily in testing the reformed code.

The values of incident radiation on the panel Q_{pnl} and temperature of the panel T_{pnl} are defined from the location data for a special material node.

$$Q_{pnl} = EXRAD(ispmloc(ISPMNOD, 2)) \quad (12)$$

$$T_{pnl} = TFC(ispmloc(ISPMNOD, 1), ispmloc(ISPMNOD, 2), ispmloc(ISPMNOD, 3)) + 273 \quad (13)$$

EXRAD is a total solar radiation incident on surface per unit area. Ispmloc calls on the location data, and ISPMNOD refers to (1-zone, 2-surface, 3-node)

Regarding electrical model, to calculate the diffuse current which is required for further power calculations, diode factor has to be determined. Equation (14) presents formula used by ESP-r to calculate diode factor:

$$DF = \frac{\left(\frac{e}{kT_{ref}}\right)\left(V_{mp} - \frac{V_{oc}}{n}\right)}{ln\left(\frac{I_{sc} - I_{mp}}{I_{sc}}\right)} \qquad (14)$$

Once the diode factor is known, it is possible to obtain diffuse current I_0

$$I_0 = 2^{\frac{T_{pnl} - T_{ref}}{EMPV}} \left(\frac{-\frac{I_{sc}}{m}}{\left[exp\left(\frac{e^{\frac{V_{oc}}{n}}}{kT_{ref}DF} \right) - 1 \right]} \right) \qquad (15)$$

Afterwards light generated current is calculated, using formula (16).

$$I_L = \frac{Q_{pnl}}{Q_{ref}} * \frac{I_{sc}}{m} \qquad (16)$$

$Q_{pnl} - incident\ shortwave\ radiation\ on\ the\ panel\ [\frac{W}{m^2}]$

$Q_{ref} - reference\ incident\ shortwave\ radiation\ 1000\ [\frac{W}{m^2}]$

$m - number\ of\ parallel\ branches\ in\ the\ module[-]$

Having diffuse and light generated currents the algorithm is able to calculate the new V_{mp} for given location and conditions at a given time step. Iteration method is used in order to obtain the value more accurately. Firstly, four different values of V_{mp} are defined:

$$V_{mp1} = \frac{kT_{pnl}DF}{e} \qquad (17)$$

$$V_{mp2} = \left(\frac{I_L}{I_0}\right) + 1 \qquad (18)$$

$$V_{mp3} = 1 + \frac{eV_{ITER}}{kT_{pnl}DF} \quad (19)$$

$$V_{mp4} = log\left(\frac{V_{mp2}}{V_{mp3}}\right) \quad (20)$$

The final voltage for a given time step:

$$V_{mpmod} = V_{mp1} * V_{mp4} \quad (21)$$

Value V_{ITER} used in the equation (19) is defined as $V_{ITER} = 0{,}4$ for the first iteration step. Then the dependency is validated. If the absolute value of $V_{ITER} - V_{mpmod}$ is greater than 0,05 and the iteration number is lower than 101 then the process starts from the beginning (V_{mp1}) assuming $V_{ITER} = |V_{mpmod}|$. The iteration repeats until the difference between these values are lower than 0,05.

Finally power output can be determined with previously obtained values.

$$P_{pv} = \left(V_{mpmod}I_L - V_{mpmod}I_0\left(exp\left[\frac{(eV_{mpmod})}{(kT_{pnl}DF)}\right] - 1\right)\right) * m * n * np\ [W] \quad (22)$$

In case the output is a minus value, then it is assumed that it is equal zero. $P_{pv} = 0$

3.3 Description of the investigated issue

The key issue investigated in this thesis relates to equation (7). In subchapter 3.1 the equation (7) states that the light generated current is a linear function of short wave radiation absorbed by the PV layer. The electrical model of ESP-r instead of absorbed values in the equation (8) uses incident shortwave radiation at the surface values. In fact, the absorbed nodal values would be more accurate and appropriate for the electrical model. The light generated current radiation should be described by equation (23):

$$I_L = \frac{a_{pnl}}{a_{ref}} * \frac{I_{sc}}{m} \quad (23)$$

At reference conditions, beam strikes the panel at 0° incident angle, therefore approximately total amount of radiation reaches tested cell or panel. If a PV panel operating in the outside environment would be constantly stimulated by radiation beams at the same incident angle all the time, it could be assumed that the fraction of actual absorbed radiation to radiation absorbed at reference condition would be very similar to the fraction of incident radiation at a given time step to the incident radiation at reference conditions.

Under previously mentioned incidence angle assumptions, the only difference between these fractions would be different absorption capabilities of material under different temperatures and also various spectral responses depending on temperature. Nevertheless, whether spectral and material absorption capability factors are significant enough in relation to PV operating temperatures should be discussed within thermal photovoltaics model of ESP-r which is out of the scope of this project.

Returning to the electrical model and absorbed radiation, the cause that the absorption and radiation fractions are different is the reflection of radiation beams. The reflection phenomenon and the angle of incidence influence on the PV output were discussed briefly in the literature review. In the electrical model the main problem is that PV panel has a layer structure, with different materials dividing PV layer from the outside environment. Figure 21 presents the layer/nodal structure of an exemplar PV panel.

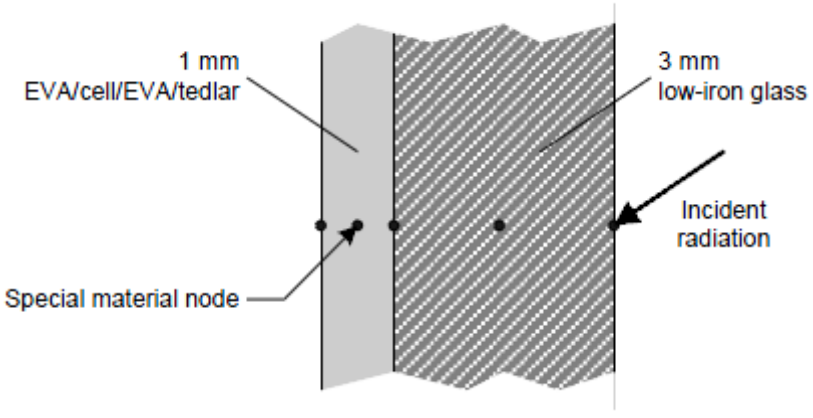

Figure 21 PV panel layers simulated in ESP-r. (Thevenard, 2005)

Each layer has a node that describes it with equations and properties. Figure 21 points out the problem in a direct way. It can be noticed that incident radiation which is considered in the electrical model for light generated current calculation strikes the first layer, which is low-iron

glass. First node represents conditions between the environment and the glass, second node defines the glass, third node is on a border between EVA layer and low-iron glass, finally the fourth node stands for the PV layer. Photovoltaic panel can be defined in various ways in ESP-r, an anti-reflective coating of many kinds can be added to prevent further reflections.

Before the radiation reaches PV layer it will reflect several times at the borders of each layer, which if we include anti-reflective coating layer makes a total of four reflection borders.

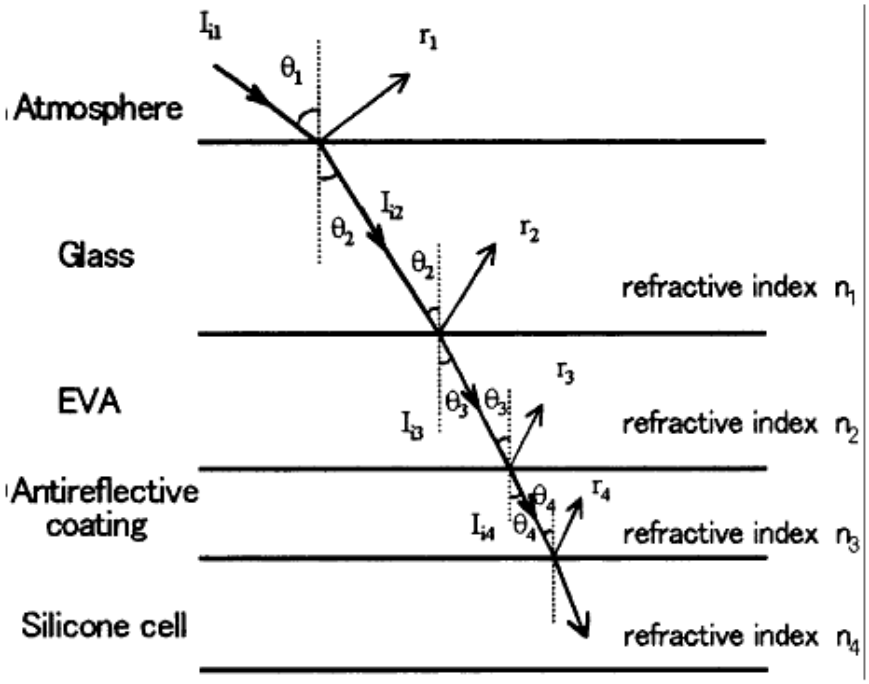

Figure 22 Radiation reflections within PV panel. (Yamada, Nakamura, Sugiura, Sakuta Koichi, & Kurokawa, 2001)

Each layer has its own refractive index n_i, which is dependent on the material properties. Since in each material the radiation spreads at different velocities, the beam becomes refracted, therefore some amount reflects from the surface at the same angle that the beam makes with perpendicular surface, while the rest is transmitted at a different angle. According to Snell's law the relation between angle of incidence and angle of refraction is the same as between the refractive index of the material with refracted wave to refractive index with original wave. (Yamada, Nakamura, Sugiura, Sakuta Koichi, & Kurokawa, 2001)

$$\frac{sin\theta_1}{sin\theta_2} = \frac{n_{\theta_2}}{n_{\theta_1}} \qquad (24)$$

Moreover each layer absorbs some amount of radiation, which also reduces the final value that reaches the PV layer.

$$G = \alpha + \tau + r \quad (25)$$

The total radiation G in each contact with different environment spreads into three components α- amount absorbed, r- amount reflected, τ-amount transmitted.

From the equation (25) it can be noticed that the higher the value of reflected radiation, the lower are values of the two other components. Nevertheless absorption highly depends on material properties, temperature and the spectral response of material. It can be assumed that when the reflection value grows, the value that drops for around the same amount is transmittance.

According to (Yamada, Nakamura, Sugiura, Sakuta Koichi, & Kurokawa, 2001) transmittance of an investigated PV module was around 0,8 for 0° angle of incidence. It has been noticed that transmittance drops with the increase of angle of incidence. First the trend is smooth and goes down quite slowly, when the angle reaches values around 60° transmittance starts to drop rapidly.

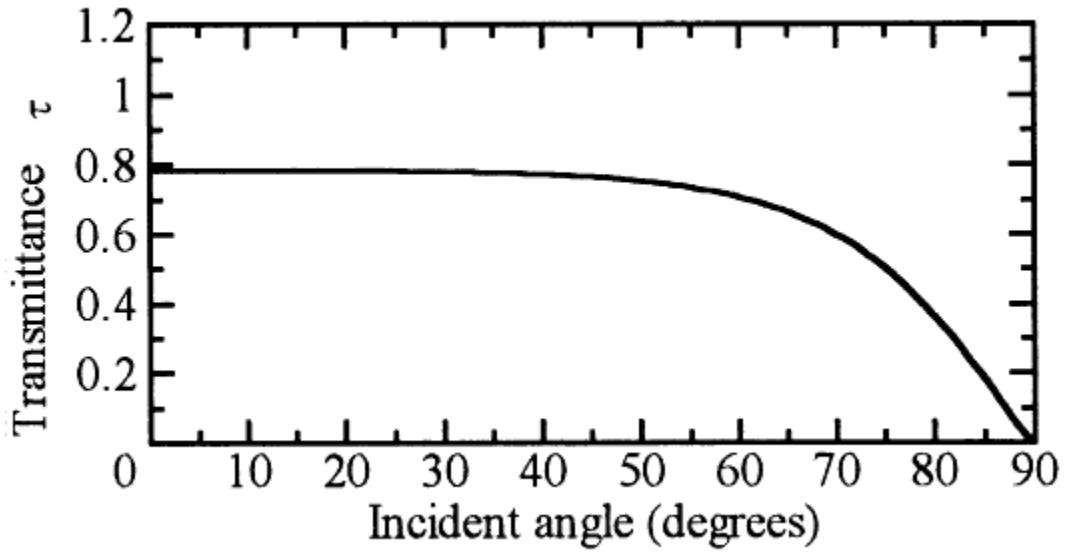

Figure 23 Transmittance in relation to the angle of incidence. (Yamada, Nakamura, Sugiura, Sakuta Koichi, & Kurokawa, 2001)

This relation is also confirmed by (Sjerps-Koomen, Alsema, & Turkenburg, 1997), they've pointed that for angles of incidence over 60° transmittance drops significantly.

Over the day, month, season and year sun takes different position on the horizon (Except for equator, which changes only during the day). If PV device doesn't have solar tracking system, its output is dependent on the suns position. For climates relatively close to equator, large reflection can occur during sunrise and sunsets, when the position of the sun is low. Nevertheless the radiation isn't very large at these times, sun's path for such climates is also relatively stable over the year, which won't cause any seasonal differences (as long as the angle of a PV is fairly optimal).

The problem might be way more complex in climate zones that are rather closer to the poles than equator. Daily, seasonal and yearly accuracy might be very different with the current electrical model. Therefore it's harder to pick an appropriate angle for PV arrays. Even for well assorted angles to optimize yearly output for some months losses could be significant and might reach around 10%. (Martin & Ruiz, 2001).

Reasonably speaking, for climates close to equator, without considering worst possible angles of PV mounting, the electrical model that uses incident radiation might give similar response as the one with absorbed values. On the other hand the very northern or very southern climates are expected to suffer various optical losses over the whole year, depending on a month or season. Therefore the outputs might differ significantly for the two versions of light generated current equations in electrical model. Careful analysis of similar and different scenarios will be performed in the results and analysis chapter, where both versions will be compared.

4. METHODOLOGY

In this chapter the main focus will be put into the logical flow and detailed description of the methods, means and data used to achieve assumed aims. First of all the general concept will be presented, covering most important activities and milestones that show the structure of pre-assumed plan and its evolution. Once the general methodology is presented, more focus will be put in the details of simulation techniques, characteristics and chosen scenarios.

4.1 General methodology

The main flow of the project followed a standard approach. First of all the investigated issue had to be briefly defined, along with the tools and means to achieve preliminary goals. Then the first attempts to access and look at the source code briefly has been commenced. Once the basic issue has been preliminary defined along with aims and objectives, the next step was to collect information about the topic and pick relevant sources regarding physical phenomenon, technical issues and previous investigations related to the main problem itself. Simultaneously, during literature review process, more in depth analysis of the source code has been done in order to validate and check whether some of the academic sources relate to the investigated issue. After getting enough knowledge and understanding of the problem and source code environment, the new code with the applied changes in light generated current calculations has been implemented. Once the new code successfully settled in, a set of simulations has been performed in order to carefully analyse and understand the outcomes of the changed code. Simultaneously, the same set of simulations has been performed for the old code to have the data for comparison. More details on the simulation methodology will be discussed further in this chapter. Obtained data from both sets of simulations had to be properly sorted to draw graphs, discover valuable relations and clearly present the outcomes. Finally at the end the analysis of the data achieved from the simulations supported by the previously gained knowledge from academic sources and the source code of ESP-r has given the opportunity to draw final conclusions and suggest further work that could be done in order to improve accuracy of ESP-r photovoltaic calculations. Figure 24 represents the block chart of the general methodology chosen for the project.

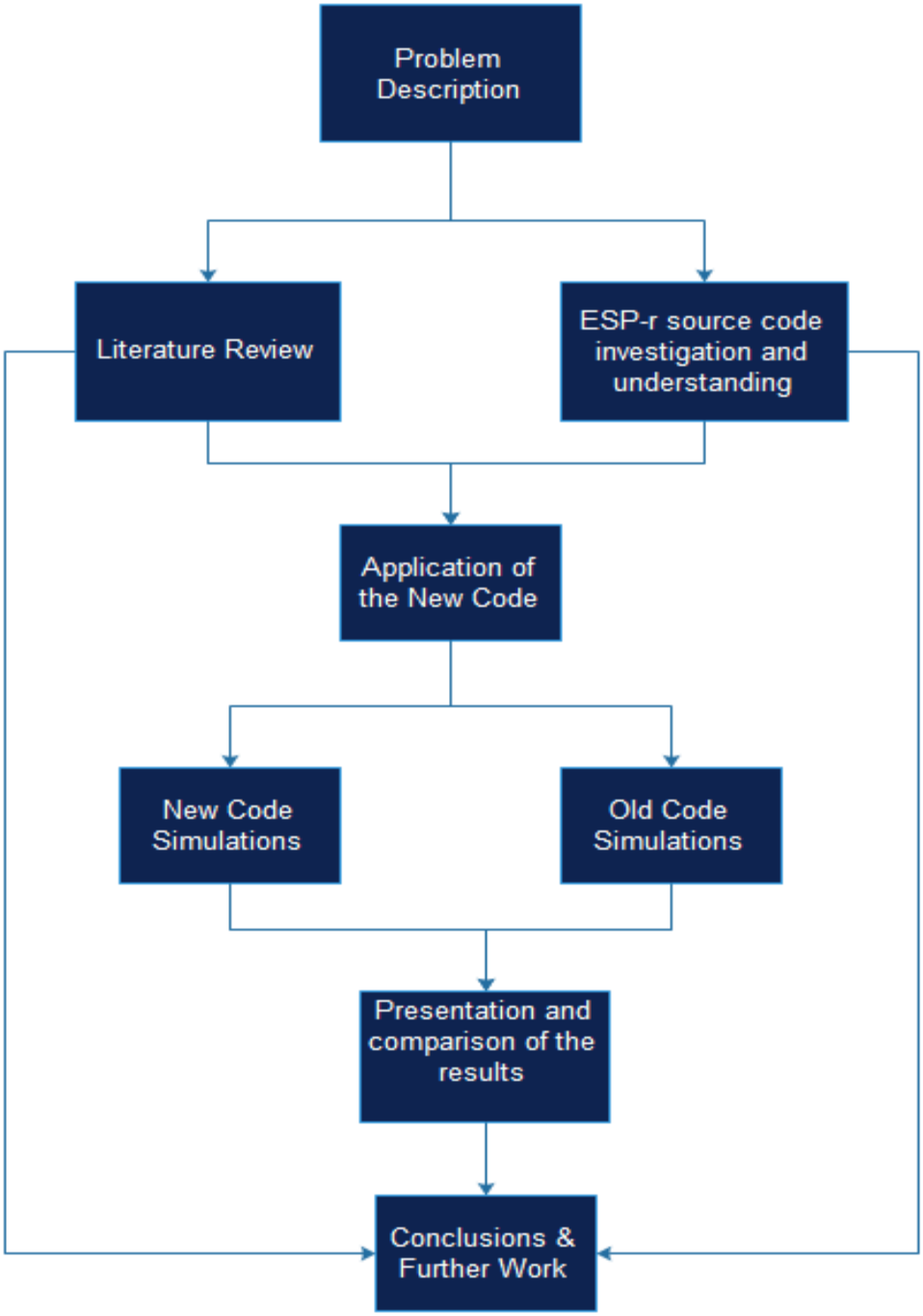

Figure 24 General methodology applied to the project.

4.2 Simulation methodology

There might be several ways of comparing the two codes through different sets of simulations. Therefore it is necessary to show the path, which has been chosen to compare the codes. Firstly, block diagram of simulation methodology will be presented (figure 25) and then each step will be briefly described to determine the purpose of chosen sets of simulations.

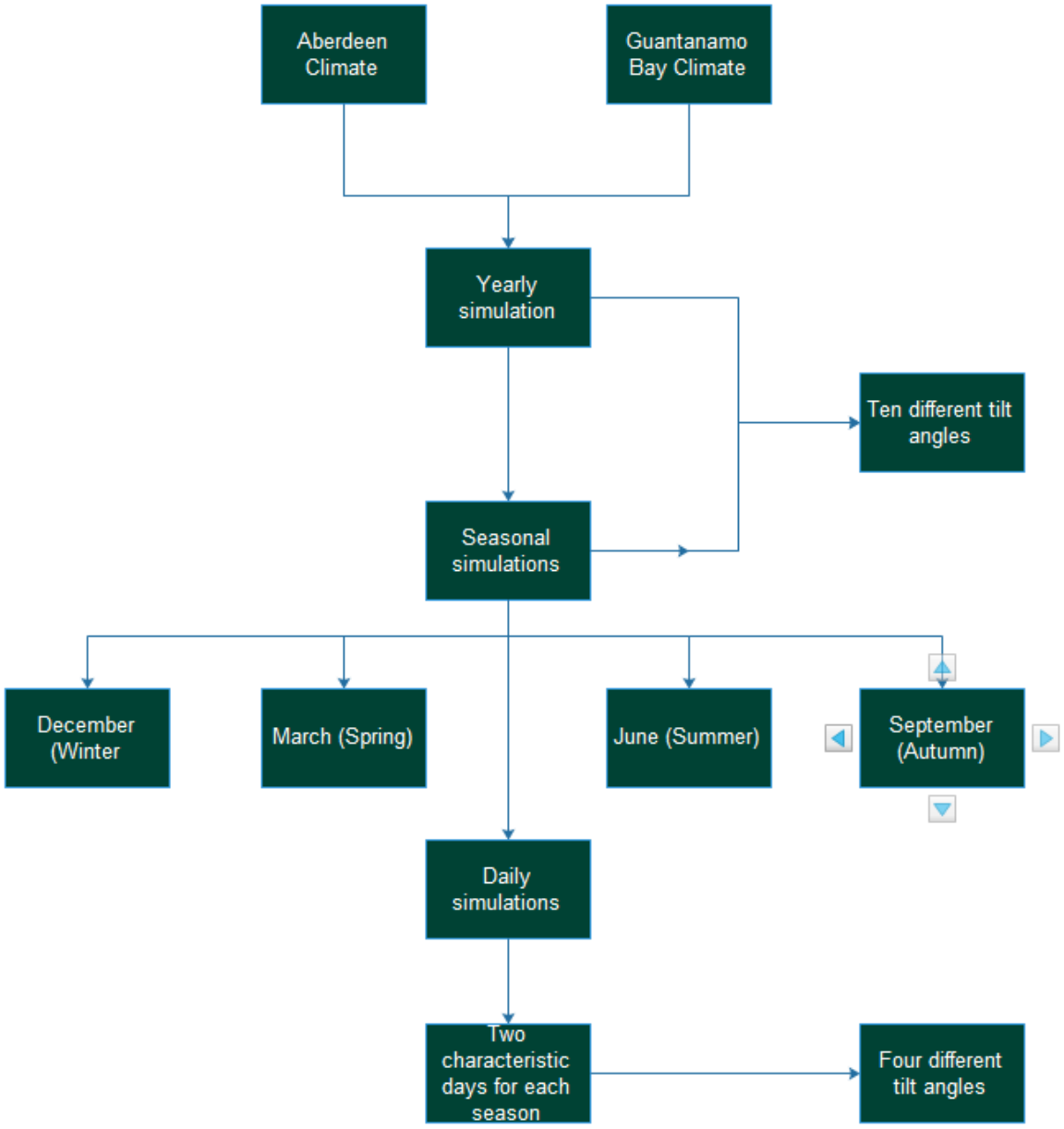

Figure 25 Simulation methodology applied to the project.

The above methodology of obtaining the data through simulations was applied to both, old and new code. The first factor determined for the simulations is a climate database. All the further simulations have been performed for two climate databases: Aberdeen and Guantanamo Bay. Once the climate has been applied, the first simulations have been run for the whole year for ten different tilt angles. Tilt angles were set from 0 ° to 90° and were linearly changed per 10° (0, 10, 20 … 90). Next step was to simulate the outputs for one month in each season for ten different tilt angles. Finally in order to show non averaged daily results of the simulations, two characteristic days have been picked for each season (cloudy day without intense direct beam radiation and a day with a clear sky and large direct radiation

values) and it has been investigated at four different tilt angles from 0° to 90° linearly changed per 30° (0, 30, 60, 90).

4.2.1 Climate zones chosen for simulations

Two climate zones have been chosen for validating the code:

- Aberdeen (57°10’N, 2°12’W)
- Guantanamo Bay (20°0’N, 75°7’E)

Both of these climate zones are in the northern hemisphere of the earth. This is convenient mainly because the seasons occur in the same periods in both of these climate zones.

Aberdeen climate represents quite far northern climate which has large amplitude in temperature and radiation levels over the whole year. Moreover the dependency of the tilt angle on the power output varies significantly over different seasons, due to different relative sun’s position.

Guantanamo Bay was chosen to contrast the issues for far northern climate and so compare how large are the differences in the two codes for a climate zone relatively close to the equator. The characteristics of this climate are: low amplitude in temperatures and radiation levels over the whole year, more stable relative suns position over the year and therefore wider range of universal tilt angles. (Due to this fact, some of the tilt angles are completely mismatched and might have large impact on the results but this will be included in the commentary.)

4.2.2 Periods and tilt angles chosen for the simulations

To have an overall look at the results and differences between them for the two codes a yearly simulations have been performed. The results obtained from simulations were averaged. The average didn’t include time steps where power outputs were equal 0, therefore it covers only the time of operation, which gives a better view on the results. Yearly simulation performed for ten different angles gave a general view on the tilt angle dependency on the differences between the two codes for given climate zones.

In order to investigate the differences more carefully, the simulations narrowed periods to one month of each season. Again the results were averaged for time steps when power output

appeared. This brings a closer view on seasonal impact on the two codes for given climates and allows understanding the yearly trends more closely. As for the yearly simulations ten different angles were put into analysis to have more data and broader view on the trends and tilt angle dependency on the codes.

The last simulations performed were daily simulations for two days of each season. The differences between codes have followed a different trend for cloudy days and days with a clear sky, therefore in order to investigate that issue, two days (cloudy and clear sky) have been picked for results presentation. Thus time average is not calculated because the purpose of these simulations was to analyse the behavior of examined values at each time step. This close analysis brings a detailed explanation what is actually happening for each code and what are the outcomes of it. Moreover it gave a better view on interpreting the yearly and monthly results. Due to large amount of daily data presented in tables the angle dependency has been narrowed to four different angles.

These three different approaches of presenting data can force misleading conclusions, therefore it is important to look at the results in iterative way and draw final conclusion which is supported by all the data simultaneously.

The same rule applies when comparing results for different tilt angles. The sun's relative position changes over the whole year, therefore some tilt angles may show higher differences between the codes due to low angle of beam incidence. Yearly view at different angle results may be misleading in drawing final conclusion; again it is important to iteratively look at the results for each angle. Moreover trends and magnitudes of differences caused by changing the tilt angle are crucial in final analysis. (I.e. for one climate large differences can occur only for one or two of the angles, while other climate may have lower magnitudes of result differences but closely distributed for each angle or large differences occur just for one season which further impact yearly results).

More simplistic view on the chosen periods and angles applied for each period is presented in table 4.

Table 2 Periods and corresponding angles used in simulations.

Investigated period	Investigated angle [°]									
One year	0	10	20	30	40	50	60	70	80	90
December (month)	0	10	20	30	40	50	60	70	80	90
March (month)	0	10	20	30	40	50	60	70	80	90
June (month)	0	10	20	30	40	50	60	70	80	90
September (month)	0	10	20	30	40	50	60	70	80	90
January (two days)	0			30			60			90
April (two days)	0			30			60			90
July (two days)	0			30			60			90
October (two days)	0			30			60			90

4.3 Simulation model

The model used for simulation was a slightly modified exemplar model representing two offices and a passageway with an integrated PV façade. In the simulations photovoltaic panel was moved from the bottom to the top position on the wall, so the model behaves more like a roof installed photovoltaic panel for lower tilt angles. Figure 26 presents the model used for simulations. Photovoltaic panel is in the rectangle area marked with red dots on its apexes. The picture to the right shows how tilt angle has been modified.

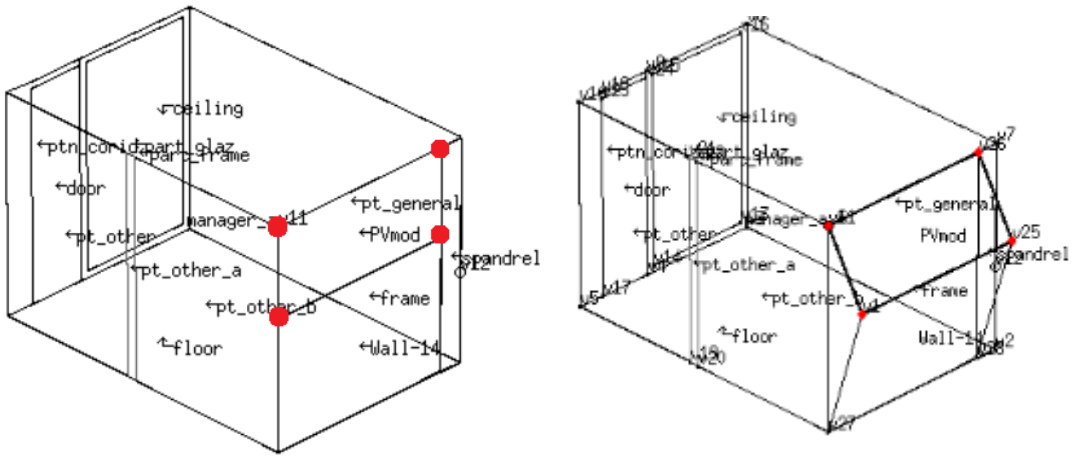

Figure 26 Model used for simulation.

The model and brand of photovoltaic panel which characteristic data has been used in simulation is presented below in table 5.

Table 3 Characteristics of photovoltaic panel used in simulations.

Model	Polycrystalline BP380
Open circuit voltage [V]	22,1
Short circuit current [A]	4,8
Voltage at maximum power point [V]	17,6

Current at maximum power point [A]	4,55
Cells in one panel	36 (in a 4x9 matrix connected in series)
Number of panels used in simulation	5
Dimensions per panel	Length: 1209mm Width: 537 mm Depth 50 mm
Area of one panel	0,649 m^2
Area of simulated array	3,246 m^2

Tilt angle adjustments were implied manually by changing vertex coordinates. To preserve dimensions of the array following set of assumptions and equations had to be implemented.

Moving bottom vertex in the (–y) direction elongated the array therefore area wouldn't be the same in each case. To prevent that from happening, the difference in Z direction between bottom and top vertexes has been calculated for each angle and applied in the program.

$$\sin\gamma = \frac{d_z}{L} \qquad (26)$$

$$d_z = \sin\gamma * L \qquad (27)$$

$\sin\gamma$ – Sin function of the tilt angle γ

L – Length of the photovoltaic array 1,209 [m]

d_z – Height difference (relative to vector [0,0,1]) [m]

With an increase of tilt angle, while length of the array remained constant, the height difference reduced. Described method allowed keeping the same area of the array during manual tilt angle adjustments.

5. RESULTS AND ANALYSIS

Results presented in this chapter will be divided for three different periods. A set of results will be shown for yearly period, monthly period and singular days. The most important values considered in the result analysis will be the differences between radiation and absorption ratio for new and old codes, differences between light generated current and its relation to the ratios, and also differences in power outputs. Analyzing these values separately for each code would produce too much data and could affect transparency of the work itself. Therefore percentage differences are used. Since the main difference in the codes lays in different ratio used for light generated current calculations, most focus will be put into investigating these ratios and their behaviors for two previously described climate zones and several tilt angles. Data which could affect transparency of the thesis and would take too much space will be placed into appendices.

5.1 Yearly results

In this section a set of yearly results will be presented in order to compare the two codes. Firstly yearly results of Aberdeen climate will be shown, which will include: differences in ratios, light generated currents and power outputs for the two codes, followed by a set of graphs representing trends formed by the ratios from the two codes in relation to tilt angle. Similar set of data will be presented for Guantanamo Bay climate further in this subchapter. Both data will be covered with a commentary to the results. Further a relation between power output and current will be presented and explained. At the end general information will be gathered and summed up to form a base for further conclusions once all the results will be analysed.

5.1.1 Yearly results for Aberdeen climate

Comparison of the average yearly results from the simulations performed on the old code and new code for Aberdeen climate are presented in Table 6. Negative values stand for higher outputs for new code simulations.

Table 4 Yearly percentage differences between codes for investigated values (Aberdeen Climate).

Tilt angle [°]	Difference in ratios [%]	Difference in light generated current [%]	Difference in power output [%]
0	0,9075	0,9077	0,9480
10	0,3550	0,3561	0,3709
20	-0,1644	-0,1636	-0,2440
30	-0,5550	-0,5550	-0,6754
40	-0,8375	0,8197	-0,9777
50	-1,0540	-1,0515	-1,2224
60	-1,2660	-1,2707	-1,4641
70	-1,4852	-1,4860	-1,7078
80	-1,6557	-1,6531	-1,8926
90	-1,7469	-1,7522	-1,9895

The difference in ratios (radiation ratio for old code, absorption ratio for new code) is followed by almost similar changes in the light generated current, with very minor differences which indicates an assumption that light generated current depends only on the ratio provided.

The fact that power output differences are noticeable higher than differences between ratios and currents is because power output also depends on a voltage, which slightly changed due to fact that for a modified geometry average temperature of the panel changed for yearly simulation and according to equations 17-21 voltage values depend on panel temperature.

For flat positioned panel the outputs are higher for the old code (around 0,9% in ratio difference per year), with the increase of tilt angle it can be noticed that the difference drops quickly and at 20° tilt angle new code outputs overgrow the old code results. With the further increase of tilt angle the differences in outputs become bigger reaching maximum for photovoltaic façade configuration (90°). The growth of difference in outputs is not linear. Figure 27 presents the trend of absorption and radiation ratio depending on the tilt angle.

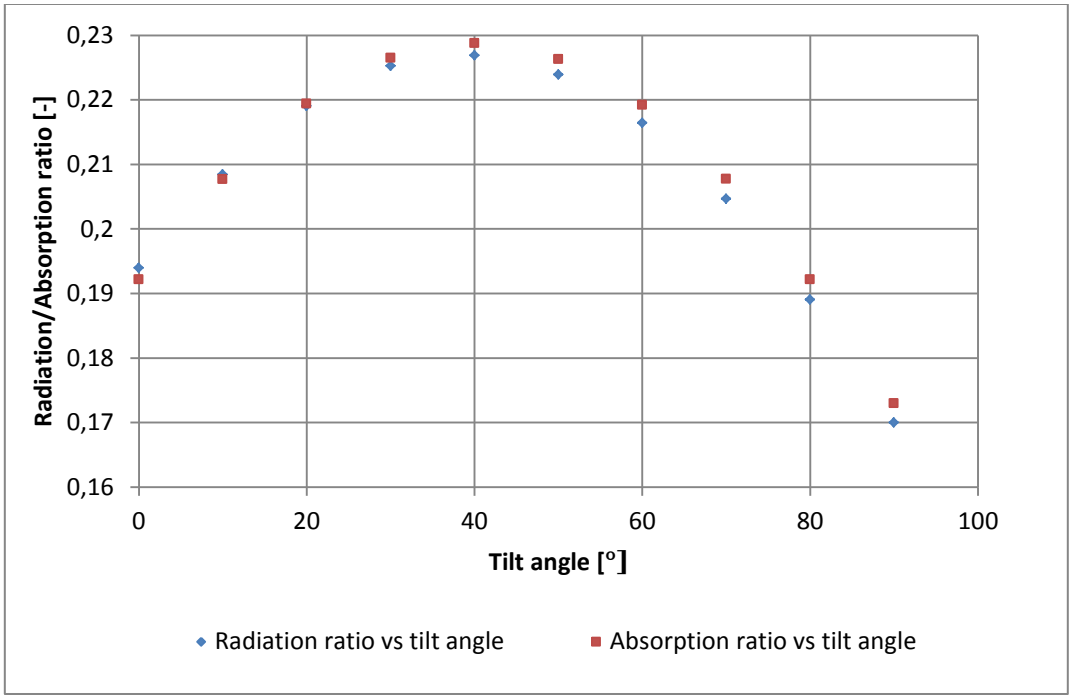

Figure 27 Yearly average radiation and absorption ratios vs tilt angle (Aberdeen climate).

The above figure not only presents the trend of the ratios vs tilt angle but also the differences between radiation and absorption ratios can be easily spotted in a similar trend to the values in tables. At the beginning radiation ratio overgrows absorption ratio, this changes around 20° tilt angle and then with an increase of tilt angle the difference gets higher (graph markers are further away for each angle).

Figures 71 and 72 confirm that the general trend is the same for light generated current and photovoltaic power output in relation to tilt angle.

5.1.2 Yearly results for Guantanamo Bay climate

Comparison of the average yearly results from the simulations performed on the old code and new code for Guantanamo Bay climate are presented in Table 7.

Table 5 Yearly percentage differences between codes for investigated values (Guantanamo Bay climate).

Tilt angle [°]	Difference in ratios [%]	Difference in light generated current [%]	Difference in power output [%]
0	1,0908	1,0910	1,1589
10	0,7532	0,7534	0,7888
20	0,6332	0,6224	0,6424
30	0,6362	0,6647	0,6826
40	0,8615	0,8976	0,9555
50	1,4004	1,4132	1,5994
60	2,2963	2,2675	2,5725
70	3,4266	3,3921	3,8215
80	4,1640	4,1658	4,6699
90	3,6895	3,6423	4,1517

Yearly output differences for Guantanamo Bay climate differ significantly from Aberdeen's differences in magnitudes. The first noticeable difference is that for Guantanamo climate there isn't any tilt angle at which the new code results are higher than the old code outputs. The differences between ratio and light generated current differences aren't significantly high, which is the same as it was in the previous example. The same rule applies to photovoltaic output differences, these are higher due to the fact that panel temperature have changed due to geometry modifications which influenced voltage and therefore PV output.

Another common thing between the two climates is the general trend. None of the values changes linearly in relation to the angle. The curve again takes shape similar to a quadratic function. Figure 28 shows the trend for Guantanamo Bay.

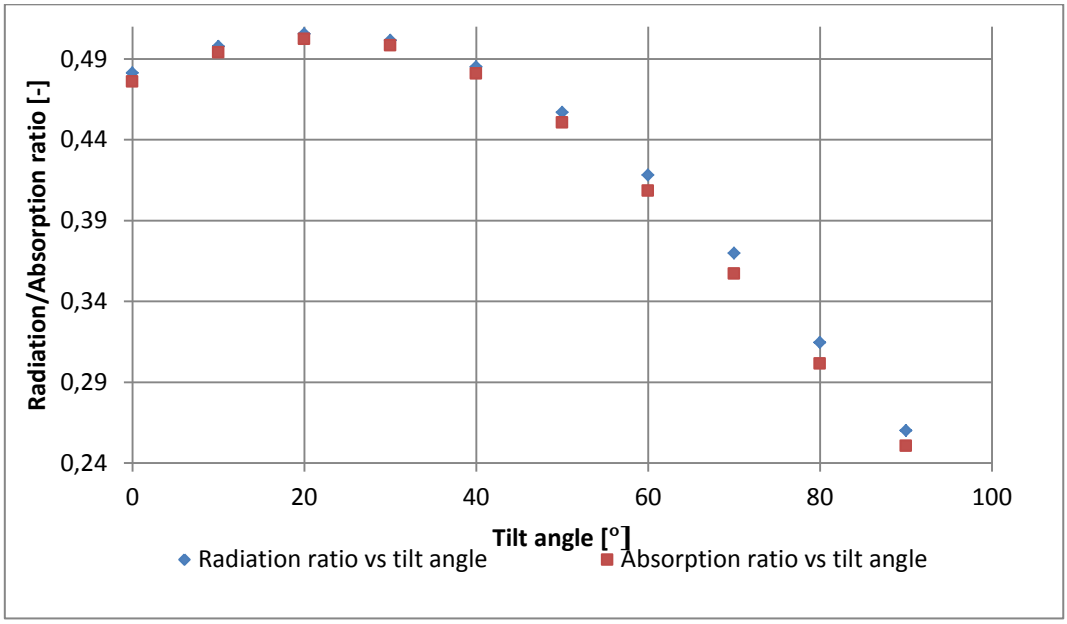

Figure 28 Yearly average radiation and absorption ratios vs tilt angle (Guantanamo Bay climate).

The differences between ratios also follow similar trend. As in the previous case at the beginning the differences are becoming smaller with the growth of angle and after reaching a given point the differences are starting to grow again with tilt angle. The difference for Guantanamo results is that the maximum difference magnitudes were obtained at 80° tilt angle and it dropped at 90°, while for Aberdeen the difference magnitudes were raising with angle without an exception.

Figures 73 and 74 confirm that the general trend is the same for light generated current and photovoltaic power output in relation to tilt angle.

5.1.3 Power to current trends for both climates

To investigate how voltage influenced the power output a power vs current characteristics have been created.

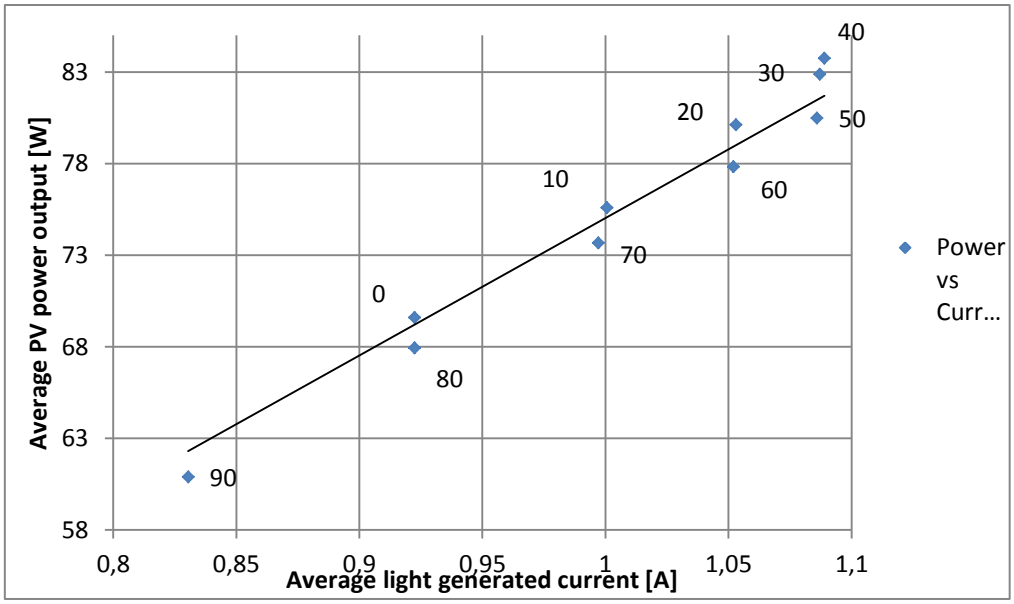

Figure 29 Yearly average power vs current at different tilt angles (Aberdeen climate).

The numbers next to the results indicate tilt angle at which the result has been obtained. The overall trend looks linear, nevertheless an interesting fact is easily noticeable. For angles higher or equal 50° the outputs seem to be beneath the trend, while for the first five angles from 0° to 40° values are above the trend line. Moreover pairs like (0, 80), (10, 70), (20,60), (30, 50) are almost at the same light generated current values, but the outputs are different. This can mean that the changes in geometry influenced the panel temperature, which slightly modified voltage and then affected power output.

Same analysis has been created for Guantanamo climate.

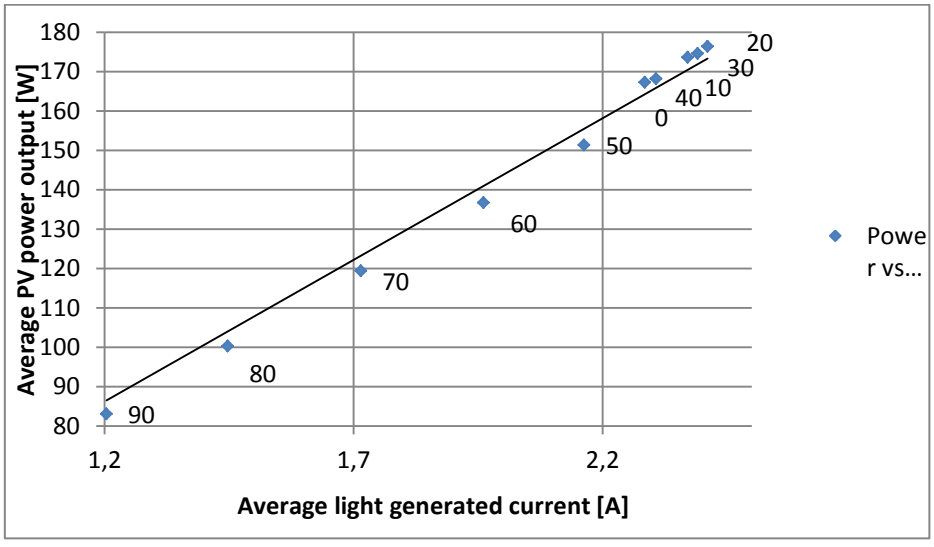

Figure 30 Yearly average power vs current at different tilt angles (Guantanamo Bay climate).

Similar trend can be observed on this graph, indicating that values obtained for tilt angles higher or equal 50° are slightly below the trend line. The difference in distribution of certain outputs between the two charts is caused by different results and shape of relations between the investigated output values and tilt angle.

5.1.4 Yearly results – discussion

Yearly analysis has shown different results for Aberdeen and Guantanamo climates. The old code seems to have lower values of radiation ratio, light generated current and power output than the new code for Aberdeen climate. Maximum difference in outputs occurs for façade integrated PV array and equals consecutive for ratios, light generated currents and power outputs: -1,747%; -1,7522%; -1,9895%. According to (Boxwell, 2015) the range of optimal angles for Aberdeen climate would be from 34° to 80° depending on when the power from photovoltaic devices is needed the most. In this optimal range the differences in yearly output between the codes would be in range approximately 1%-1.9% higher for the new code.

Guantanamo climate result differences were always higher for old code simulation and they grew until achieving values of 4,164%; 4,166%; 4,67% for tilt angle 80°. Optimal angles for Guantanamo climate are in range from -4° to 44° (Boxwell, 2015) which indicates that for optimal angles the differences in yearly output would vary in range from 0,64%-1,16%, higher for the old code.

Power output in relation to current in both cases has shown that for tilt angles equal or over 50° power outputs are below the trend line, which indicates changes in voltage that could be explained by the panel's temperature slight change with the modification of model's geometry.

General yearly output gave an overall view on yearly trends and differences between the codes. Considering the whole set of tilt angles, larger yearly differences occur for Guantanamo Bay climate, although if we look at optimum angles Aberdeen climate shows higher differences between the codes. The main difference between the climates is that for Guantanamo Bay the investigated values appear to be higher for old code, while for Aberdeen in most configurations the new code values overgrow the ones simulated with the old code.

5.2 Monthly seasonal analysis

The main focus of this subchapter is put into how differences between codes change in relation to given season for investigated climates. For each characteristic month of a given season, simulations have been performed for the new and old code at ten different tilt angles. Moreover, analyzing differences between codes for multiple tilt angles at each season can give a better view on yearly outputs presented in the previous subchapter.

For each season and climate zone relation between the radiation and absorption ratio to tilt angle will be presented in order to monitor trends for different seasons, compare them with yearly trends and have a better view on optimum angles.

5.2.1 Winter results for Aberdeen climate (December)

Comparison of the differences of average results obtained for old and new codes is presented in table 8.

Table 6 Percentage differences between codes for investigated values in December (Aberdeen climate).

Tilt angle [°]	Difference in ratios [%]	Difference in light generated current [%]	Difference in power output [%]
0	-0,24061	-0,25586	-0,21416
10	-0,843501	-0,81607	-0,921029
20	-1,10843	-1,10442	-1,25788
30	-3,17298	-3,11168	-3,51449
40	-3,99274	-3,98866	-4,49689
50	-4,25354	-4,23758	-4,76186

60	-4,26204	-4,29135	-4,80436
70	-4,45469	-4,41388	-4,92876
80	-4,5977	-4,62815	-5,16251
90	-4,86275	-4,85294	-5,41278

Looking at the monthly differences between the codes, similar relations can be noticed as for yearly analysis. Ratio differences doesn't differ much from light generated current differences, while power output differences are slightly higher in most cases. General trend for winter simulation shows that from 0° to 90° tilt angle differences in results between the codes is constantly increasing. The magnitudes are higher than the ones for yearly output, which indicates that winter is a crucial season for Aberdeen climate in comparison between the codes. All the average values obtained for winter season are higher for new code simulations.

The trend of ratios related to tilt angle is presented on figure 31

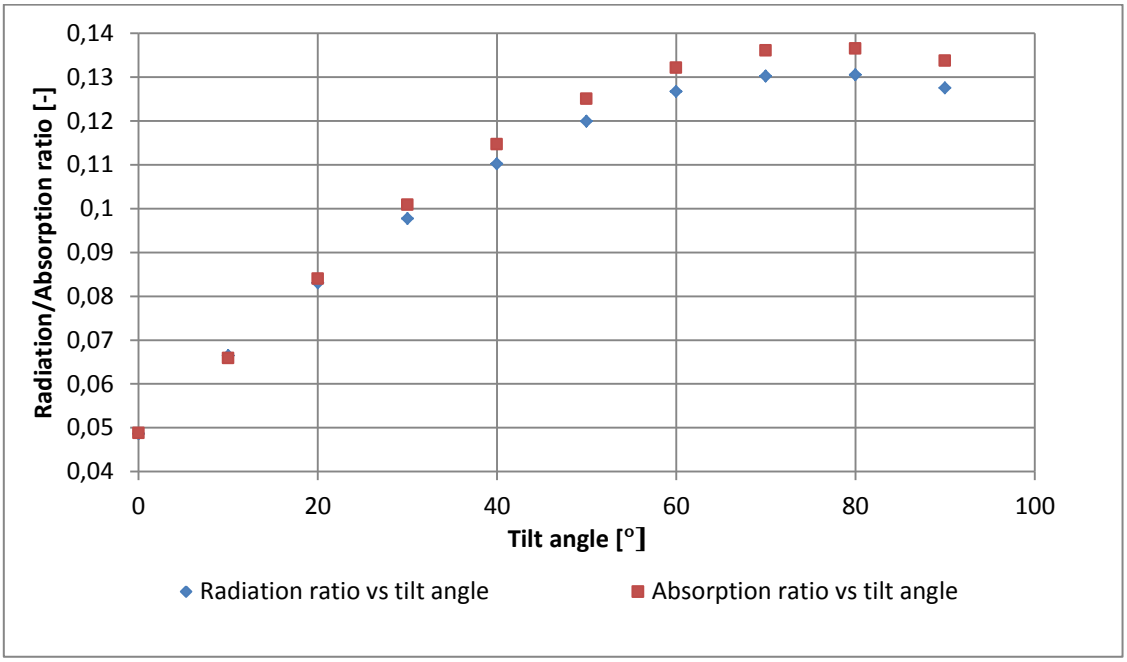

Figure 31 Average radiation and absorption ratios vs tilt angle in December (Aberdeen climate).

The highest ratio (and therefore power output) in both cases is obtained at tilt angle of 80°, which is confirmed as the most optimum angle for Aberdeen in December. (Boxwell, 2015).The gaps between markers are constantly increasing which confirms the previously commented trend of value differences between the codes.

5.2.2 Winter results for Guantanamo Bay climate (December)

Comparison of the differences of average results obtained for old and new codes is presented in table 9.

Table 7 Percentage differences between codes for investigated values in December (Guantanamo Bay climate).

Tilt angle [°]	Difference in ratios [%]	Difference in light generated current [%]	Difference in power output [%]
0	-0,52016	-0,48754	-0,64873
10	-1,65289	-1,6517	-1,91224
20	-2,10084	-2,06293	-2,38501
30	-2,35709	-2,35886	-2,6773
40	-2,60962	-2,55272	-2,85063
50	-2,70997	-2,58276	-2,95105
60	-2,73513	-2,72059	-3,08394
70	-2,76861	-2,75019	-3,12518
80	-2,66876	-2,6574	-3,00898

90	-1,67282	-1,67497	-1,86866

The differences in results obtained for Guantanamo climate are smaller in winter than for Aberdeen climate. Although this time for both climate zones new code results are bigger than the old code outputs. The trend of differences in results related to tilt angle is slightly different than for Aberdeen climate. The differences grow from 0° until 70° and then suddenly drop at 90° by 1% for 10° difference between 80° and 90° tilt angle.

Trend of ratios in relation to tilt angle is presented at the figure 32:

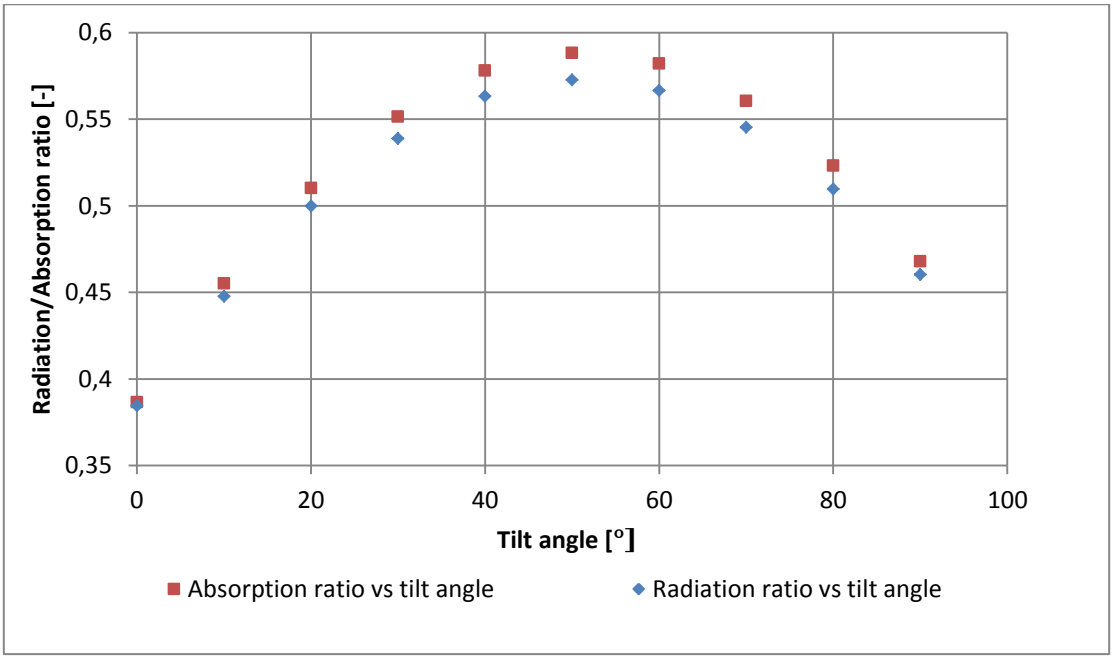

Figure 32Average radiation and absorption ratios vs tilt angle in December (Guantanamo Bay climate).

Similar as for Aberdeen climate, the highest ratio and output represents the most appropriate angle for given climate zone in December. New code results appeared to be higher in December for Guantanamo climate, relating it with the yearly output where for every tilt angle differences are higher for old code it means that winter outputs for Guantanamo climate doesn't influence the yearly output as much as the other seasons.

5.2.3 Spring results for Aberdeen climate (March)

Comparison of the differences of average results obtained for old and new codes is presented in table 10.

Table 8Percentage differences between codes for investigated values in March (Aberdeen climate).

Tilt angle [°]	Difference in ratios [%]	Difference in light generated current [%]	Difference in power output [%]
0	1,174497	1,165501	1,162791
10	-0,34619	-0,30896	-0,46923
20	-1,21786	-1,2218	-1,42733
30	-1,69492	-1,67549	-1,88006
40	-1,87144	-1,86441	-2,12743
50	-2,08167	-2,08507	-2,37284
60	-2,29746	-2,267	-2,60474
70	-2,49066	-2,50865	-2,82223
80	-2,71572	-2,64599	-3,05196
90	-2,94257	-2,96736	-3,29337

For spring period differences between codes in Aberdeen climate follow similar trend as in winter with one exception. The magnitudes for flat PV array (0°) are different from further tilt angles trends and indicate around 1,16% higher power output for old code. Further differences in investigated values are increasing with tilt angle up to around 3,3% higher power output for the new code.

The relation between ratios and tilt angle for both codes is presented on figure 33

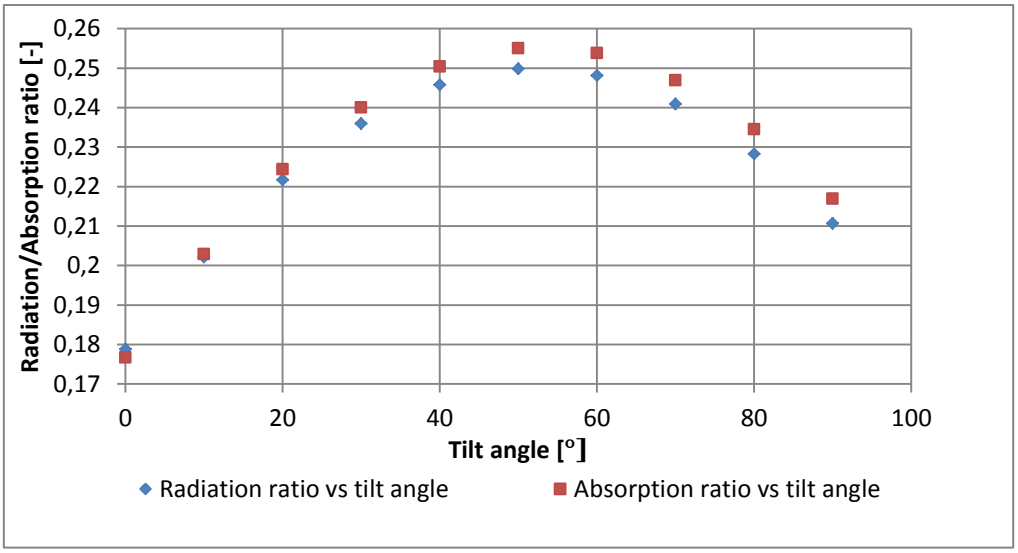

Figure 33Average radiation and absorption ratios vs tilt angle in March (Aberdeen climate).

Again as for winter simulation the ratios vs tilt angle graph shows the highest ratio closely to the most optimum angle for spring period (57° for Aberdeen) (Boxwell, 2015). The graph forms shape close enough to quadratic function as it was in previous cases.

5.2.4 Spring results for Guantanamo Bay climate (March)

Comparison of the differences of average results obtained for old and new codes is presented in table 11.

Table 9 Percentage differences between codes for investigated values in March (Guantanamo Bay climate).

Tilt angle [°]	Difference in ratios [%]	Difference in light generated current [%]	Difference in power output [%]
0	1,058801	1,059556	1,12673
10	0,743158	0,755287	0,798187
20	0,63358	0,623396	0,646357
30	0,650535	0,694191	0,734816

40	0,824521	0,85885	0,874591
50	1,147911	1,109804	1,240681
60	1,731161	1,839295	2,023659
70	3,390216	3,412322	3,737781
80	6,259947	6,246545	6,872719
90	10,30422	10,29312	11,33793

The magnitudes of differences between codes for Guantanamo climate in March are varying significantly with tilt angle. In region between 0° until 50° the differences aren't that large (in range 0,65%-1,24% higher power output for old code). Nevertheless for each increase of tilt angle by 10° further than 50° induces way larger differences between the codes, reaching 11,33 % higher output for old code at 90° tilt angle. These high differences are caused by the fact, that tilt angles from 60° to 90° are highly inefficient for this climate zone. Incident radiation values are relatively large, but poor angle adjustment causes high reflection losses causing the absorption values way lower than expected.

The graph representing relation between the ratios and tilt angle is presented below:

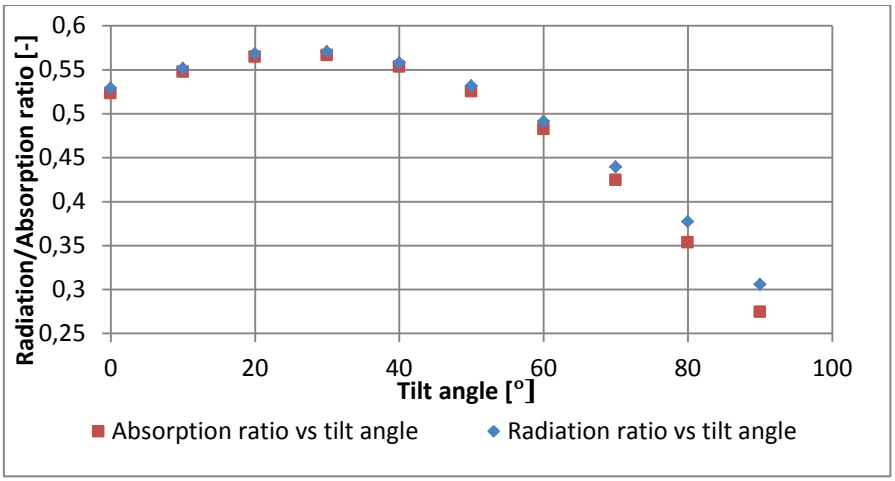

Figure 34 Average radiation and absorption ratios vs tilt angle in March (Guantanamo Bay climate).

The differences between radiation and absorption ratios can be easily noticed for higher angles of incidence. The ratio values form quadratic function shape as for each analysis, the apex of this hypothetical quadratic function is around the 20° tilt angle, which again confirms the most optimum angle in March for Guantanamo Bay climate.

5.2.5 Summer results for Aberdeen climate (June)

Comparison of the differences of average results obtained for old and new codes is presented in table 12.

Table 10 Percentage differences between codes for investigated values in June (Aberdeen climate).

Tilt angle [°]	Difference in ratios [%]	Difference in light generated current [%]	Difference in power output [%]
0	1,187384	1,160093	1,219512
10	1,048825	1,055011	1,07846
20	0,898311	0,973054	0,963429
30	0,800582	0,788476	0,84712
40	0,713749	0,782473	0,752577
50	0,593589	0,659522	0,625142
60	0,511291	0,44405	0,503376
70	0,422734	0,391773	0,420282
80	0,532198	0,443951	0,555384

90	0,746733	0,751782	0,85284

The differences between the codes for June submit a slightly different trend than for previous months. First of all it appears that values obtained for old code overgrow the new code values. This indicates that absorption ratio becomes lower with the increase of radiation ratio, which could mean larger reflection losses at some of the day periods. From 0° tilt angle until 70° the differences between the codes are getting smaller and for the last two tilt angles they start increase again. Nevertheless there isn't any value that highly differs from the rest. The results for June look relatively similar for every angle, comparing to other months. The fact that values are higher for old code opposes the general yearly trend for Aberdeen climate, where new code values overgrow the old code.

The relation between ratios and tilt angle is presented on the figure 35:

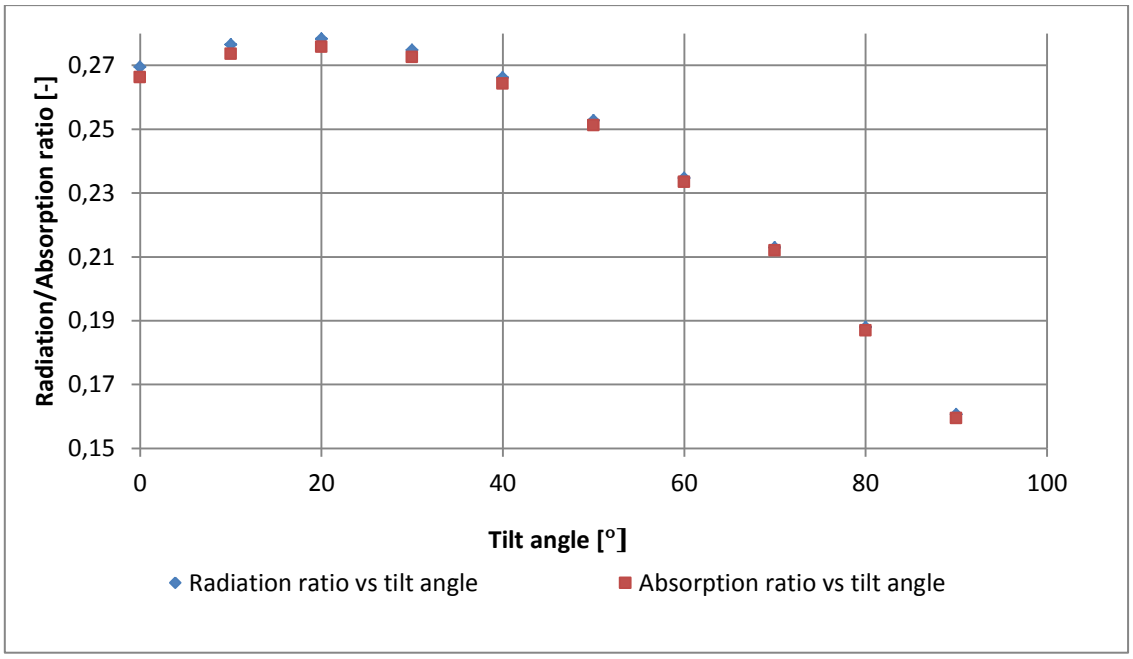

Figure 35 Average radiation and absorption ratios vs tilt angle in June (Aberdeen climate).

The shape of this graph is slightly different than the ones formed for previous months. At the beginning it follows the shape of quadratic function, although from 40° tilt angle onwards the shape forms more like a linear trend. Another thing which is different than for the other months is that the highest ratio wasn't obtained close to the most optimum tilt angle, which is 34° for this case, while highest ratios were at 20° tilt angle.

5.2.6 Summer results for Guantanamo Bay climate (June)

Comparison of the differences of average results obtained for old and new codes is presented in table 13.

Table 11 Percentage differences between codes for investigated values in June (Guantanamo Bay climate).

Tilt angle [°]	Difference in ratios [%]	Difference in light generated current [%]	Difference in power output [%]
0	1,949803	1,944685	2,002377
10	2,118366	2,138308	2,329357
20	2,423677	2,427184	2,660532
30	3,05499	3,023873	3,354481
40	4,396552	4,371257	4,849485
50	6,572295	6,601124	7,304761
60	10,09975	10,12987	11,25398
70	13,43202	13,37143	14,96488
80	9,275136	9,2827	10,42563
90	-1,90476	-2,38095	-2,66387

The differences between codes for Guantanamo Bay climate in June are following totally different trend than in Aberdeen case. Moreover values are varying significantly for each 10° increase of tilt angle. The lowest differences are for flat PV array and façade, the difference

between these cases is the fact that for 0° case values obtained for old code are higher than the ones for the new code, while in façade case it's the opposite. The highest differences are obtained consecutive for angles 80°, 60°, 70°. Maximum difference in power output reaches almost 15%, which indicates very large difference between the codes and these results definitely affect yearly average. Interesting fact is that every time a large difference occurs for Guantanamo climate, the corresponding incident angle is far from optimal angle. This may imply that the reflection losses become very large for inefficiently adjusted angles in such climate zone.

The relation between ratios and tilt angle is presented on the figure 36:

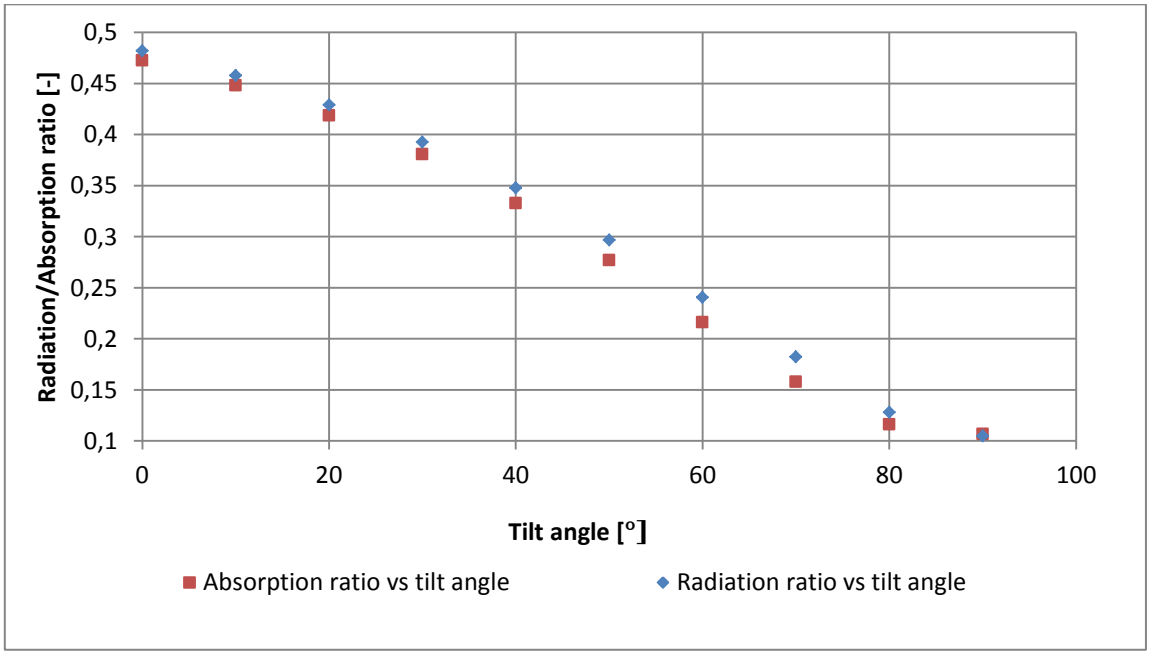

Figure 36 Average radiation and absorption ratios vs tilt angle in June (Guantanamo Bay climate).

The above trend seems to be very different from the ones presented on yearly analysis or different months. The trend is more similar to linear function than quadratic one. The differences in ratios are highly visible in the range 50°-80° tilt angles. The most optimum angle for Guantanamo climate in summer is -4° and in fact flat position (0°) which is the closest to optimum from analysed tilt angles has the higher output.

5.2.7 Autumn results for Aberdeen climate (September)

Comparison of the differences of average results obtained for old and new codes is presented in table 14.

Table 12 Percentage differences between codes for investigated values in September (Aberdeen climate).

Tilt angle [°]	Difference in ratios [%]	Difference in light generated current [%]	Difference in power output [%]
0	0,355872	0,497238	0,584112
10	-0,09877	-0,10284	-0,17806
20	-0,51716	-0,48972	-0,66311
30	-0,77697	-0,7619	-0,90875
40	-0,95195	-1,0397	-1,13892
50	-1,19266	-1,18479	-1,37573
60	-1,42045	-1,48075	-1,64001
70	-1,69745	-1,70567	-1,93319
80	-1,99246	-1,98586	-2,27973
90	-2,2646	-2,36025	-2,60542

September analysis for Aberdeen climate has similar trend to spring outcomes as expected. The differences between the codes are lower for September than March. The only configuration when old code values are higher is flat positioned PV array, rest of the results show that new code gives higher values. The highest differences are for façade configuration, same as for winter and spring periods. Magnitudes of differences in autumn aren't out of norm for any tilt angle and preserve fairly linear trend.

The relation between ratios and tilt angle is presented on the figure 37:

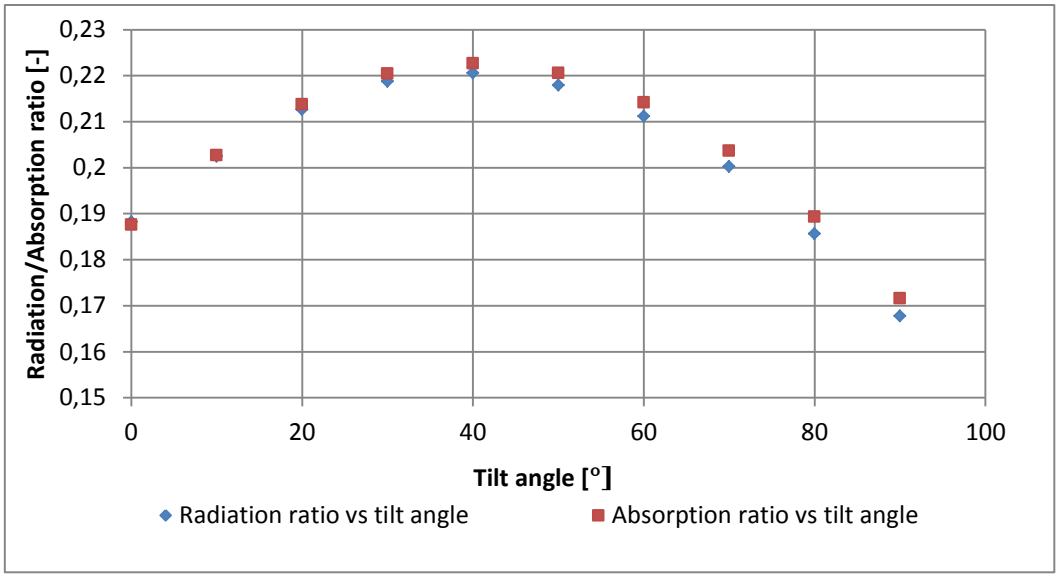

Figure 37 Average radiation and absorption ratios vs tilt angle in September (Aberdeen climate).

Figure 37 presents similar shape as in the spring analysis. The difference is that the graph looks like slightly moved closer to the Y axis. The values form previously noticed trend for most of the ratios to tilt angle graphs (except June's relation).

5.2.8 Autumn results for Guantanamo Bay climate (September)

Comparison of the differences of average results obtained for old and new codes is presented in table 15.

Table 13 Percentage differences between codes for investigated values in September (Guantanamo Bay climate).

Tilt angle [°]	Difference in ratios [%]	Difference in light generated current [%]	Difference in power output [%]
0	1,542416	1,524516	1,648568
10	1,355276	1,331182	1,432507
20	1,330505	1,325674	1,411312
30	1,456406	1,435603	1,54295

40	1,773196	1,761168	1,895009
50	2,311111	2,296296	2,540142
60	3,537853	3,530928	3,917405
70	5,814953	5,847255	6,459795
80	9,351012	9,353877	10,34696
90	13,16271	13,12381	14,59984

The differences in September follow the trend of March results, although on the contrary to Aberdeen climate, the differences in September are higher between the codes than in March. The usual trend for Guantanamo Bay climate can be noticed, that for non-optimum tilt angles the differences are huge and reaching 14,6% difference in power output at 90° tilt angle. This fact will be explained later in this chapter. For every tilt angle values of the old code overgrow the new code values.

Radiation and absorption ratios in relation to tilt angle are presented on the figure 38:

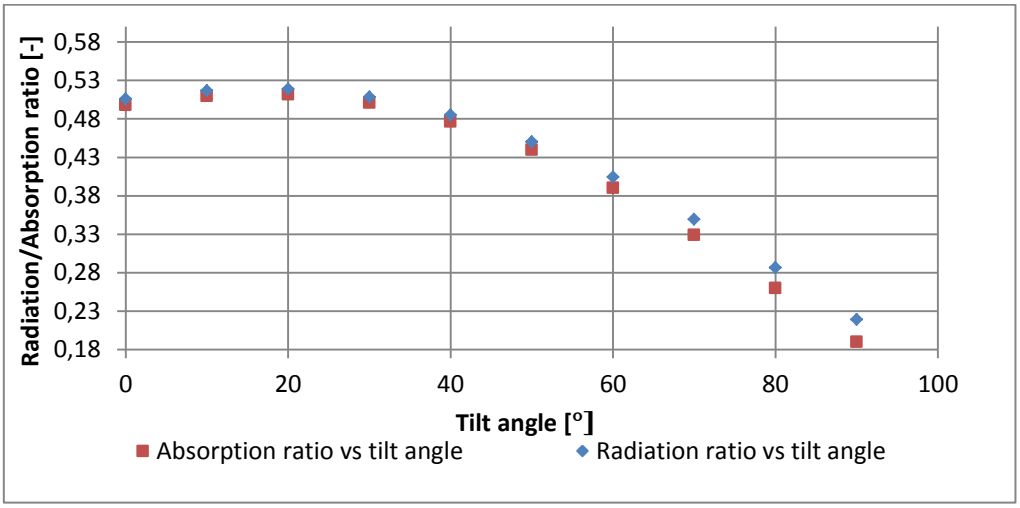

Figure 38 Average radiation and absorption ratios vs tilt angle in September (Guantanamo Bay climate).

Figure 38 presents the usual trend without any unexpected behaviors. Differences between ratios are highly noticeable especially for high tilt angles.

5.2.9 Monthly (seasonal) results – discussion

For Aberdeen climate the monthly analysis appeared to be very stable in trends. The differences between the codes were changing fairly linear with the increase of tilt angle and for three out of four months have shown a maximum difference values for façade configuration. The biggest differences have been spotted for winter period when the sun's position is the lowest. Except June's analysis the values for new code were higher than the ones for the old code. This can be explained by the fact that for larger direct beam radiation for time steps when incident angle becomes small, the reflection losses become significant enough to create visible difference between the codes.

The fact that the differences between the codes aren't extremely large for any tilt angle is due to the large relative displacement of sun and its path over the whole year, which doesn't really allow for any extreme tilt angle (among investigated ones). Maximum values for radiation and absorption ratios for every month were approximately close to the most optimum tilt angle for a given season. Light generated current and power output trends have similar shape therefore only ratio relations have been shown.

The case in Guantanamo Bay climate appeared different. The trends of ratio relations to tilt angle were fairly stable except the summer one, which was closer to linear shape than quadratic function, although if more angles would be considered it may have shown more quadratic shape. The differences values in most cases, (except winter results) were on average larger than in Aberdeen climate, and have proven to give higher outputs for old code with radiation ratio. Interesting fact has been noticed, that for non-optimum tilt angles the differences between the codes were extremely large in comparison to the optimum tilt angles. This can be explained by the fact that sun's path over the whole year for Guantanamo Bay is relatively stable and doesn't vary much (82° east of due south in December and 100° east of due south in June). Significantly large differences between the codes for large tilt angles (60°-90°) influenced yearly output differences, which were relatively large for these angles.

Comparing the two climates it can be noticed that Aberdeen climate's results are fairly stable without extreme differences for different tilt angles. If optimum angles would be considered

in analysis it could be noticed that the differences between the codes for Aberdeen climate are on average higher than for Guantanamo Bay. Another difference is the fact that in three out of four months Aberdeen analysis gave results higher for the new code, which is the opposite for Guantanamo case. It follows to a conclusion that absorption doesn't grow linearly with radiation levels and less amount of radiation becomes absorbed for larger radiation intensity levels. This could be linked with the temperature of the climate and the way it's used for absorption calculations.

5.3 Daily analysis

To investigate the differences between the two codes in more detail, a set of simulations has been performed. For each season and climate, two days have been picked. One day represents the most cloudy day for a given climate and season. The other represents the brightest day with a clear sky for a given climate and season. Analysis whether the day is cloudy or not was performed based on radiation ratio analysis. Since the denominator is constant, the higher the ratio is, the higher the direct beam radiation occurs. In the analysis following sets have been prepared:

Table 14 Periods chosen for daily analysis (Aberdeen climate).

Aberdeen Climate							
Winter (January)		**Spring (April)**		**Summer (July)**		**Autumn (October)**	
Cloudy day	Bright day	Cloudy day	Bright day	Cloudy day	Bright day	Cloudy day	Bright day
03.01	01.01	02.04	03.04	03.07	05.07	07.10	02.10

Table 15 Periods chosen for daily analysis (Guantanamo Bay climate).

Guantanamo Bay Climate							
Winter (January)		Spring (April)		Summer (July)		Autumn (October)	
Cloudy day	Bright day	Cloudy day	Bright day	Cloudy day	Bright day	Cloudy day	Bright day
04.01	01.01	01.04	06.04	06.07	07.07	07.10	01.10

Each day's output has been simulated for four different tilt angles: 0°, 30°, 60°, 90°. This is to monitor daily differences for multiple tilt angles in order to have a better view on average results versus angle in monthly and yearly analysis.

5.3.1 Aberdeen climate daily analysis

Winter

Data for winter days (Figures 39, 40, 41, 42, Table 19)

The two winter days analysed for Aberdeen climate have shown similar tendency for bright and cloudy day. For 0° tilt angle the trend for bright day was different from other tilt angles. The difference between ratios was favorable for old code (higher output values for old code). With the increase of tilt, trend of sunny days became similar to cloudy day's trend and the only further dissimilarity was an increase of magnitude of ratios difference for higher angles.

Cloudy day preserved trend for each angle. Although magnitudes of ratio differences between codes changed. For flat positioned PV array differences for each times step are implying higher values for the old code. The same situation applies for 30° and 60° tilt angles although the differences between the values are reducing. At 90° the magnitudes of ratio differences became negative, which implies that outputs of the new code became higher. This can be noticed at figure 42.

For bright day the situation looks slightly different when analyzing values. Only for 0° tilt angle magnitudes of ratio differences are higher in favor of old code. For next three tested tilt

angles large differences can be spotted, (around 6% in ratio difference) and values obtained by new code became significantly higher. Comparing these results with the average obtained for December, it can be noticed that bright days have main influence especially for higher tilt angles on the average differences between the codes outputs. For 30° tilt angle it is visible that cloudy day possesses opposite trend, which temper a bit the winter's average.

Spring

Data for spring days (Figures 47, 48, 49, 50, Table 23)

The situation and trends in chosen spring days form fairly stable shapes, which don't change a lot with an increase of tilt angle. The situation is similar to winter analysis, nevertheless the main difference is that for early and late time steps (sunrise, sunset) the old code values become significantly bigger than new code values (6%-12% over 3-5 time steps). This is the cause of optical losses, with low sun's position. During sunrises and sunsets incident radiation approaches the array at low angles of incidence, causing large losses due to beam reflections. For time steps while sun's position is fairly high, the scenario changes and the new code values become significantly higher than the old code values. Since at these time steps the power output is most significant, then the overall spring average has proven to give higher outputs for the new code.

The analysis for the cloudy day is almost exactly the same as for winter days. It preserves the same trend for every investigated tilt angle case, at 60° tilt angle the ratio differences between the codes balance for most time steps around 0% value. With the increase of angle they start to have negative values which mean higher outputs for new code.

Summer

Data for summer days (Figures 55, 56, 57, 58, Table 21)

The trend for summer bright day looks slightly chaotic. This is caused due to the fact, that in the analysed day, for some time steps, clouds could have occurred. This is more natural for Aberdeen's summer that the sky is not clear the whole time. That's why for some time steps values of cloudy day cover with values of bright day. Approximate trend could be deduced from data provided on the figures. Firstly it can be noticed that middle range doesn't vary

with angle and remains stable. For the very first time steps values remain similar with the change of angle, although the region between sunrise and noon and between noon and sunset varies the most with the angle.

Cloudy day trend remains fairly stable (slightly more chaotic than for other seasons) and behaves similar to previously explained cloudy day trends, changing ratio differences sign for angles higher than 60°.

In the analysis those points that are most vulnerable for sudden rises during time steps with low incidence angle occurrence, show relatively high values (5%-7%) of ratio differences, which can be an explanation for summer average trend that gives higher outputs for old code simulations.

Autumn

Data for autumn days (Figures 63, 64, 65, 66, Table 25)

The analysis for October has proven to be fairly similar to April days. One of the main differences is that for spring sunrise periods there were large spikes of ratio differences increase. In October same behavior was recorded for sunsets. Despite that, the middle time steps when the output is the highest appear to be in the negative region of ratio differences as it was for spring. This implies higher outputs for new code and also explains the monthly outputs calculated for autumn.

The cloudy day trend behaves in the same way as for previous months. The only thing worth mentioning here is that every time the highest ratio differences for cloudy days were for sunrise period, then it drops during the major time of operation and rises again when it comes to sunset. This can be explained by reflection losses for low incident angles of solar beams during these periods of the day.

5.3.2 Guantanamo Bay climate daily analysis

Winter

Data for winter days (Figures 43, 44, 45, 46, Table 20)

The trends for winter days analysed for Guantanamo Bay are stable and preserve similar trend with an increase of tilt angle. For bright days the ratio differences are in majority negative values. For every angle, they become positive only at sunrise and sunset time steps (reflection losses). The shape changes slightly with an increase of angle, for 30° the values drop during earlier time steps to around -4% which gives a constant shape during time of major operation. For 60° the shape looks smooth with slow increase in ratio differences per time step, this becomes even smoother further for 90° tilt angle. Overall the main time of operation is in range where new code values are higher, therefore if days like that dominate in winter, it explains monthly trend for winter differences in Guantanamo climate.

The trend for cloudy day preserves fairly similar shape for each angle, with minor differences. The trend for 90° tilt angle stands out in shape from shapes at other tilt angles. Considering 0° tilt angle most of the values are close to 0%, except the differences at sunrise time steps, with increased angle the values start to drop slightly. The difference between values at 0° and 30° tilt angle aren't so significant, and still may be assumed as close to 0%. At 60° tilt angle, values start to drop below 0% favoring the new code values, while at 90° the drop becomes even bigger making the values obtained for the new code higher. It is worth mentioning that for every angle, sunrise time steps are positive, which again stands for occurred reflection losses.

Spring

Data for spring days (Figures 51, 52, 53, 54, Table 24)

The differences between cloudy day and bright day in spring for Guantanamo climate aren't very large. It can be caused due to the fact that for this climate there aren't many opportunities for cloudy day, therefore a day with relatively lower radiation levels have been chosen. It can be noticed that for tilt angles 0° 30° 60° the behavior is similar with slight differences between ratio difference magnitudes. For main time frame of operation the differences between the codes aren't very big, for 30 ° tilt angle they are close to 0%. On the other hand in each case for sunset and sunrise time steps, large spikes are recorded in difference between the codes, this is again caused due to reflection losses.

For the tilt angle of 90° the difference suddenly becomes very large in favor of old code results. This can be explained by the fact, that for façade configuration the angles of incidence

on PV array are very low causing dramatic reflection losses, which can be also noticed in the difference between obtained values for spring period in table 24.

Summer

Data for summer days (59, 60, 61, 62, Table 22)

Summer trend for bright day in Guantanamo climate for 0° tilt angle, doesn't point any significant differences between the codes for the major period of operation, and points out reflection losses for sunrise and sunset time steps. With an increase of tilt angle the ratio differences grow making old code values higher than new code ones. This happens due to the fact that once the tilt angle significantly overgrows the optimum tilt angle for the summer (-4°) the incident beam radiation will create low angle of incidence with PV array causing reflection losses and therefore provide higher output for old code. For 60° tilt angle the reflection losses are even more visible, once the tilt becomes perpendicular to the surface suddenly for both bright and cloudy day the trend shapes in the same way, favoring new code results.

The cloudy day's trend follows the bright day trend with exceptions at several time steps; this is due to the climate zone, where totally cloudy days are extremely rare cases.

Autumn

Data for autumn days (Figures 67, 68, 69, 70, Table 26)

Cloudy day's trend looks almost exactly the same for every tilt angle. The maximum value drops slightly with an increase of tilt angle, but the shape preserves almost completely. Reflection losses occur for sunrise and sunset time steps as for previous months.

When analyzing bright day, similar as in autumn case for Aberdeen climate the differences between codes ratios spike during the sunset. The main period of operation balances around -1% of ratio differences for three tilt angles: 0°, 30°, 60°. For 90° tilt angle, similar as in spring case, bright day differences become way higher in comparison with previous angles. This is again due to the fact that façade position is unsuitable for this climate zone and period,

causing the beams to approach PV array at very low incident angles and therefore producing large reflection losses, which cause disproportion between the codes.

5.3.3 Daily results – discussion

For Aberdeen climate the analysis and graphs have proven that for 60° tilt angle, during cloudy days there aren't almost any differences between the codes during the major period of operation. It only affected the sunset and sunrise time steps where reflection losses had to be considered due to low angles of incidence. For first two angles cloudy days could slightly influence the monthly average, as the trend in general was above the X axis, in general for major time steps of operation the values were no more than 2% of ratio differences. For 90° tilt angles the cloudy day trends also had an influence on the average, although then these trends favored new code values.

Bright days followed different trends depending on a season. For every season and every angle it can be noticed that for time steps corresponding to sunsets and sunrises the values of old code became higher, this is due to the reflection losses considered by the new code (absorption ratio instead of incident radiation ratio). For the time steps with highest radiation for every season it has been noticed that new code values become higher than the old code values. In the summer the drop in values for major time of operation isn't long and large enough to overgrow reflection losses caused in earlier and later time steps, which is why summer's average favors the old code values.

In Guantanamo climate, while looking at spring, autumn and summer at first two angles, which are in the optimum range, the outputs look very stable. During the major period of operation there aren't significant differences between the codes, only at the border time steps (sunset, sunrise) where reflection losses occur. For 60° tilt angle the differences start to rise during the time steps of main operation, this is also caused by the reflection, because beams approaching wrongly adjusted tilt angle strike at low incidence angles. For 90° tilt angle the situation looks very bad and the large disproportion between codes cannot be neglected at any point. The only period that stands out from these results for Guantanamo Bay climate is winter. During winter period results obtained through simulating the new code are higher than for the old code, for every angle of incidence (Except sunset and sunrise time steps).

6. CONCLUSIONS AND FURTHER WORK

This chapter will present the conclusions, outcomes and new ideas that came out during the result and analysis part. This will be followed by recommendation for further improvements to ESP-r models and validation of investigated issue.

6.1 Conclusions

This paper has focused on comparison between the two versions of ESP-r source codes responsible for electrical model algorithm definition. New code replaced previously used incident shortwave radiation to reference radiation ratio in electrical model with absorbed radiation by the PV layer to absorbed radiation at the reference conditions ratio. Therefore light generated current is calculated in a different way which was described in previous chapters. Validation of how accurate the new code is would require specific experimental data for the same device under same conditions. Nevertheless comparison between the two versions provided logical outcomes which allow assessing the impact of applied changes.

Yearly analysis has shown that the radiation and absorption ratio, light generated current and PV power output have similar trends in relation to incident angle. The only difference was diagnosed for PV power output, which was caused by the flaws of the software. Geometry changes provoked different PV array temperatures, which influenced in different voltages for higher tilt angle. Lower voltage influenced PV power output.

Yearly difference between the codes outcomes appeared to be in general larger for Guantanamo Bay climate. Further monthly analysis have shown that high difference values have been pointed for angles which were far from optimum tilt angles for Guantanamo climate. These tilt angles have been defined for each season. The extreme differences between power outputs and corresponding angles have been placed in the table 18.

Table 16 Poorly adjusted tilt angles for a given season in Guantanamo Bay climate.

	Winter	Spring	Summer	Autumn
50°			7,3 %	
60°	-3,084 %		11,25 %	3,92 %
70°	-3,13 %	3,74 %	14,96 %	6,46 %
80°	-3,009 %	6,87 %	10,43 %	10,35 %
90°		11,34 %		14,6 %

The daily analysis has proven that these large spikes in differences in that case were caused by the large reflection losses connected with inefficient adjustment of PV tilt angle in relation to relative sun's position. Guantanamo Bay is close to equator therefore the relative sun's position doesn't change a lot over the whole year, which implies that the set of effective tilt angles is narrowed. On the other hand, narrowed set of effective tilt angles makes them more universal over the year.

For autumn and spring periods there weren't significant differences between the codes for the range of optimum angles (0°-45°), the only difference occurred during sunrise and sunset time steps which is due to reflection losses. Winter period analysis has shown that in the main operation period the values were bigger for new code, which could be the cause of the way qtmca formula (applied in the source code) calculates absorption values for periods with lower temperature.

Aberdeen climate appeared more stable in analysis due to the fact that sun's position changes significantly over the whole year, which gives broader range of tilt angles that could be applied for a given period. The drawback of this is the period might be relatively too short, and the tilt should be readjusted.

Most of the seasons investigated excluding summer, have proven to give higher outputs for the new code for Aberdeen climate. Even though for each daily case, reflection losses

connected with sun's position during sunrise and sunset were observed, they weren't large enough to cover differences that occurred during the main operation period. This scenario has only happened in summer, where the reflection losses overgrown relatively small differences between the codes during main operation period. The explanation for larger values of new code simulations over the old code must be within the use of temperature in the new code's absorption calculation. Such trends have been noticed only for winter periods in both climates and spring/autumn period for Aberdeen climate, which might be considered as periods of low temperature as well.

While considering optimum tilt angles, Aberdeen climate has proven to be more vulnerable on reflection losses. For the range of optimum angles 34°-80° (minimum most appropriate angle for a given month until maximum most appropriate angle for a given month) Aberdeen climate would suffer yearly losses in range of 1%-1.9%. Guantanamo climate is more resistive for difference between the codes for optimum angles and equals 0,64%-1,16% for angles in range -4°-44°. Academic sources agreed on the fact that for generally effective tilt angles the losses will always be higher for northern climate due to the longer sun's path.

Reflection losses took a large part in the differences between the codes. For some ineffective configurations the differences were extremely large (even around 15%). Nevertheless for most cases reflection losses appeared generally during sunrise and sunset time steps, and badly adjusted tilt angles (as expected from the literature review). The new code copes perfectly with the reflection losses and gives a better view on estimating the absorbed radiation for colder climates.

Lastly in order to obtain the above conclusions it was necessary to iteratively look on the results. For solar energy yield estimation it is never wise to look at one time period, but ideally analyze multiple time periods and draw valuable conclusion from each of them to form the final point of view.

6.2 Further work

There is still a lot to be done in order to improve ESP-r software. It is understandable that ESP-r is a tool to analyse performance of many different configurations of energy systems, nevertheless accuracy is a key point to reflect reality in performance analysis. Based on the knowledge gained from literature review, in depth look into the solar photovoltaic model of

ESP-r and conclusions arisen from the analysis, few suggestions to further improvements can be highlighted.

First of all the core of electrical model (equivalent circuit) itself lacks in accuracy. Few proposed solutions in (Thevenard, 2005) could be a way to improve the model. Shunt and series resistances should be included in the circuit, application of Sandia model would also be a good idea, although access to the database might be troubling.

Secondly, absorption of different electromagnetic wave spectrum bits depending on the material and temperature of the PV layer should be included in the thermal model. Moreover temperature effects on light generated current could be investigated. Even though the effect is relatively small (approximately +0,065%/°C depending on a module (Markvart & Castaner, 2003)) it could still cover some of the power losses provided by the voltage drop with temperature.

Involvement of ageing and environmental factors could also be a part of a further improvement to ESP-r photovoltaic model. There are still many flaws that require investigation and application to the electrical and thermal models of ESP-r. The development of ESP-r is a constant process that reflects reality better with each slight improvement.

Regarding the issue analysed in the thesis, it would be wise to compare the results with real data, the difficulty with that, is that the device would have to be analysed at the same conditions in the same climate zones, which might be troubling. Another, simpler way is to perform analysis based on data available for particular device in a given climate. Once compared, the new code could be fully validated.

REFERENCES

Alamri, S. N., & Benghanem, M. S. (2008). Modeling of photovoltaic module and experimental determination of serial resistance. *Journal for Science of Taibah University*, 95-105.

Beckman, W. A., De Soto, W., & Klein, S. A. (2005). Improvement and validation of a model for photovoltaic array performance. *Elsevier Solar Energy*, 78-88.

Benghanem, M. S., & Alamri, S. N. (2008). Modeling of photovoltaic module and experimental determination of serial resistance. *Journal of Taibah University for science*, 94-105.

Boxwell, M. (2015). *Solar Electricity Handbook - 2015 Edition.* Greenstream Publishing.

Donsion, M. P., & Skocil, T. (n.d.). *Mathematical Modeling and Simulation of Photovoltaic Array.*

Dubey, S., Sarvaiya, J. N., & Seshadri, B. (2012). Temperature Dependent Photovoltaic (PV) Efficiency and Its Effect on PV Production in the World A Review. *PV Asia Pacific Conference* (pp. 311-321). Singapore: Elsevier.

Duffie, J. A., & Beckman, W. A. (2013). *Solar Engineering of Thermal Processes Fourth Edition.* New Jersey: John Wiley & Sons Inc.

Ghitas, A. E. (2012). Studying the effect of spectral variations intensity of the incident solar radiation on the Si solar cells performance. *NRIAG Journal of Astronomy and Geophysics*, 165-171.

Habbati Bellia, R. Y. (2014). A Detailed Modeling of Photovoltaic Module using MATLAB. *NRIAG Journal of Astronomy and Geophysics*.

Honsberg, C., & Bowden, S. (n.d.). *Solar cell operation - resistive effects*. Retrieved August 05, 2015, from Photovoltaic Education Network: http://www.pveducation.org/pvcdrom/solar-cell-operation/shunt-resistance

Ishaque, K., Salam, Z., & Taheri, H. (2010). Simple, fast and accurate two-diode model for photovoltaic modules. *Elsevier Solar Energy Materials & Solar Cells* , 586-594.

Ishii, T., Otani, K., Itagaki, A., & Utsunomiya, K. (2013). A simplified methodology for estimating solar spectral spectralinfluence on photov oltaic energy yield using average photon energy. *Energy Science & Engineering*, 18-26.

Islam, N., Rahman, M. Z., & Mominuzzaman, S. M. (2014). The Effect of Irradiation on Different Parameters of Monocrystalline Photovoltaic Solar Cell. *Developments in Renewable Energy Technology (ICDRET), 2014 3rd International Conference* (pp. 1-6). Dhaka, Bangladesh: IEEE.

Kaplani, E. (2012). Degradation Effects in sc-Si PV Modules Subjected to Natural and Induced Ageing after Several Years of Field Operation. *JOURNAL OF Engineering Science and Technology Review*, 18-23.

Kelly, N. J. (1998). *TOWARDS A DESIGN ENVIRONMENT FOR BUILDING INTEGRATED ENERGY SYSTEMS: THE INTEGRATION OF ELECTRICAL POWER FLOW MODELLING WITH BUILDING SIMULATION.* Glasgow: University of Strathclyde.

King, D. L., & Pratt, L. (n.d.). *THE EFFECT OF UNCERTAINTY IN MODELING COEFFICIENTS USED TO PREDICT ENERGY PRODUCTION USING THE SANDIA ARRAY PERFORMANCE MODEL.* Albuquerque: Sandia National Laboratories.

King, D. L., Boyson, W. E., & Kratochvill, J. A. (2004). *Photovoltaic Array Performance Model.* Oak Ridge: U.S. Department of Energy.

King, D. L., Kratochvil, J. A., & Boyson, W. E. (2002). *ANALYSIS OF FACTORS INFLUENCING THE ANNUAL ENERGY PRODUCTION OF PHOTOVOLTAIC SYSTEMS.* Albuquerque: IEEE.

Klise, G. T., & Stein, J. S. (2009). *Models Used to Assess the Performance of Photovoltaic Systems.* Livermore, CA: Sandia Report.

Krauter, S. (2006). *Solar Electric Power Generation - Photovoltaic Energy Systems.* Berlin: Springer.

Labouret, A., & Villoz, M. (2010). *Solar Photovoltaic Energy.* London: The Institution of Engineering and Technology.

Luque, A., & Hegedus, S. (2003). *Handbook of Photovoltaics Science and Engineering.* Chichester: John Wiley & Sons Ltd.

Markvart, T., & Castaner, L. (2003). *Practical Handbook of Photovoltaics Fundamentals and Applications.* Elsevier.

Martin, N., & Ruiz, J. M. (2001). *Calculation of the PV modules angular losses under field conditions by means of an analytical model.* London: Elsevier.

Navabi, R., Abedi, S., Pal, R., & Hosseinian, S. H. (2014). On the fast convergence modeling and accurate calculation of PV output energy for operation and planning studies. *Elsevier Energy Conversion and Management*, 497-506.

Roedern, B., & Ullal, H. (2008). The role of polycrystalline thin film PV technologies in competitive PV module markets. *33rd IEEE photovoltaic specialists conference proceedings.* IEEE.

Salam, Z., & Ishaque, K. (n.d.). An Improved Two-Diode Photovoltaic (PV) Model for PV System.

Sjerps-Koomen, E. A., Alsema, E. A., & Turkenburg, W. C. (1997). *A SIMPLE MODEL FOR PV MODULE REFLECTION LOSSES UNDER FIELD CONDITIONS.* London: Elsevier.

Sturcbecher, J. J., & Larue, J. C. (1994). The mini-flasher: a solar array test system. *Solar Energy Materials and Solar Cells ELSEVIER*, 91-98.

Swanson, M. (2007). Developments in silicon solar cells. *IEEE international*, 359-362.

Thevenard, D. (2005). REVIEW AND RECOMMENDATIONS FOR IMPROVING THE MODELLING OF BUILDING INTEGRATED PHOTOVOLTAIC SYSTEMS. *Ninth International IBPSA Conference*, (strony 1221-1228). Montreal.

Tiwari, G. N., Mishra, R. K., & Solanki, S. C. (2011). Photovoltaic modules and their applications: A review on thermal modelling. *Applied Energy Elsevier*.

Wagner, A. (2000). *PEAK-POWER AND INTERNAL SERIES RESISTANCE MEASUREMENT UNDER NATURAL AMBIENT CONDITIONS.* Copenhagen: EuroSun.

Wenham, S. R. (2007). *Applied Photovoltaics.* Earthscan.

Yamada, T., Nakamura, H., Sugiura, T., Sakuta Koichi, & Kurokawa, K. (2001). *Reflection loss analysis by optical modeling of PV module.* London: Elsevier.

APPENDIX A – GRAPHS OBTAINED FROM DAILY SIMULATIONS.

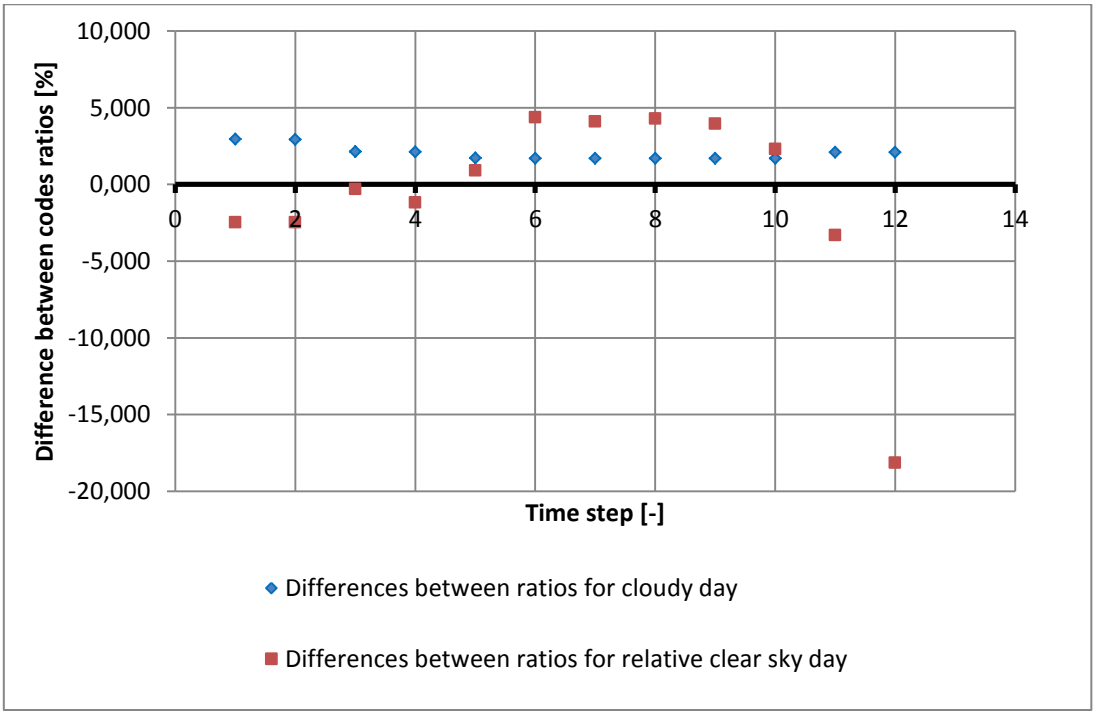

Figure 39 Percentage differences between ratios per time step for cloudy and bright days. (January Aberdeen 0° tilt angle).

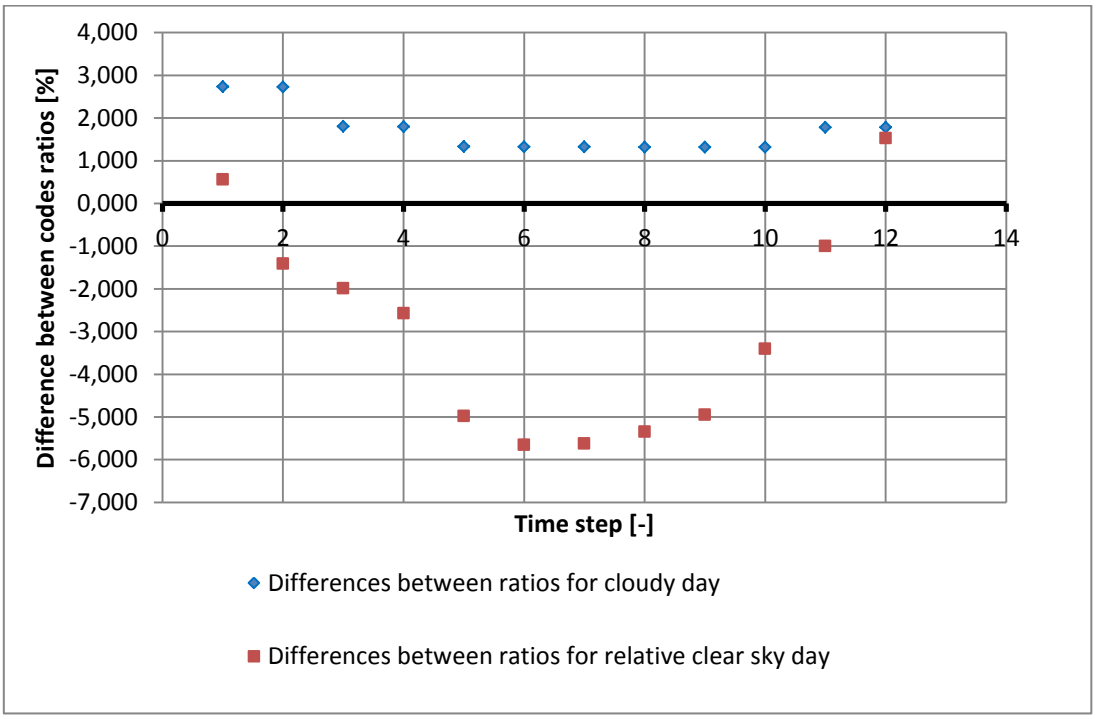

Figure 40 Percentage differences between ratios per time step for cloudy and bright days. (January Aberdeen 30° tilt angle).

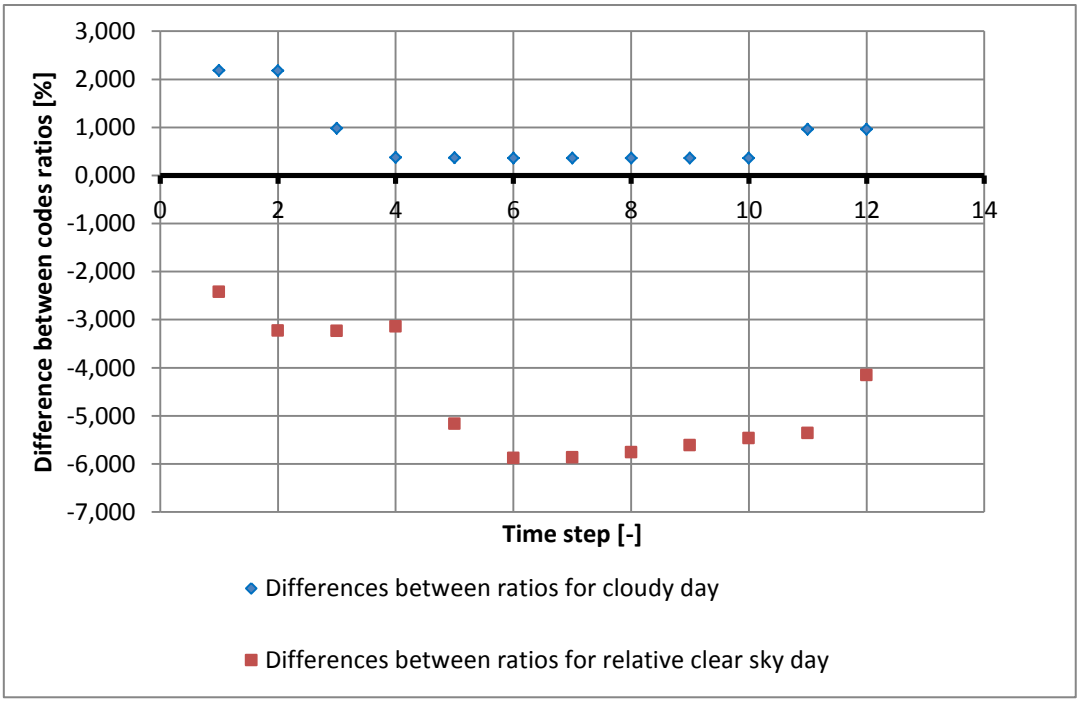

Figure 41 Percentage differences between ratios per time step for cloudy and bright days. (January Aberdeen 60° tilt angle).

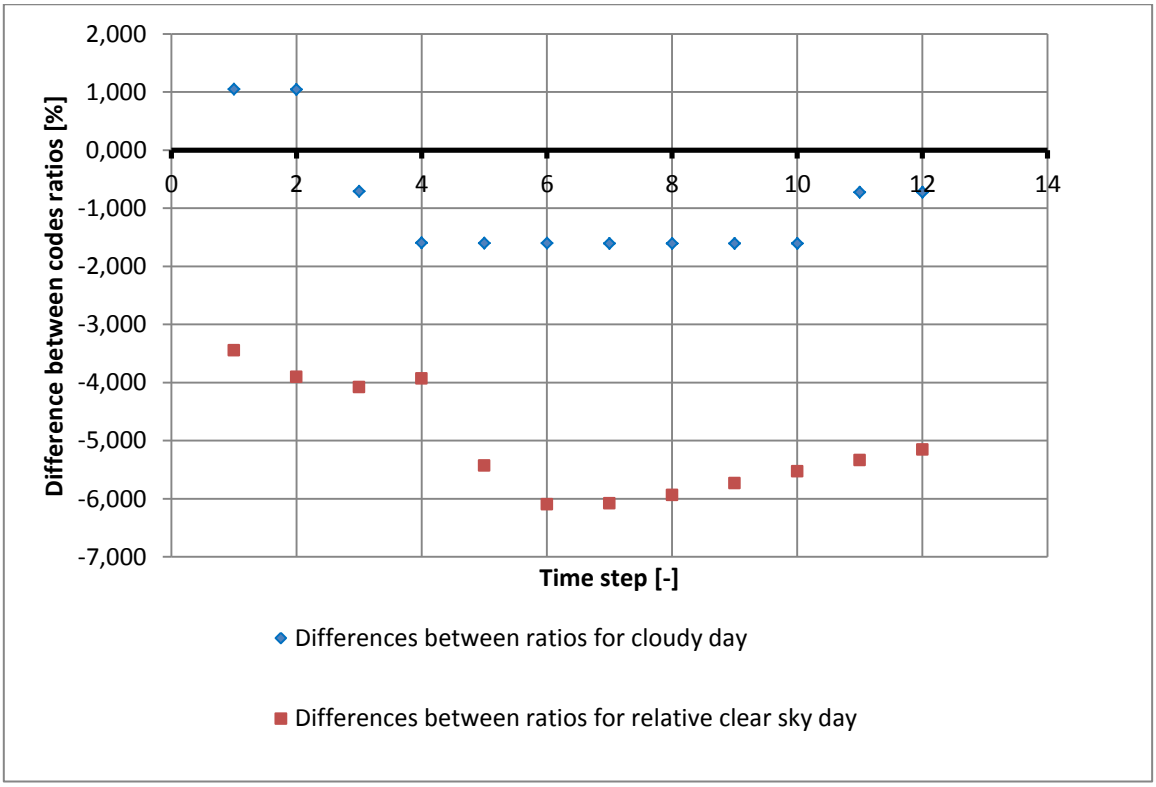

Figure 42 Percentage differences between ratios per time step for cloudy and bright days. (January Aberdeen 90° tilt angle).

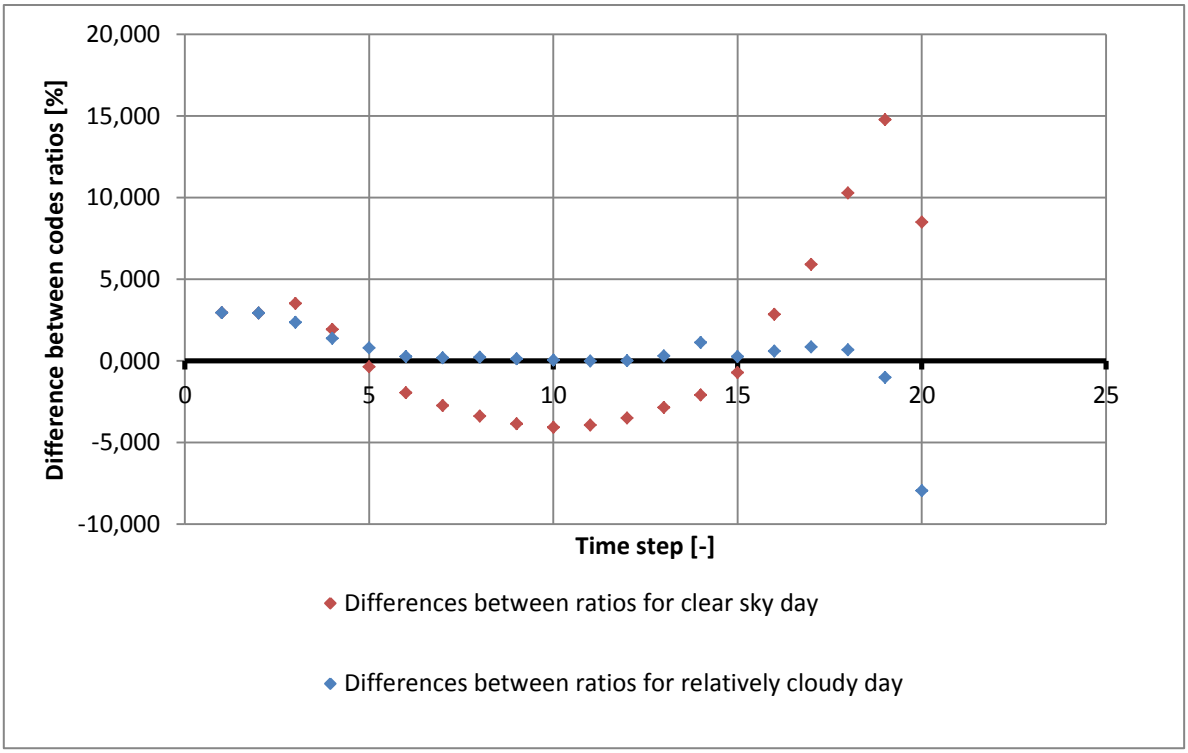

Figure 43 Percentage differences between ratios per time step for cloudy and bright days. (January Guantanamo Bay 0° tilt angle).

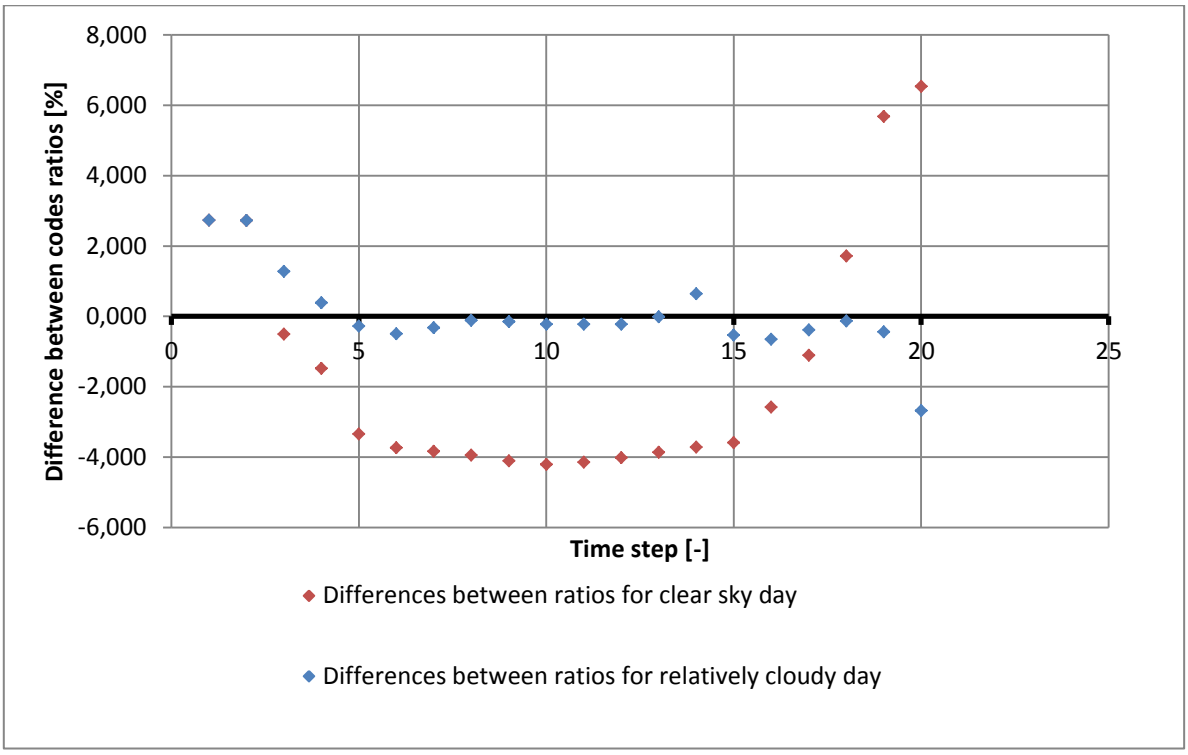

Figure 44 Percentage differences between ratios per time step for cloudy and bright days. (January Guantanamo Bay 30° tilt angle).

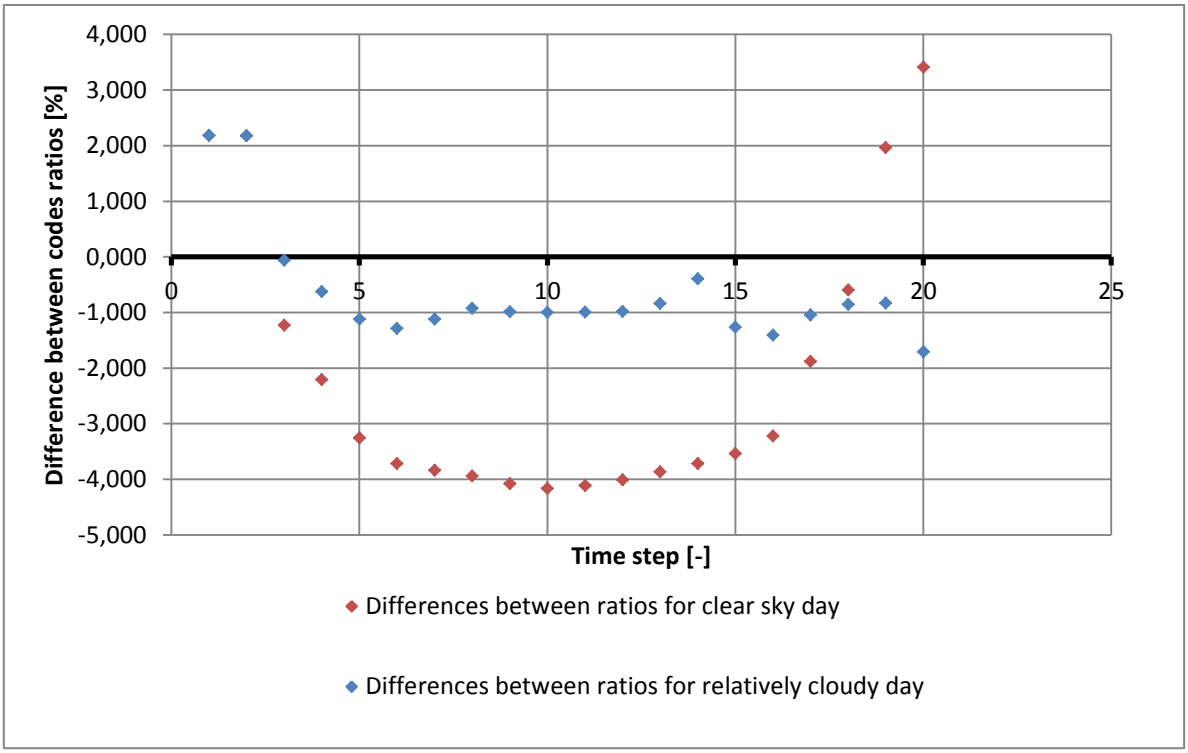

Figure 45 Percentage differences between ratios per time step for cloudy and bright days. (January Guantanamo Bay 60° tilt angle).

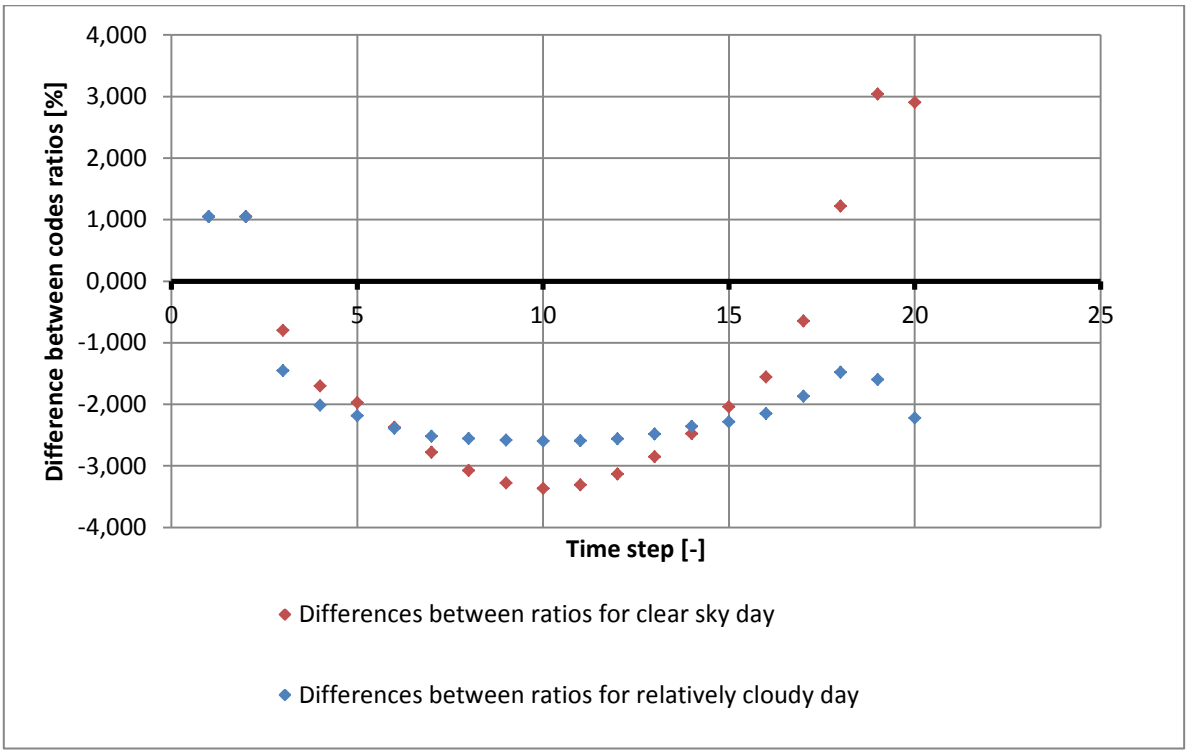

Figure 46 Percentage differences between ratios per time step for cloudy and bright days. (January Guantanamo Bay 90° tilt angle).

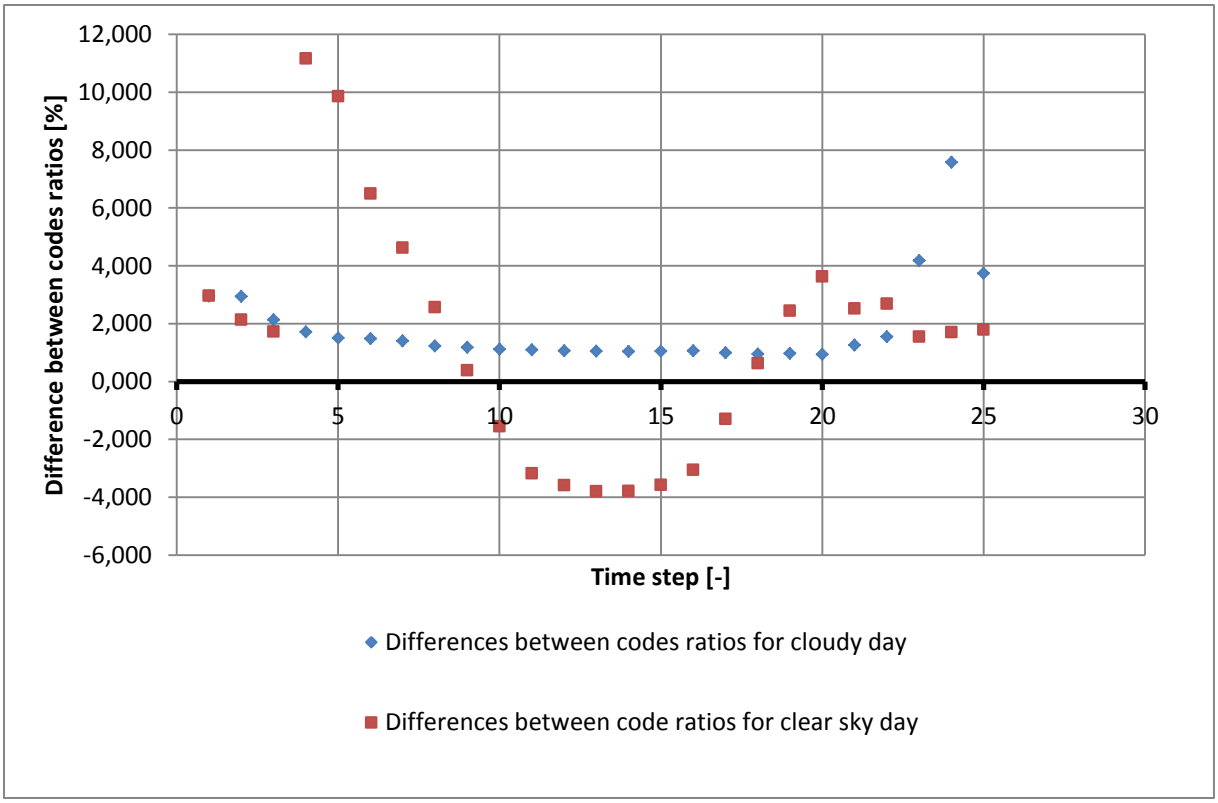

Figure 47 Percentage differences between ratios per time step for cloudy and bright days. (April Aberdeen 0° tilt angle).

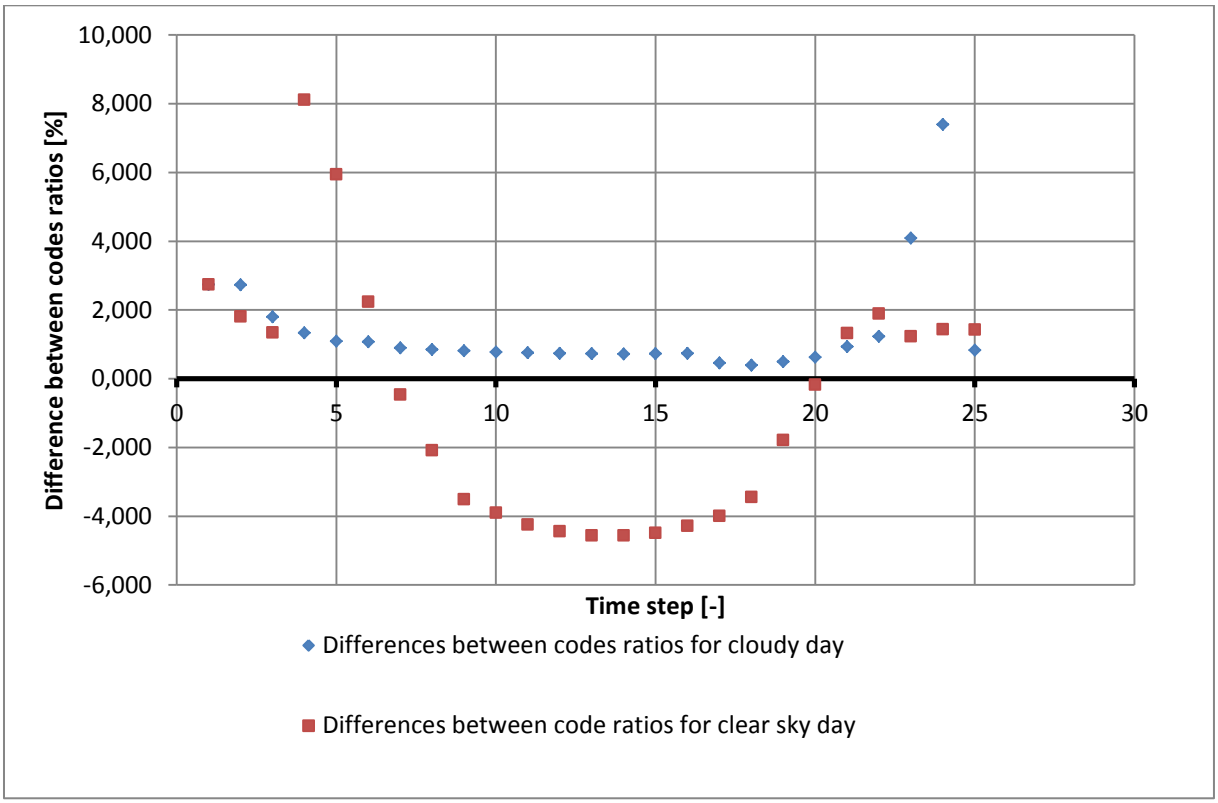

Figure 48 Percentage differences between ratios per time step for cloudy and bright days. (April Aberdeen 30° tilt angle).

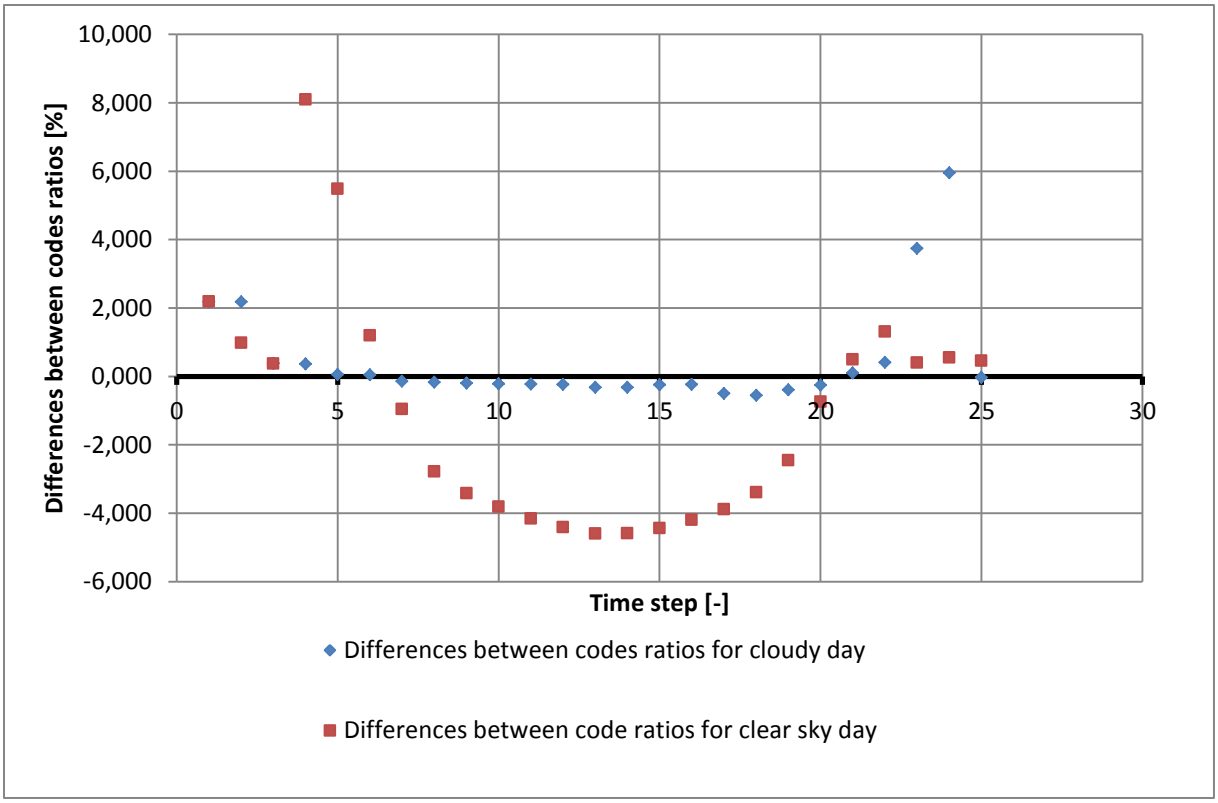

Figure 49 Percentage differences between ratios per time step for cloudy and bright days. (April Aberdeen 60° tilt angle).

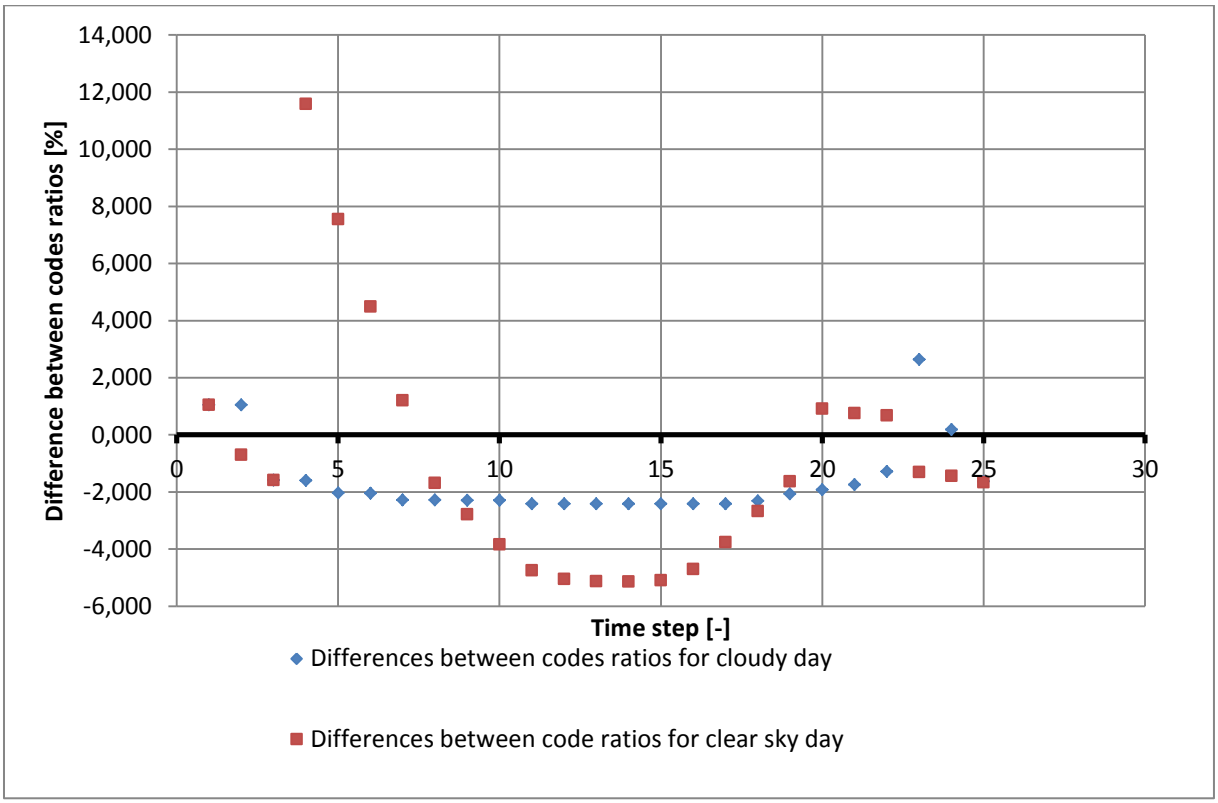

Figure 50 Percentage differences between ratios per time step for cloudy and bright days. (April Aberdeen 90° tilt angle).

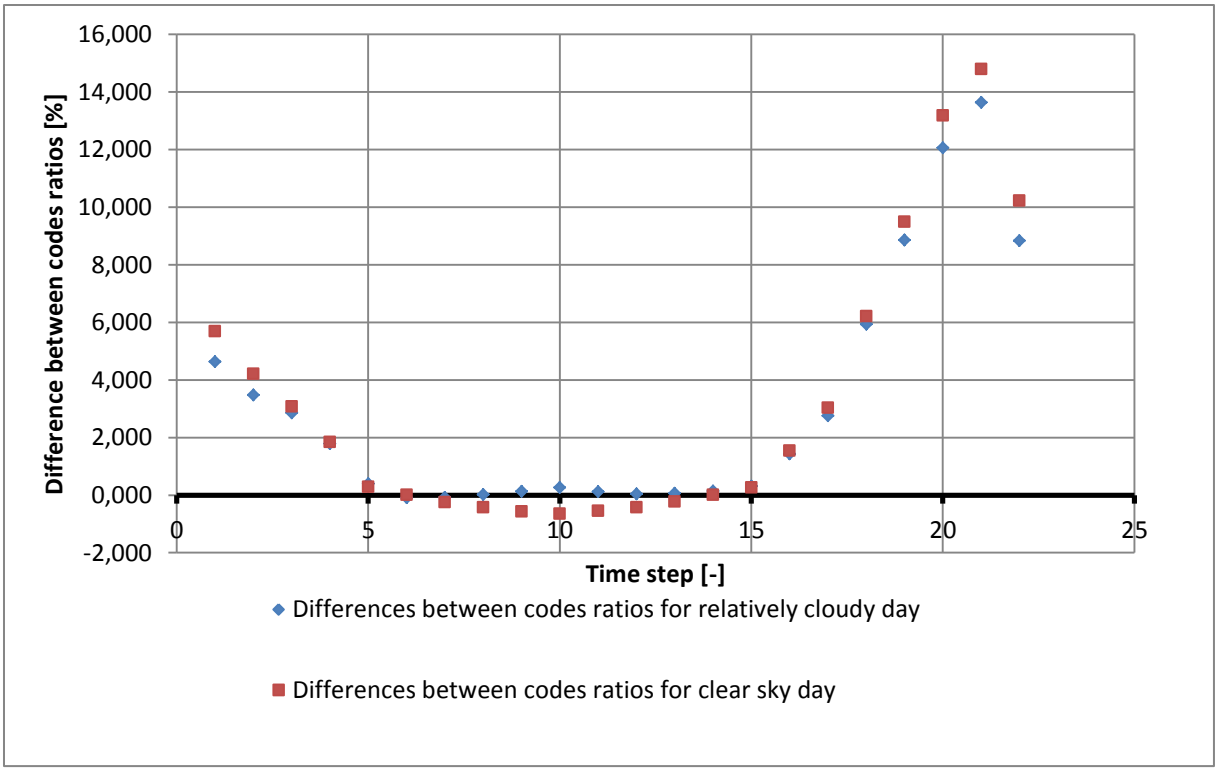

Figure 51Percentage differences between ratios per time step for cloudy and bright days. (April Guantanamo Bay 0° tilt angle).

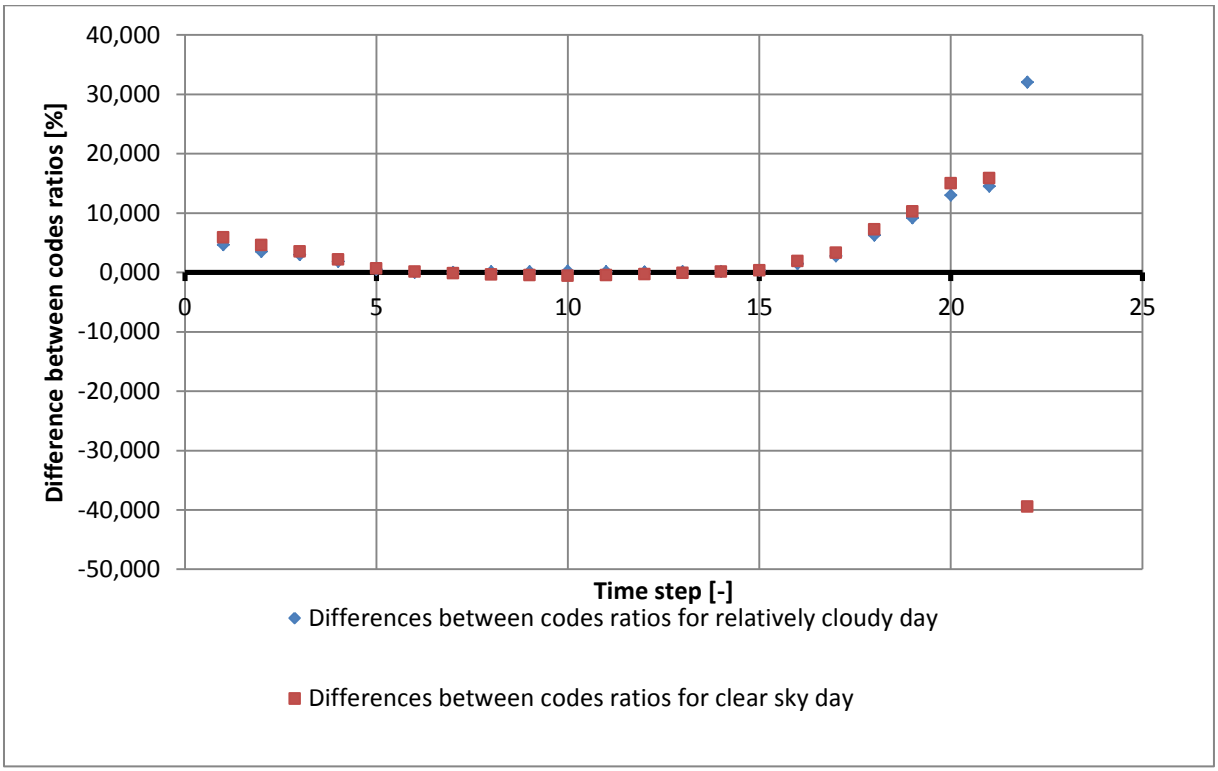

Figure 52 Percentage differences between ratios per time step for cloudy and bright days. (April Guantanamo Bay 30° tilt angle).

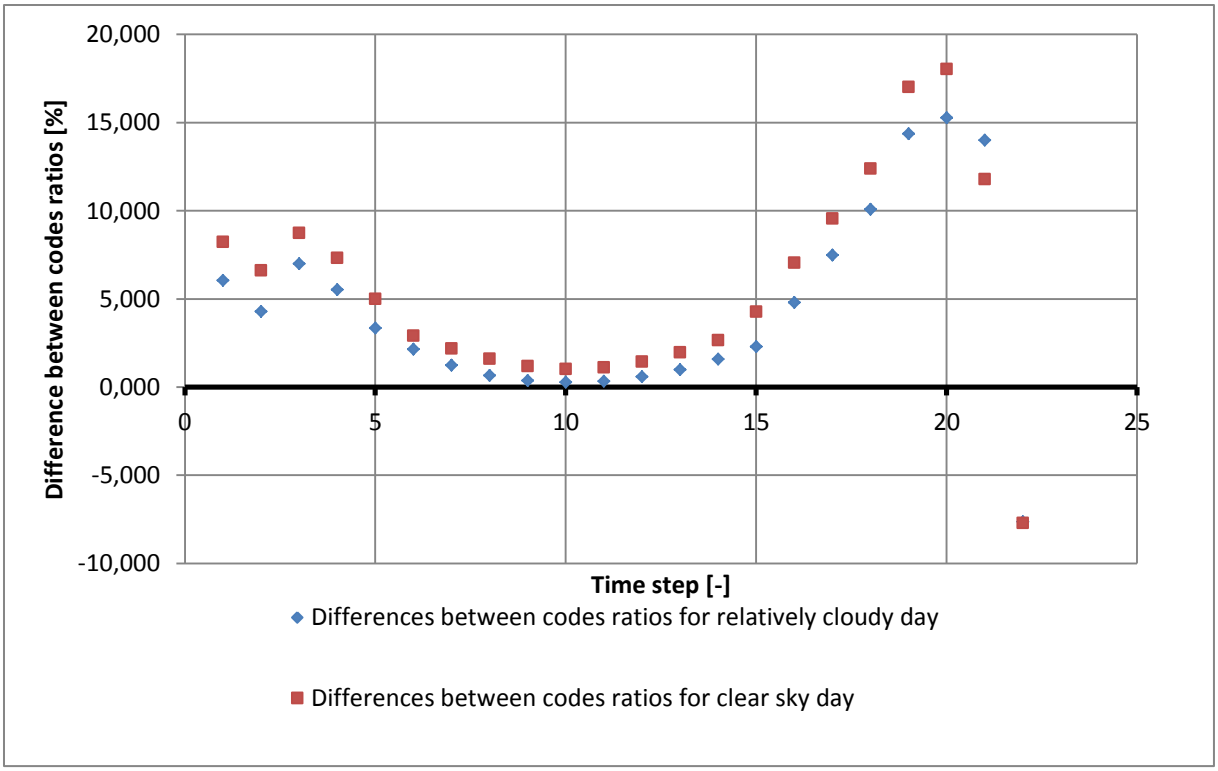

Figure 53 Percentage differences between ratios per time step for cloudy and bright days. (April Guantanamo Bay 60° tilt angle).

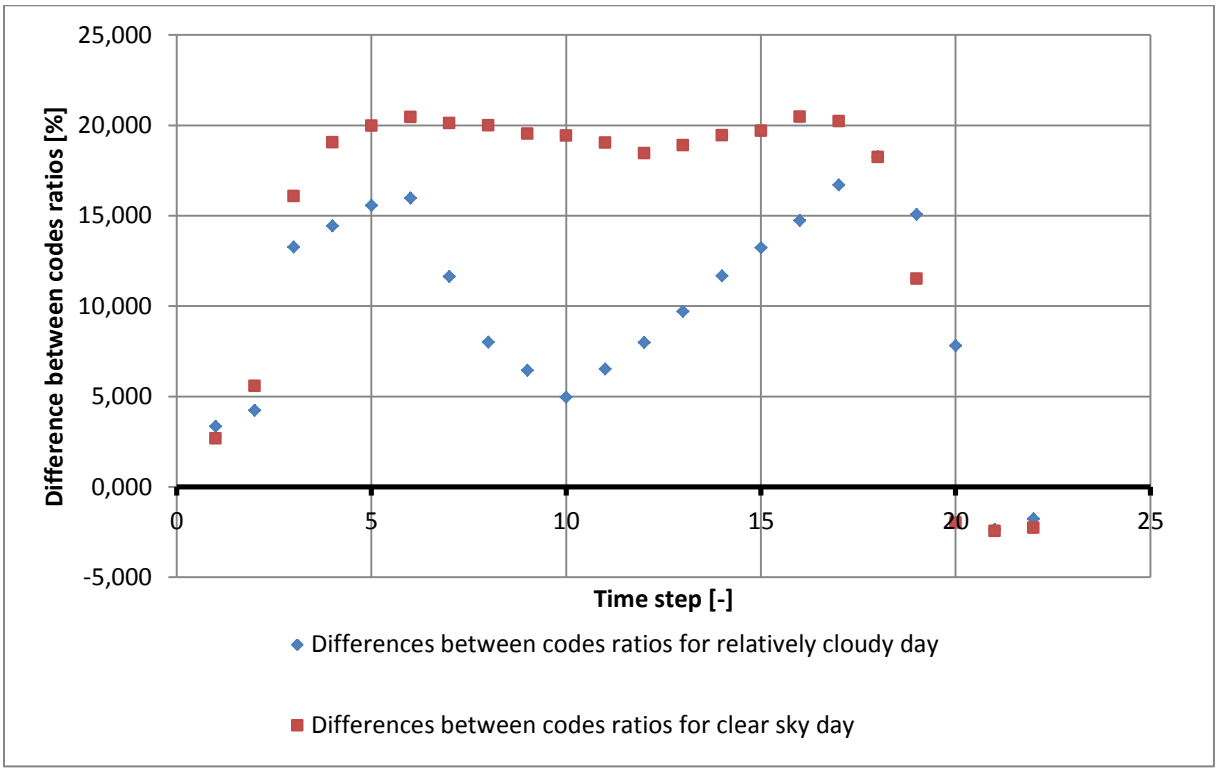

Figure 54 Percentage differences between ratios per time step for cloudy and bright days. (April Guantanamo Bay 90° tilt angle).

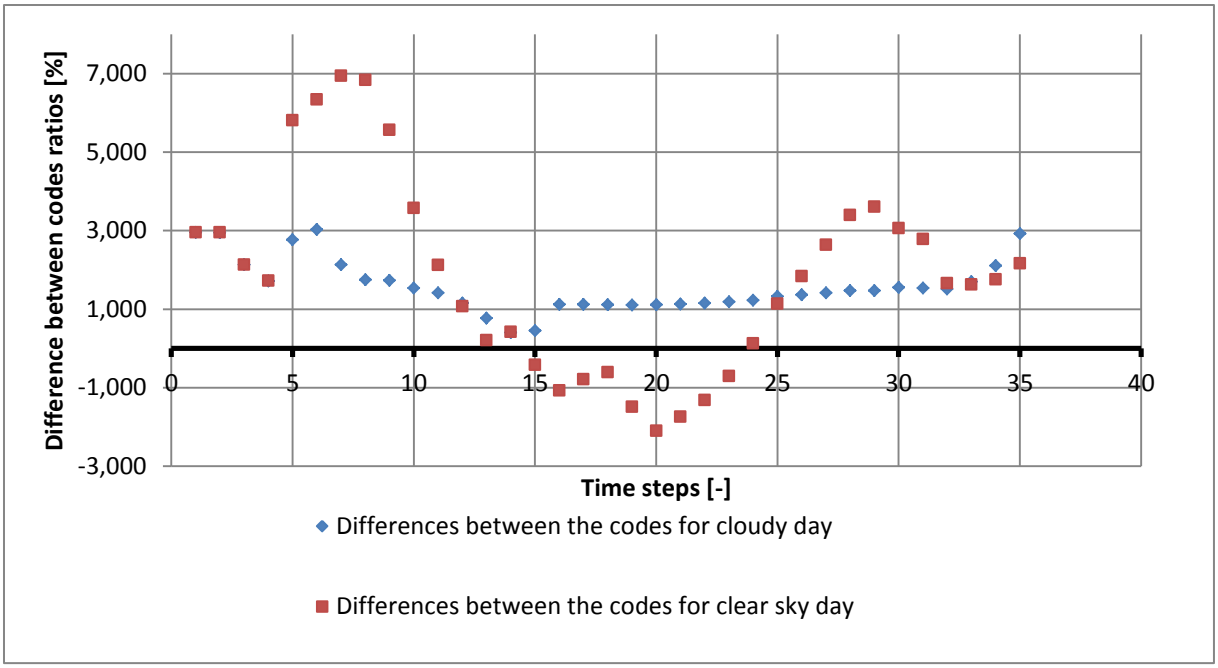

Figure 55 Percentage differences between ratios per time step for cloudy and bright days. (July Aberdeen 0° tilt angle).

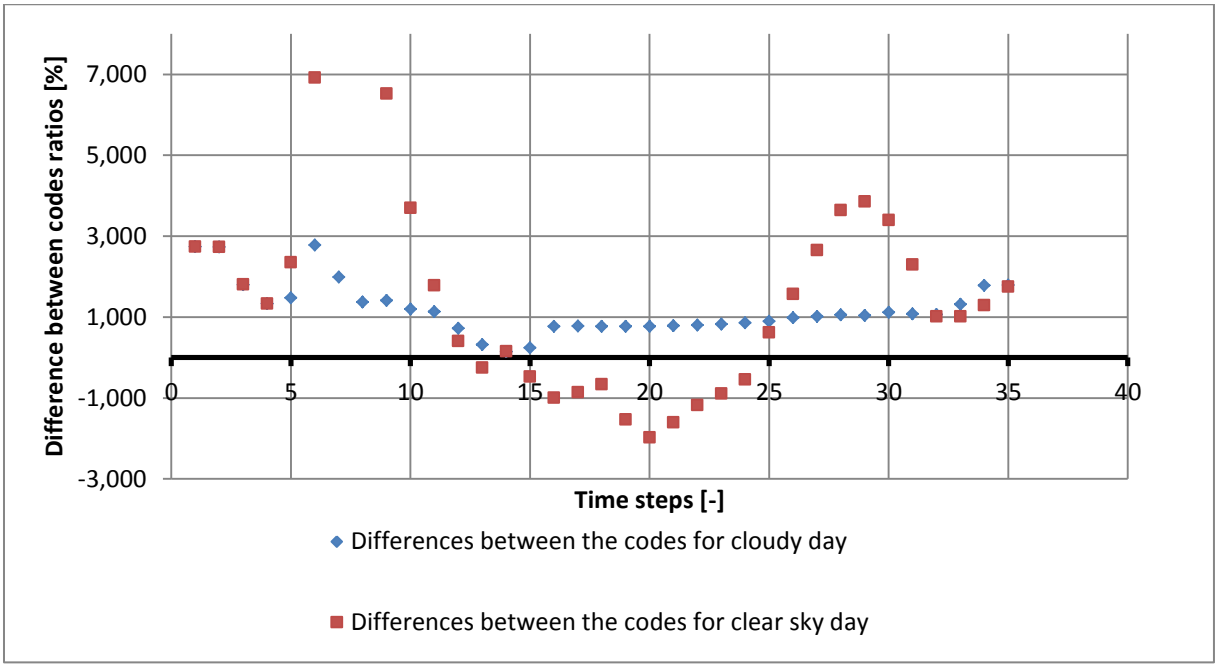

Figure 56 Percentage differences between ratios per time step for cloudy and bright days. (July Aberdeen 30° tilt angle).

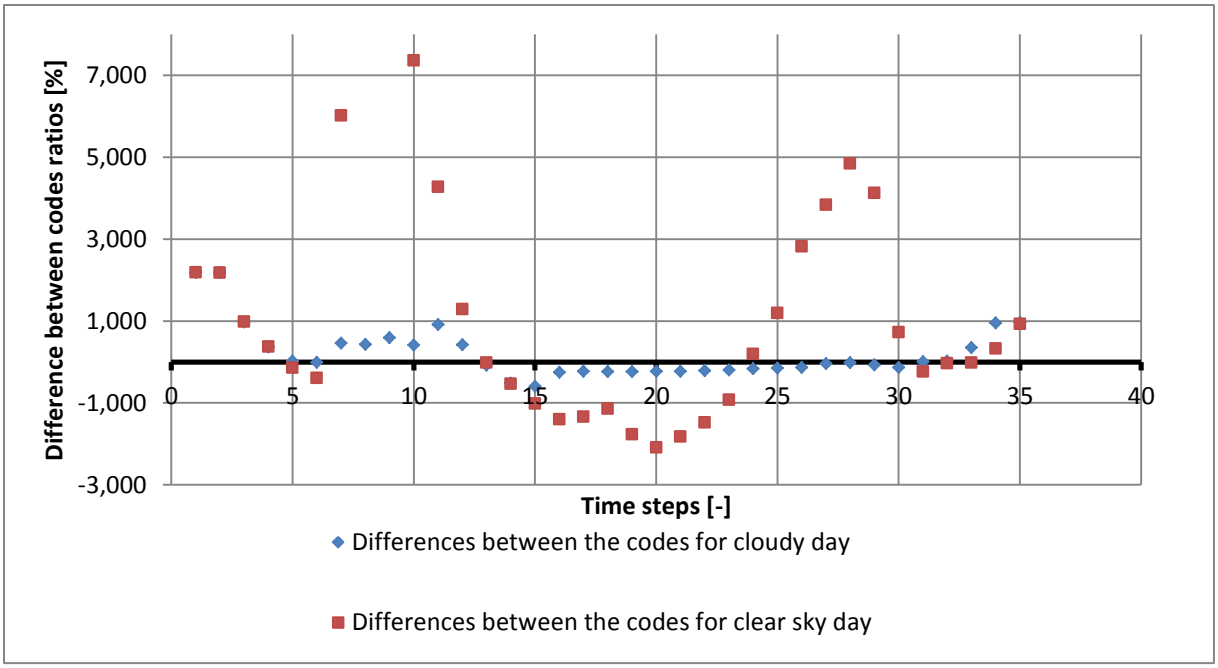

Figure 57 Percentage differences between ratios per time step for cloudy and bright days. (July Aberdeen 60° tilt angle).

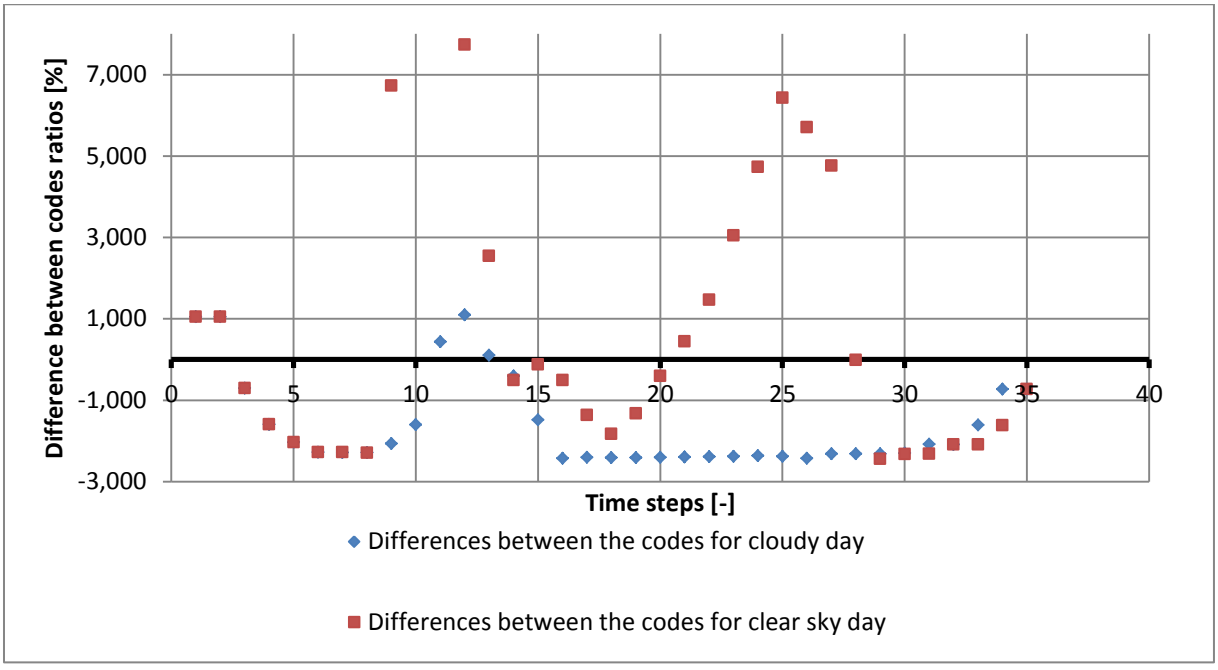

Figure 58 Percentage differences between ratios per time step for cloudy and bright days. (July Aberdeen 90° tilt angle).

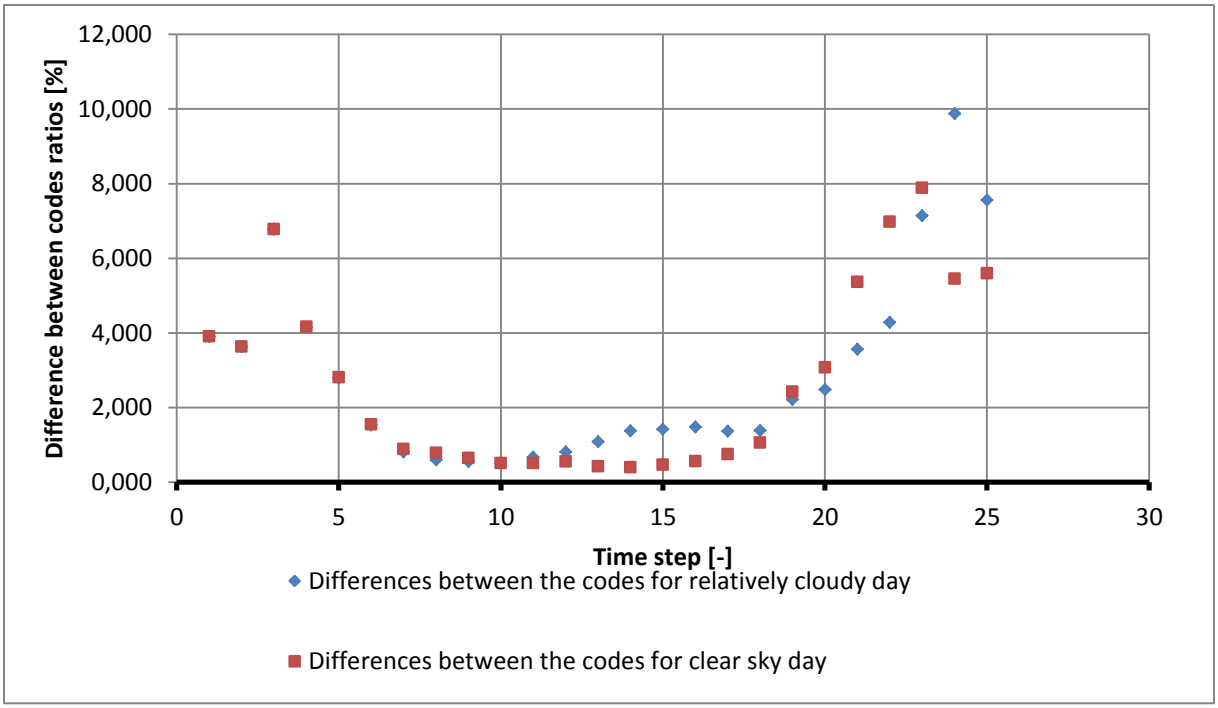

Figure 59 Percentage differences between ratios per time step for cloudy and bright days. (July Guantanamo Bay 0° tilt angle).

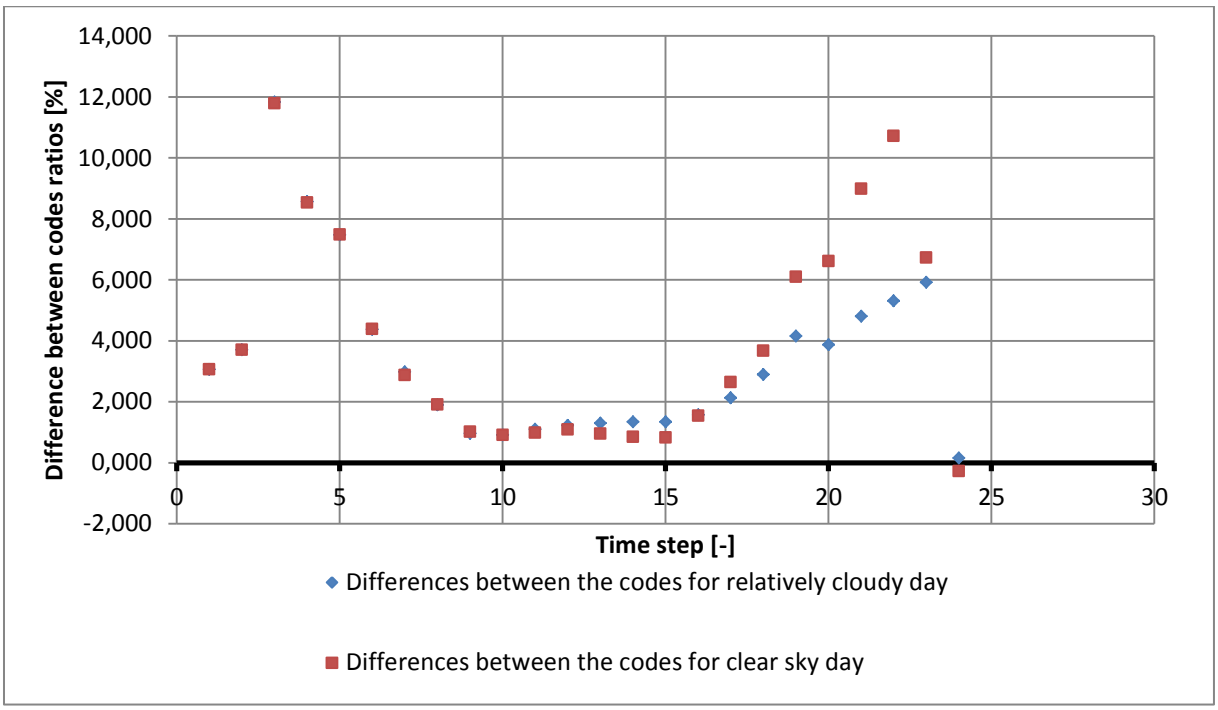

Figure 60 Percentage differences between ratios per time step for cloudy and bright days. (July Guantanamo Bay 30° tilt angle).

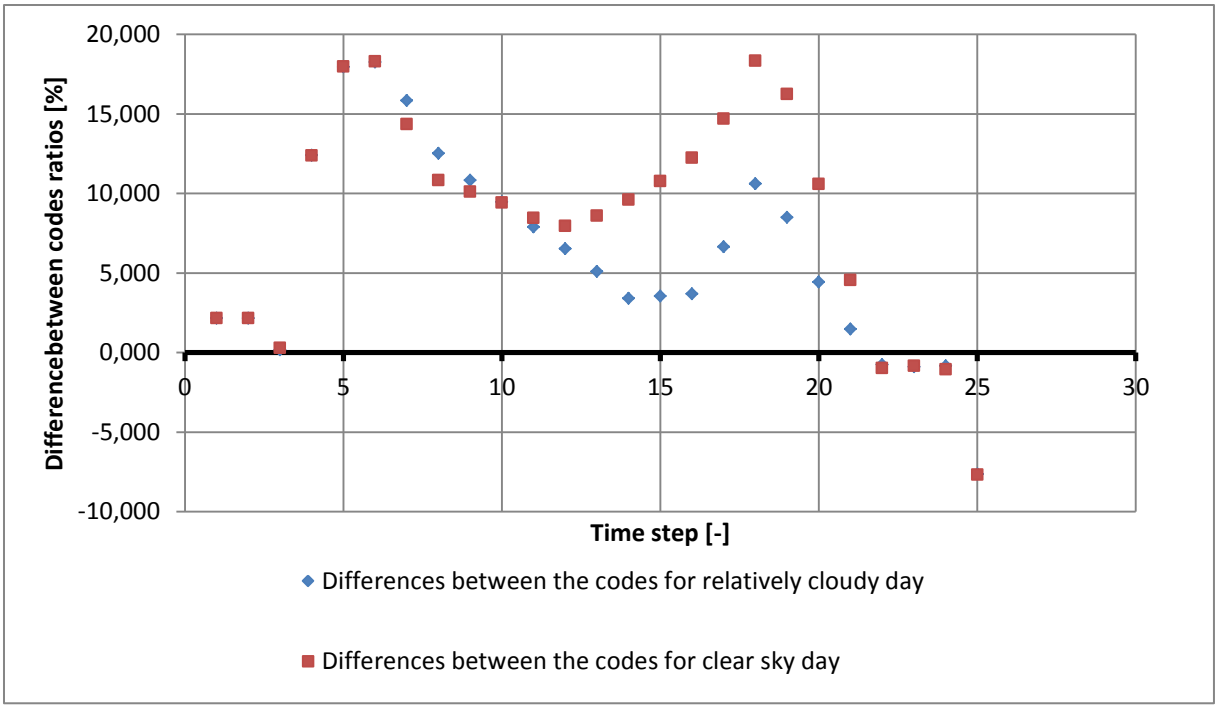

Figure 61 Percentage differences between ratios per time step for cloudy and bright days. (July Guantanamo Bay 60° tilt angle).

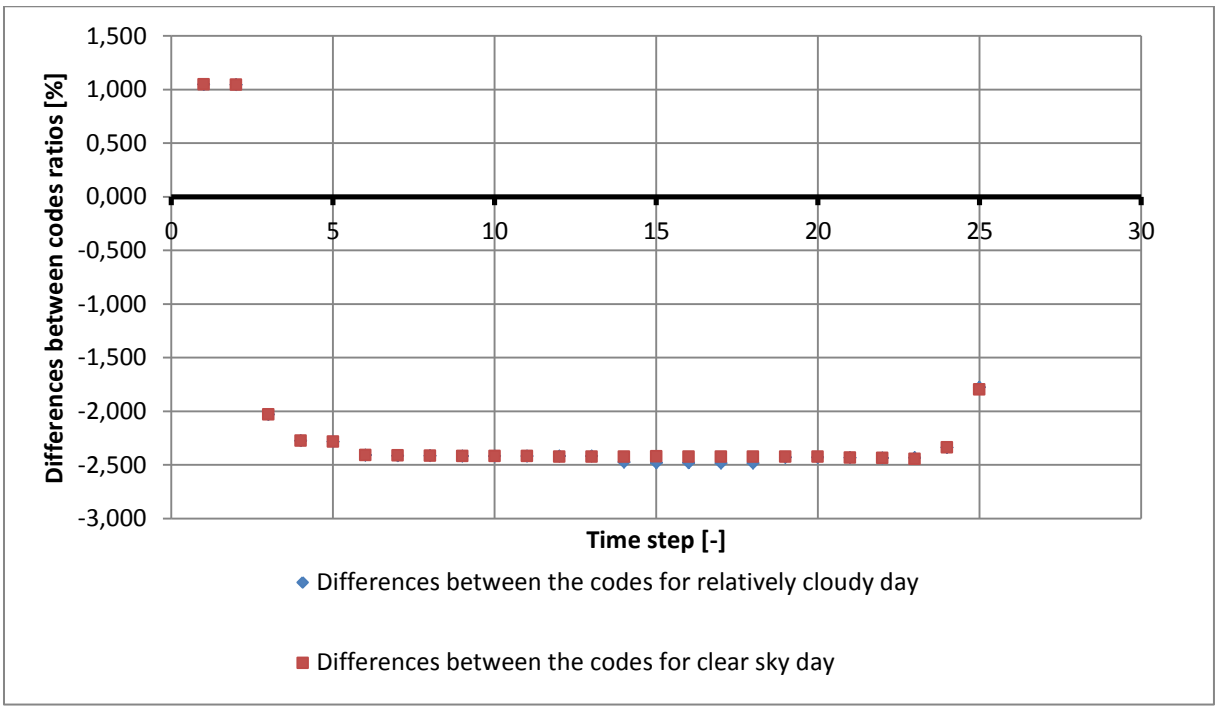

Figure 62 Percentage differences between ratios per time step for cloudy and bright days. (July Guantanamo Bay 90° tilt angle).

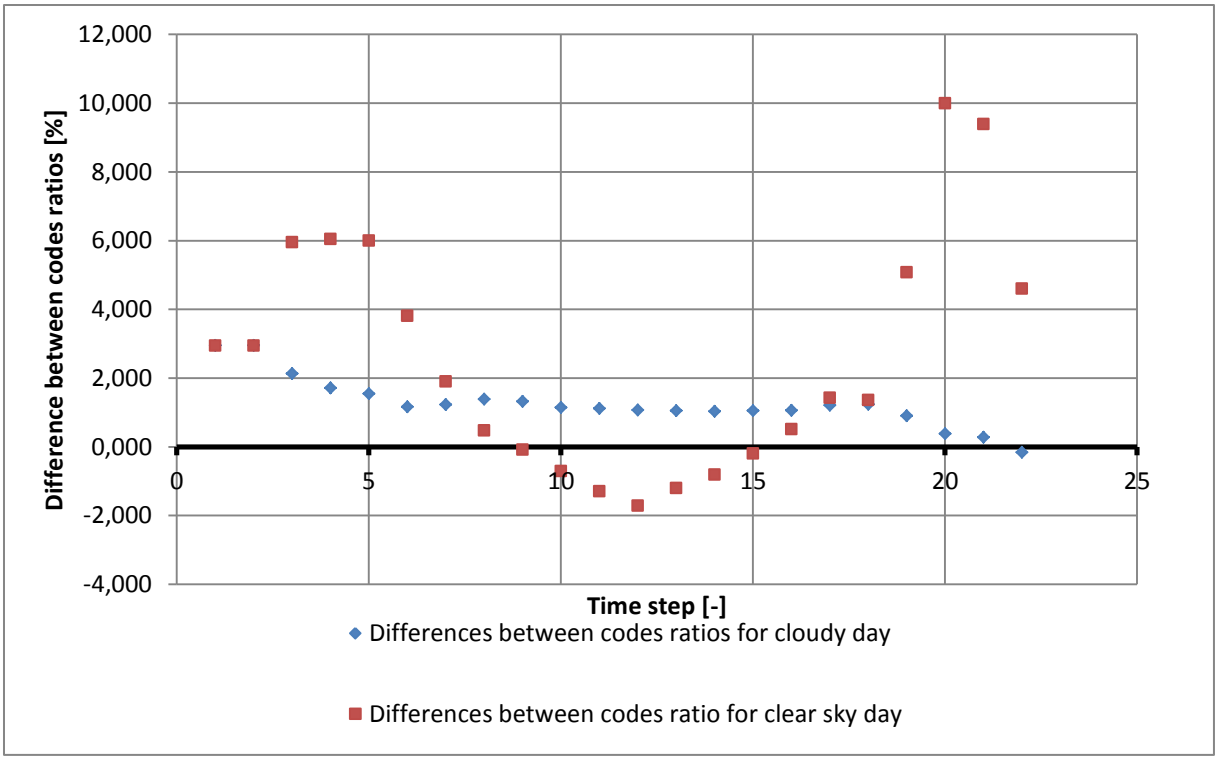

Figure 63 Percentage differences between ratios per time step for cloudy and bright days. (October Aberdeen 0° tilt angle).

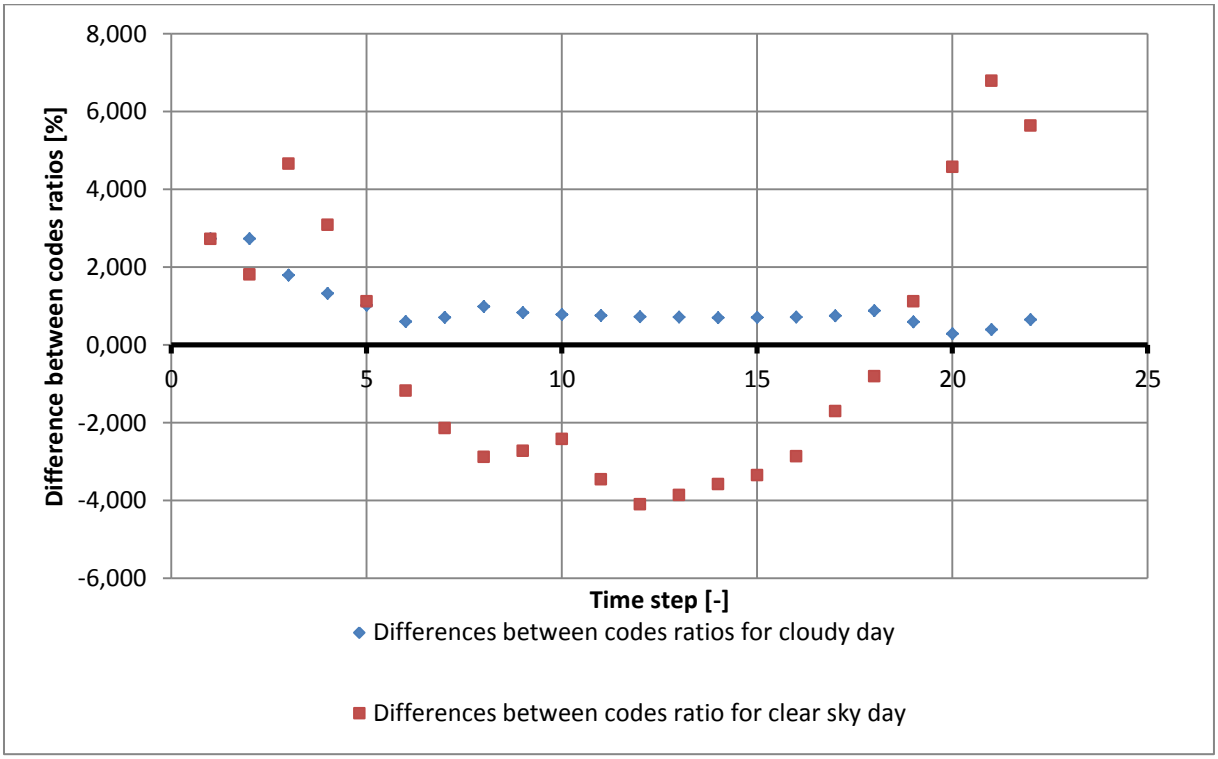

Figure 64 Percentage differences between ratios per time step for cloudy and bright days. (October Aberdeen 30° tilt angle).

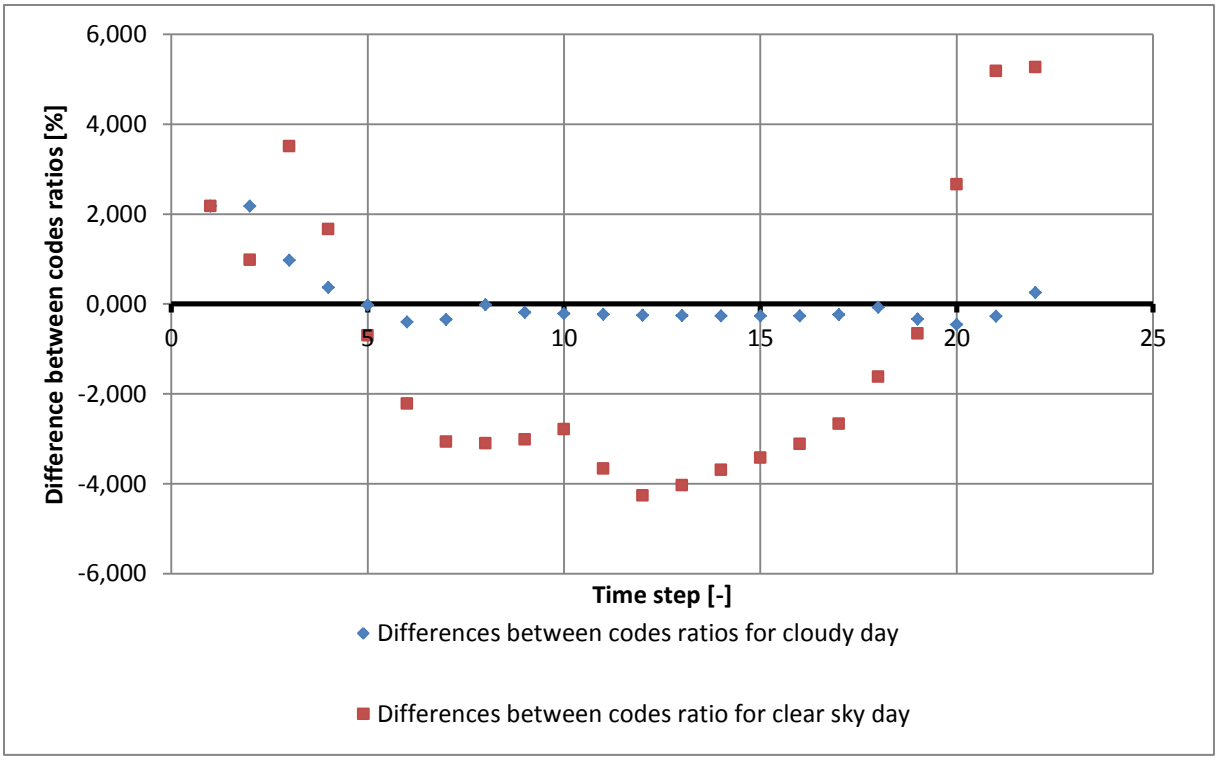

Figure 65 Percentage differences between ratios per time step for cloudy and bright days. (October Aberdeen 60° tilt angle).

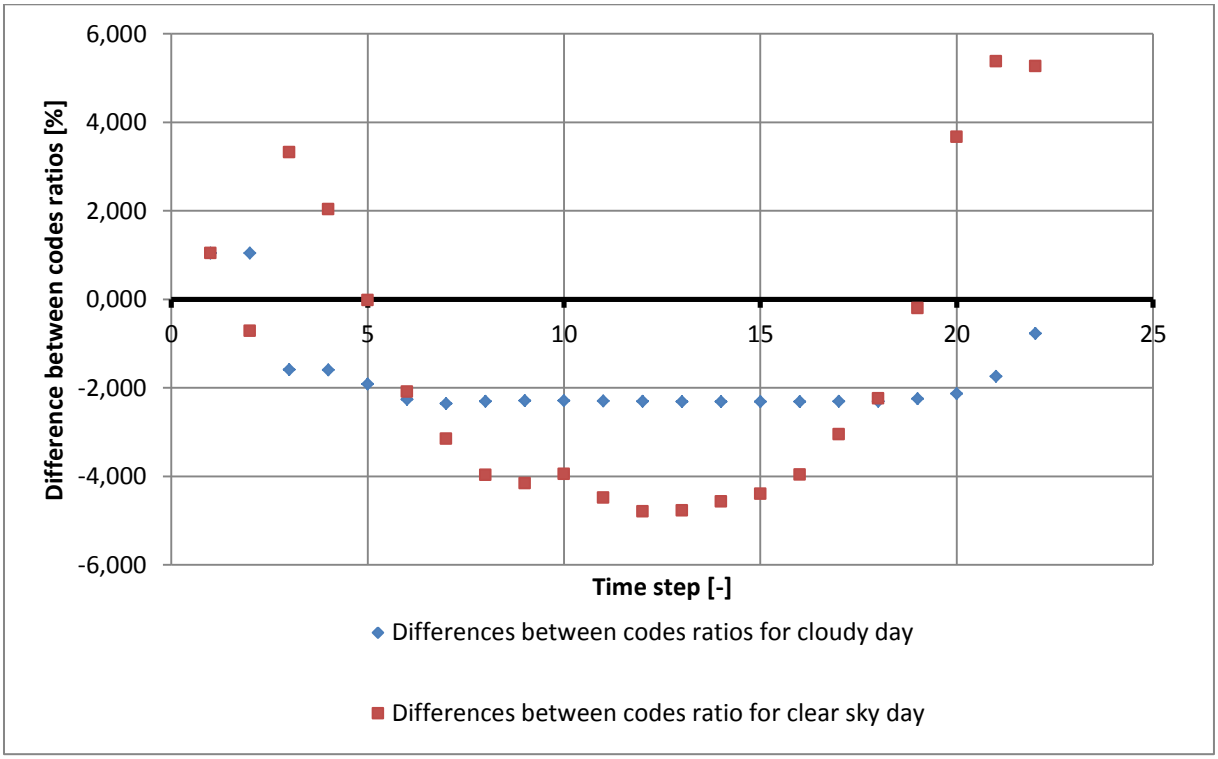

Figure 66 Percentage differences between ratios per time step for cloudy and bright days. (October Aberdeen 90° tilt angle).

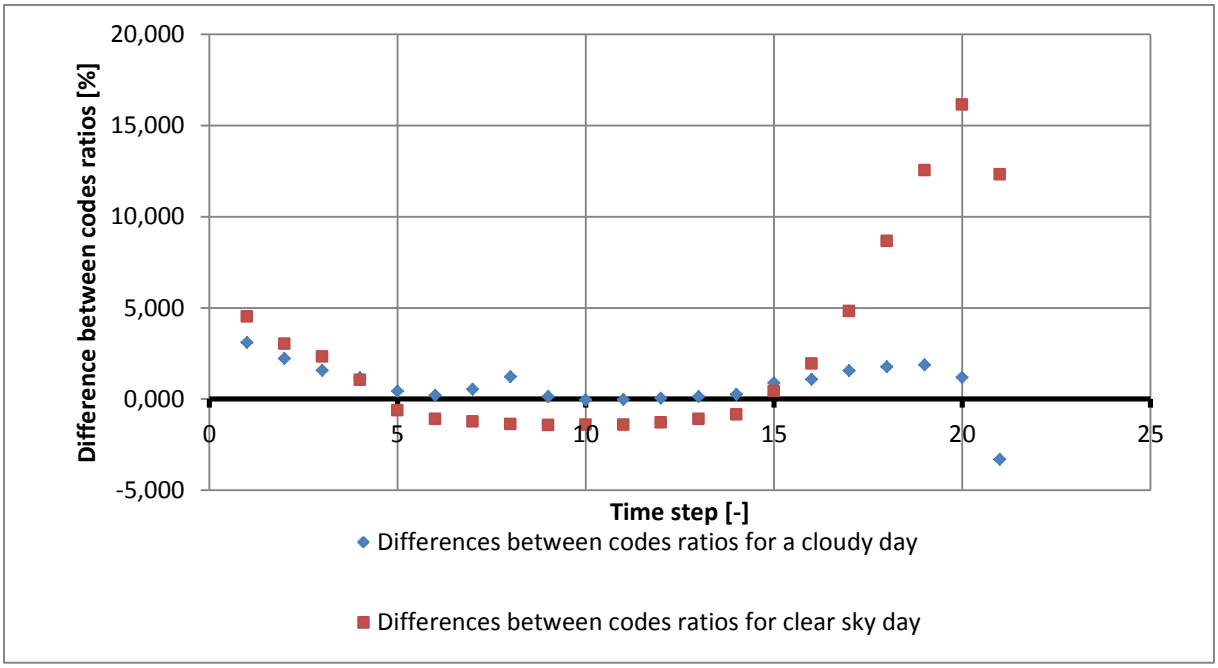

Figure 67 Percentage differences between ratios per time step for cloudy and bright days. (October Guantanamo Bay 0° tilt angle).

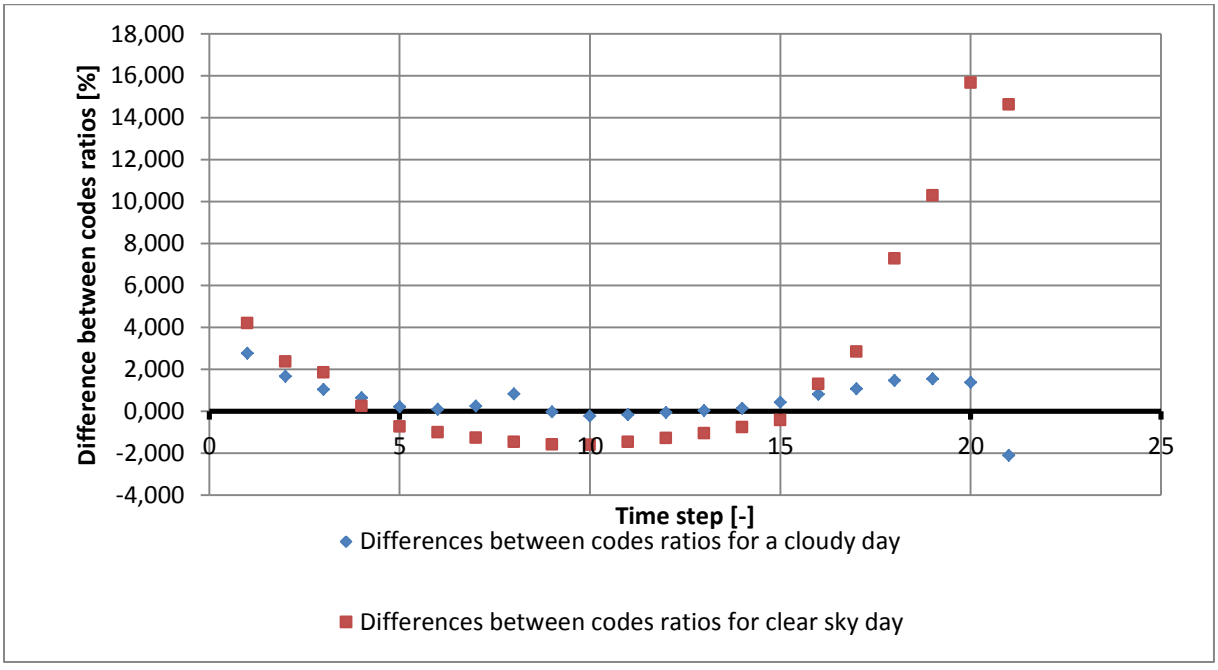

Figure 68 Percentage differences between ratios per time step for cloudy and bright days. (October Guantanamo Bay 30° tilt angle).

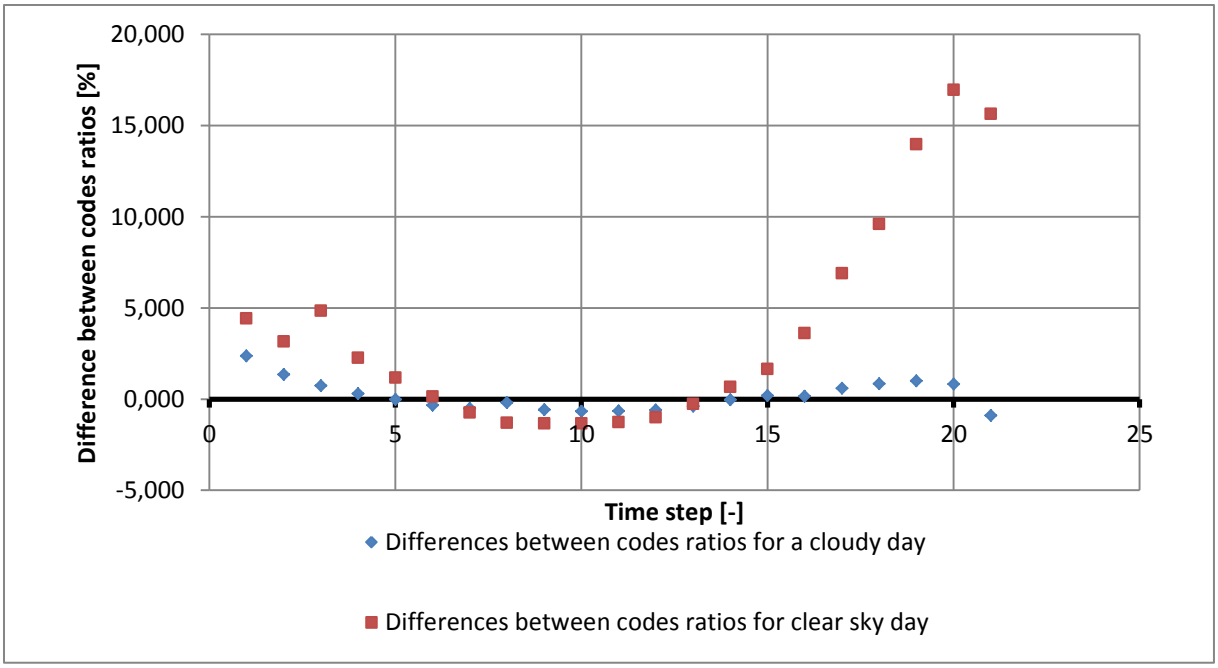

Figure 69 Percentage differences between ratios per time step for cloudy and bright days. (October Guantanamo Bay 60° tilt angle).

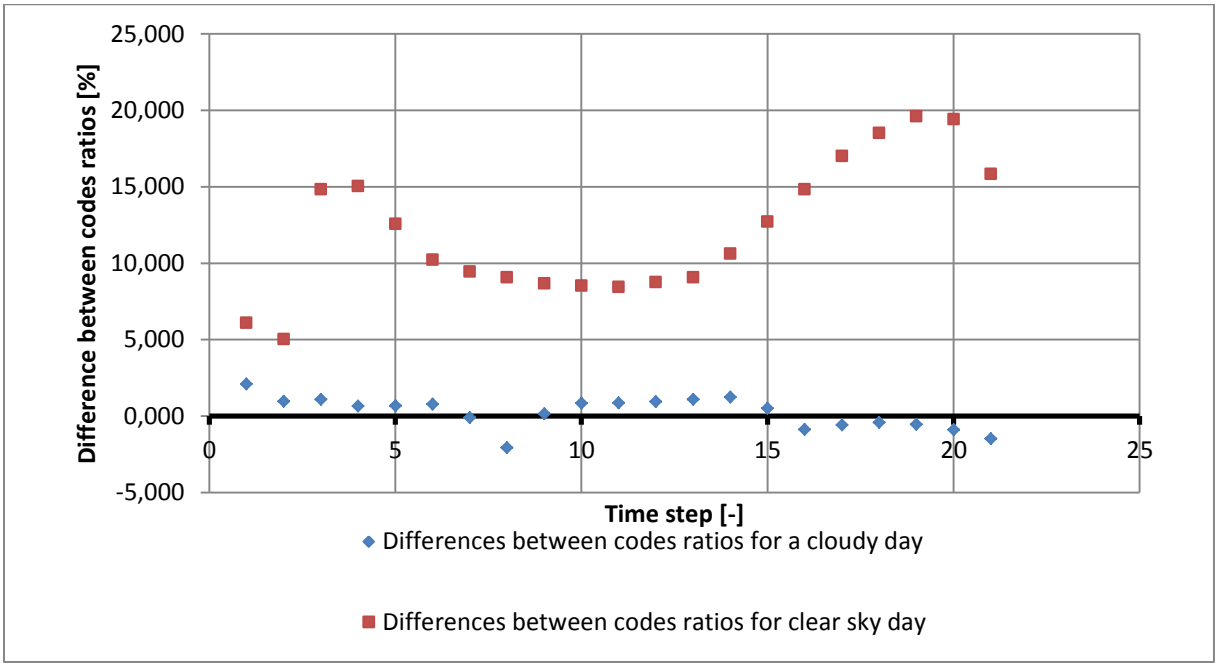

Figure 70 Percentage differences between ratios per time step for cloudy and bright days. (October Guantanamo Bay 90° tilt angle).

APPENDIX B – RESULTS GATHERED FOR DAILY SIMULATIONS.

Table 17 Daily differences between codes for 1st and 3rd of January (Aberdeen climate).

Aberdeen climate 1st and 3rd of January							
0° 01.01	0° 03.01	30° 01.01	30° 03.01	60° 01.01	60° 03.01	90° 01.01	90° 03.01
-2,468	2,954	0,554	2,732	-2,424	2,185	-3,449	1,047
-2,465	2,947	-1,416	2,725	-3,228	2,179	-3,906	1,044
-0,294	2,139	-1,993	1,803	-3,233	0,983	-4,084	-0,711
-1,163	2,127	-2,573	1,792	-3,141	0,378	-3,935	-1,598
0,906	1,726	-4,979	1,330	-5,165	0,370	-5,432	-1,602
4,376	1,718	-5,656	1,323	-5,879	0,366	-6,098	-1,603
4,115	1,714	-5,624	1,321	-5,861	0,363	-6,081	-1,606
4,296	1,711	-5,345	1,318	-5,755	0,361	-5,938	-1,606
3,963	1,712	-4,950	1,318	-5,612	0,360	-5,737	-1,609
2,319	1,712	-3,410	1,318	-5,464	0,360	-5,530	-1,609

-3,310	2,110	-1,001	1,777	-5,356	0,959	-5,337	-0,729
-18,126	2,113	1,526	1,779	-4,150	0,961	-5,156	-0,729

Table 18 Daily differences between codes for 1st and 4th of January (Guantanamo Bayclimate).

Guantanamo Bay climate 1st and 4th of January							
0° 01.01	**0° 04.01**	**30° 01.01**	**30° 04.01**	**60° 01.01**	**60° 04.01**	**90° 01.01**	**90° 04.01**
2,954	2,955	2,732	2,732	2,184	2,185	1,047	1,047
2,945	2,946	2,724	2,724	2,178	2,178	1,044	1,044
3,521	2,370	-0,510	1,275	-1,231	-0,060	-0,803	-1,457
1,940	1,385	-1,488	0,385	-2,205	-0,623	-1,704	-2,019
-0,360	0,802	-3,351	-0,283	-3,253	-1,121	-1,977	-2,189
-1,943	0,273	-3,738	-0,505	-3,713	-1,284	-2,378	-2,390
-2,725	0,203	-3,842	-0,324	-3,835	-1,119	-2,781	-2,520
-3,372	0,228	-3,953	-0,122	-3,942	-0,925	-3,077	-2,558
-3,850	0,130	-4,114	-0,160	-4,079	-0,985	-3,280	-2,585
-4,063	0,058	-4,219	-0,226	-4,165	-0,995	-3,368	-2,598

-3,919	0,006	-4,150	-0,233	-4,110	-0,994	-3,312	-2,593
-3,498	0,011	-4,023	-0,230	-4,009	-0,981	-3,137	-2,566
-2,852	0,308	-3,866	-0,023	-3,866	-0,835	-2,854	-2,486
-2,078	1,136	-3,721	0,634	-3,717	-0,393	-2,479	-2,363
-0,713	0,269	-3,597	-0,535	-3,538	-1,262	-2,041	-2,290
2,855	0,614	-2,582	-0,660	-3,220	-1,405	-1,558	-2,153
5,916	0,870	-1,113	-0,391	-1,881	-1,045	-0,647	-1,874
10,295	0,691	1,711	-0,133	-0,597	-0,852	1,219	-1,483
14,789	-1,006	5,681	-0,446	1,966	-0,832	3,040	-1,601
8,513	-7,934	6,531	-2,689	3,411	-1,708	2,900	-2,226

Table 19Daily differences between codes for 3rd and 5th of July (Aberdeen climate).

Aberdeen climate 3rd and 5th of July							
0° 03.07	**0° 05.07**	**30° 03.07**	**30° 05.07**	**60° 03.07**	**60° 05.07**	**90° 03.07**	**90° 05.07**
2,956	2,959	2,733	2,735	2,186	2,187	1,047	1,047
2,953	2,955	2,730	2,732	2,183	2,184	1,044	1,044

2,133	2,136	1,798	1,801	0,980	0,982	-0,708	-0,708
1,722	1,725	1,328	1,330	0,371	0,373	-1,596	-1,596
2,772	5,816	1,473	2,348	0,027	-0,139	-2,040	-2,039
3,028	6,340	2,776	6,918	-0,011	-0,394	-2,282	-2,281
2,131	6,943	1,988	10,025	0,458	6,019	-2,288	-2,285
1,749	6,839	1,371	8,034	0,430	12,505	-2,289	-2,296
1,736	5,570	1,405	6,521	0,595	11,026	-2,070	6,728
1,541	3,581	1,190	3,692	0,415	7,367	-1,603	13,565
1,419	2,122	1,127	1,778	0,914	4,281	0,429	11,521
1,151	1,075	0,718	0,399	0,423	1,288	1,093	7,732
0,772	0,208	0,312	-0,258	-0,075	-0,018	0,099	2,544
0,408	0,422	0,142	0,147	-0,519	-0,528	-0,413	-0,511
0,450	-0,419	0,234	-0,476	-0,593	-1,016	-1,485	-0,128
1,125	-1,069	0,765	-1,003	-0,247	-1,400	-2,433	-0,512
1,125	-0,790	0,773	-0,864	-0,227	-1,338	-2,408	-1,373
1,113	-0,608	0,763	-0,669	-0,234	-1,143	-2,413	-1,837

1,109	-1,490	0,762	-1,534	-0,234	-1,765	-2,414	-1,328
1,114	-2,097	0,768	-1,979	-0,230	-2,090	-2,410	-0,410
1,130	-1,742	0,780	-1,609	-0,223	-1,818	-2,404	0,439
1,153	-1,313	0,798	-1,182	-0,211	-1,479	-2,394	1,462
1,189	-0,706	0,823	-0,895	-0,195	-0,920	-2,384	3,041
1,230	0,131	0,851	-0,545	-0,166	0,196	-2,368	4,725
1,325	1,140	0,889	0,616	-0,147	1,194	-2,387	6,427
1,370	1,838	0,979	1,569	-0,133	2,822	-2,428	5,705
1,420	2,636	1,013	2,649	-0,040	3,838	-2,318	4,760
1,472	3,399	1,051	3,637	-0,018	4,846	-2,318	-0,017
1,476	3,611	1,033	3,853	-0,067	4,131	-2,320	-2,447
1,557	3,061	1,111	3,390	-0,130	0,731	-2,308	-2,331
1,538	2,787	1,078	2,295	0,012	-0,231	-2,086	-2,324
1,510	1,663	1,058	1,011	0,023	-0,029	-2,089	-2,090
1,703	1,632	1,310	1,012	0,352	-0,016	-1,617	-2,093
2,113	1,762	1,778	1,287	0,958	0,330	-0,736	-1,624

2,924	2,167	1,783	1,749	0,963	0,935	-0,730	-0,734

Table 20 Daily differences between codes for 6th and 7th of July (Guantanamo Bay climate).

Guantanamo Bay climate 6th and 7th of July							
0° 06.07	0° 07.07	30° 06.07	30° 07.07	60° 06.07	60° 07.07	90° 06.07	90° 07.07
3,904	3,904	3,059	3,055	2,173	2,173	1,047	1,047
3,631	3,636	3,702	3,702	2,162	2,162	1,044	1,044
6,784	6,785	11,826	11,787	0,177	0,294	-2,031	-2,031
4,150	4,168	8,558	8,533	12,410	12,395	-2,276	-2,276
2,801	2,812	7,467	7,478	17,975	17,993	-2,287	-2,287
1,535	1,544	4,374	4,378	18,263	18,305	-2,410	-2,410
0,811	0,883	2,973	2,865	15,848	14,366	-2,418	-2,416
0,591	0,780	1,892	1,903	12,528	10,850	-2,417	-2,417
0,554	0,646	0,962	1,013	10,836	10,123	-2,419	-2,420
0,509	0,509	0,912	0,911	9,478	9,438	-2,419	-2,421

0,671	0,505	1,096	0,980	7,897	8,471	-2,420	-2,421
0,809	0,548	1,220	1,085	6,526	7,955	-2,421	-2,427
1,085	0,420	1,291	0,947	5,099	8,607	-2,421	-2,425
1,374	0,396	1,338	0,849	3,414	9,623	-2,477	-2,425
1,421	0,463	1,332	0,819	3,553	10,779	-2,484	-2,424
1,480	0,557	1,573	1,541	3,703	12,256	-2,484	-2,426
1,369	0,752	2,129	2,643	6,648	14,698	-2,487	-2,427
1,382	1,055	2,889	3,671	10,623	18,354	-2,485	-2,426
2,218	2,424	4,150	6,090	8,498	16,263	-2,432	-2,426
2,482	3,078	3,871	6,612	4,450	10,607	-2,433	-2,426
3,564	5,366	4,806	8,979	1,484	4,553	-2,436	-2,436
4,285	6,976	5,310	10,716	-0,759	-0,977	-2,438	-2,437
7,146	7,887	5,917	6,726	-0,899	-0,837	-2,435	-2,447
9,879	5,452	0,154	-0,278	-0,826	-1,051	-2,339	-2,341
7,566	5,595	-39,261	-39,136	-7,642	-7,683	-1,778	-1,799

Table 21 Daily differences between codes for 2nd and 3rd of April (Aberdeen climate).

Aberdeen climate 2nd and 3rd of April							
0° 02.04	0° 03.04	30° 02.04	30° 03.04	60° 02.04	60° 03.04	90° 02.04	90° 03.04
2,955	2,963	2,732	2,739	2,185	2,190	1,047	1,047
2,947	2,138	2,725	1,803	2,179	0,984	1,044	-0,707
2,133	1,728	1,798	1,333	0,384	0,375	-1,591	-1,595
1,721	11,168	1,327	8,105	0,369	8,101	-1,598	11,582
1,509	9,860	1,086	5,939	0,060	5,486	-2,043	7,538
1,485	6,496	1,067	2,235	0,047	1,198	-2,046	4,485
1,404	4,624	0,894	-0,473	-0,142	-0,953	-2,286	1,204
1,233	2,566	0,844	-2,088	-0,170	-2,781	-2,289	-1,696
1,181	0,390	0,809	-3,510	-0,196	-3,418	-2,301	-2,791
1,123	-1,543	0,769	-3,910	-0,214	-3,805	-2,302	-3,840
1,093	-3,175	0,748	-4,247	-0,226	-4,158	-2,417	-4,757
1,060	-3,589	0,727	-4,448	-0,237	-4,410	-2,418	-5,060
1,052	-3,792	0,722	-4,566	-0,318	-4,592	-2,421	-5,137

1,041	-3,783	0,715	-4,566	-0,322	-4,586	-2,421	-5,139
1,054	-3,572	0,722	-4,489	-0,241	-4,440	-2,424	-5,095
1,062	-3,050	0,729	-4,291	-0,237	-4,193	-2,424	-4,706
1,003	-1,298	0,453	-3,997	-0,495	-3,879	-2,424	-3,769
0,958	0,634	0,390	-3,452	-0,554	-3,384	-2,316	-2,673
0,980	2,444	0,490	-1,792	-0,393	-2,455	-2,072	-1,642
0,939	3,629	0,619	-0,184	-0,247	-0,739	-1,930	0,905
1,265	2,530	0,927	1,317	0,105	0,499	-1,747	0,748
1,552	2,689	1,224	1,883	0,408	1,307	-1,289	0,670
4,185	1,555	4,084	1,222	3,744	0,407	2,639	-1,316
7,577	1,701	7,393	1,427	5,950	0,552	0,180	-1,442
3,739	1,798	0,822	1,424	-0,030	0,457	-1,633	-1,670

Table 22 Daily differences between codes for 1st and 6th of April (Guantanamo Bay climate).

Guantanamo Bay climate 1st and 6th of April							
0° 01.04	**0° 06.04**	**30° 01.04**	**30° 06.04**	**60° 01.04**	**60° 06.04**	**90° 01.04**	**90° 06.04**

4,636	5,692	4,604	5,840	6,053	8,232	3,332	2,676
3,485	4,219	3,467	4,544	4,303	6,622	4,221	5,568
2,856	3,078	2,956	3,483	6,996	8,741	13,263	16,082
1,791	1,849	1,821	2,151	5,534	7,323	14,431	19,047
0,399	0,287	0,454	0,651	3,354	5,003	15,565	19,962
-0,088	0,008	0,005	0,081	2,158	2,914	15,964	20,452
-0,077	-0,244	-0,021	-0,154	1,236	2,195	11,630	20,108
0,021	-0,426	0,067	-0,374	0,665	1,602	7,998	19,983
0,138	-0,571	0,098	-0,520	0,369	1,192	6,434	19,531
0,263	-0,639	0,216	-0,588	0,282	1,031	4,960	19,426
0,125	-0,540	0,081	-0,498	0,335	1,126	6,512	19,023
0,044	-0,417	0,065	-0,335	0,589	1,439	7,979	18,451
0,063	-0,216	0,086	-0,143	0,991	1,972	9,704	18,882
0,150	0,015	0,170	0,078	1,590	2,657	11,663	19,438
0,317	0,264	0,328	0,332	2,293	4,279	13,216	19,687
1,433	1,546	1,427	1,849	4,809	7,056	14,733	20,460

2,754	3,040	2,762	3,273	7,499	9,553	16,687	20,214
5,940	6,217	6,214	7,184	10,088	12,387	18,254	18,240
8,860	9,497	9,142	10,241	14,363	17,013	15,073	11,498
12,061	13,186	12,963	15,003	15,282	18,030	7,810	-1,995
13,642	14,802	14,492	15,860	14,016	11,797	-2,363	-2,450
8,839	10,225	31,999	-39,472	-7,640	-7,703	-1,777	-2,268

Table 23 Daily differences between codes for 2nd and 7th of October (Aberdeen climate).

Aberdeen climate 2nd and 7th of October							
0° 02.10	**0° 07.10**	**30° 02.10**	**30° 07.10**	**60° 02.10**	**60° 07.10**	**90° 02.10**	**90° 07.10**
2,947	2,953	2,726	2,731	2,180	2,184	1,047	1,047
2,941	2,950	1,807	2,728	0,986	2,181	-0,711	1,044
5,954	2,131	4,655	1,797	3,515	0,979	3,322	-1,590
6,048	1,719	3,089	1,325	1,669	0,368	2,037	-1,598
5,998	1,544	1,121	1,021	-0,698	-0,023	-0,015	-1,916
3,813	1,169	-1,175	0,596	-2,216	-0,400	-2,090	-2,263

1,901	1,228	-2,142	0,706	-3,061	-0,341	-3,153	-2,358
0,478	1,389	-2,881	0,991	-3,103	-0,012	-3,970	-2,305
-0,082	1,326	-2,726	0,832	-3,014	-0,183	-4,154	-2,291
-0,711	1,150	-2,425	0,780	-2,783	-0,214	-3,946	-2,292
-1,293	1,116	-3,456	0,756	-3,666	-0,228	-4,484	-2,295
-1,716	1,073	-4,104	0,720	-4,258	-0,252	-4,789	-2,305
-1,204	1,058	-3,862	0,713	-4,035	-0,258	-4,773	-2,309
-0,809	1,035	-3,583	0,697	-3,691	-0,266	-4,569	-2,308
-0,196	1,053	-3,354	0,709	-3,421	-0,262	-4,394	-2,313
0,517	1,063	-2,867	0,712	-3,117	-0,260	-3,960	-2,312
1,430	1,209	-1,705	0,745	-2,668	-0,238	-3,052	-2,304
1,356	1,236	-0,811	0,883	-1,620	-0,074	-2,241	-2,305
5,082	0,906	1,117	0,591	-0,652	-0,334	-0,198	-2,248
9,997	0,381	4,576	0,284	2,667	-0,453	3,672	-2,134
9,390	0,276	6,789	0,390	5,186	-0,274	5,377	-1,740
4,603	-0,160	5,634	0,653	5,270	0,259	5,267	-0,771

Table 24 Daily differences between codes for 1st and 7th of October (Guantanamo Bay climate).

Guantanamo Bay climate 1st and 7th of October							
0° 01.10	0° 07.10	30° 01.10	30° 07.10	60° 01.10	60° 07.10	90° 01.10	90° 01.10
4,529	3,100	4,195	2,763	4,430	2,371	6,077	2,090
3,043	2,223	2,366	1,651	3,160	1,351	5,013	0,957
2,333	1,578	1,840	1,027	4,840	0,732	14,829	1,073
1,058	1,173	0,242	0,638	2,260	0,306	15,029	0,643
-0,617	0,445	-0,739	0,200	1,172	-0,019	12,565	0,661
-1,098	0,209	-1,016	0,083	0,146	-0,335	10,207	0,776
-1,233	0,535	-1,271	0,231	-0,740	-0,506	9,445	-0,107
-1,376	1,230	-1,470	0,813	-1,294	-0,200	9,056	-2,093
-1,425	0,134	-1,596	-0,039	-1,330	-0,581	8,667	0,146
-1,410	-0,043	-1,605	-0,234	-1,325	-0,658	8,523	0,828
-1,408	-0,015	-1,476	-0,172	-1,267	-0,647	8,424	0,844
-1,284	0,052	-1,290	-0,077	-0,995	-0,604	8,753	0,942

-1,095	0,135	-1,058	0,025	-0,257	-0,388	9,065	1,074
-0,847	0,261	-0,773	0,134	0,666	-0,043	10,608	1,227
0,438	0,900	-0,429	0,426	1,656	0,194	12,697	0,491
1,951	1,089	1,284	0,807	3,619	0,162	14,828	-0,893
4,827	1,567	2,827	1,067	6,898	0,594	16,995	-0,594
8,667	1,777	7,277	1,460	9,611	0,837	18,500	-0,430
12,557	1,872	10,280	1,535	13,971	0,994	19,590	-0,556
16,156	1,195	15,669	1,366	16,954	0,820	19,395	-0,919
12,324	-3,312	14,622	-2,115	15,635	-0,901	15,822	-1,506

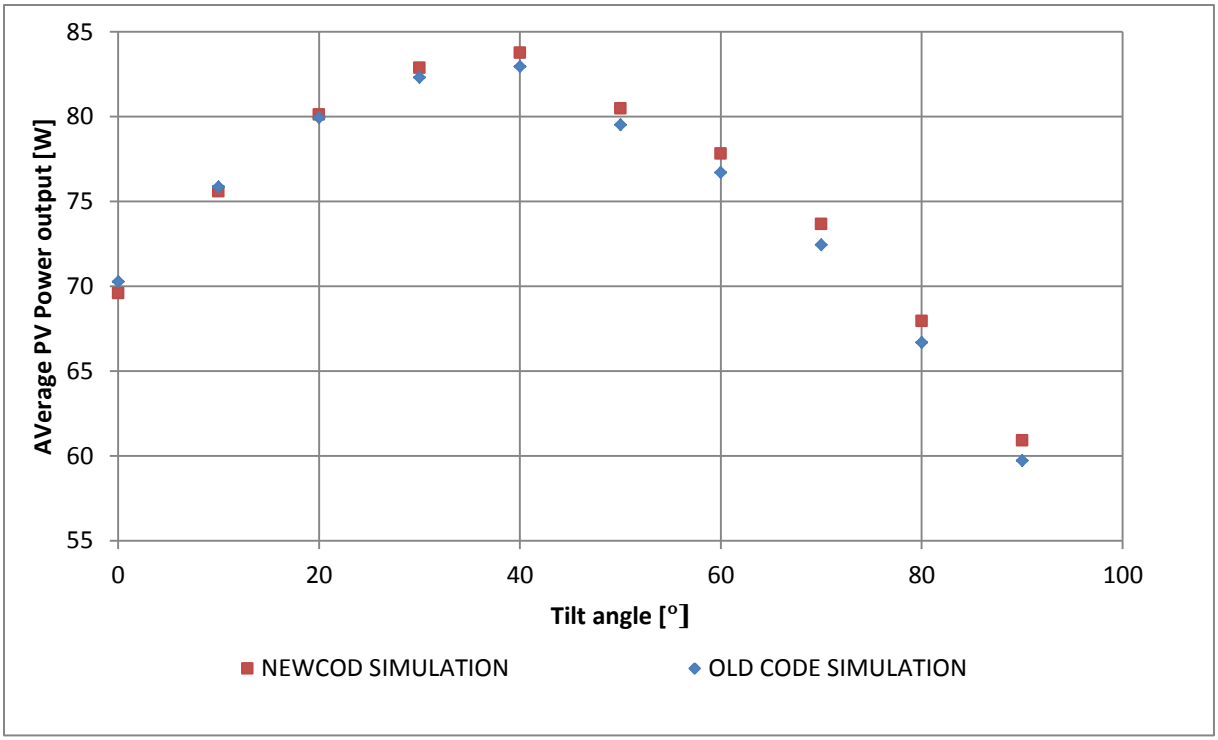

Figure 71 Yearly average PV power output vs tilt angle (Aberdeen climate).

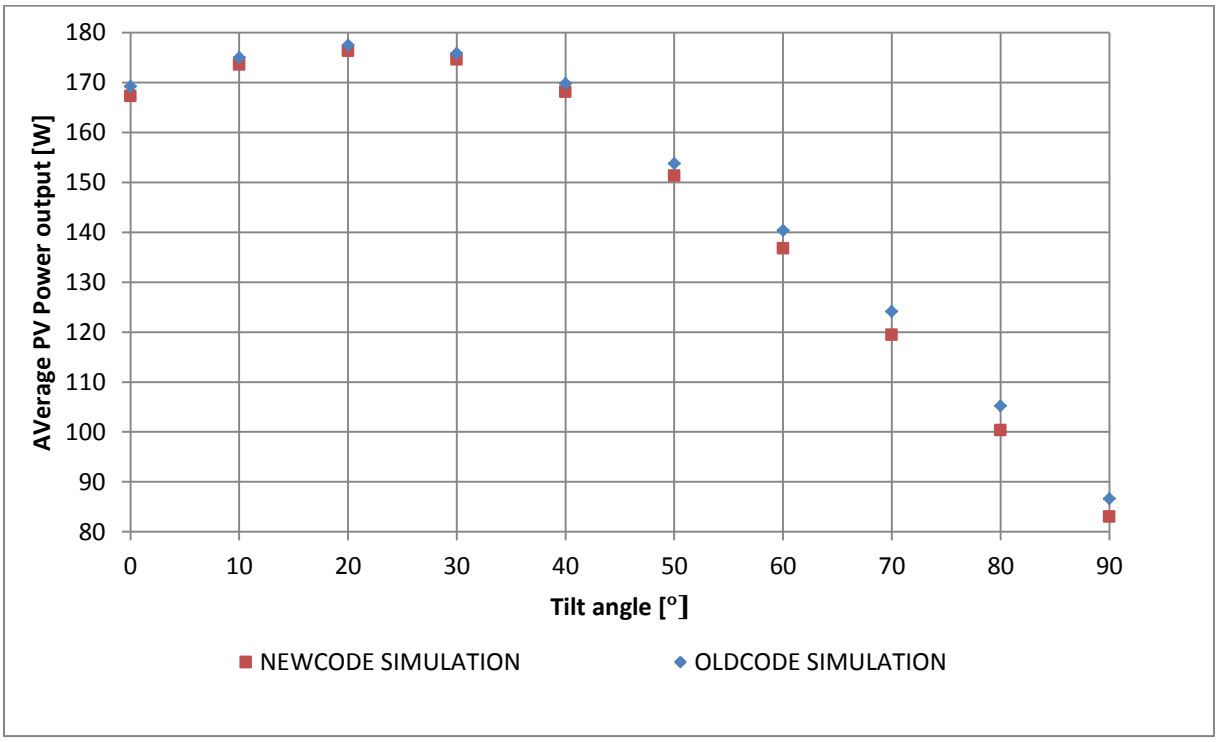

Figure 72 Yearly average PV power output vs tilt angle (Guantanamo Bay climate).

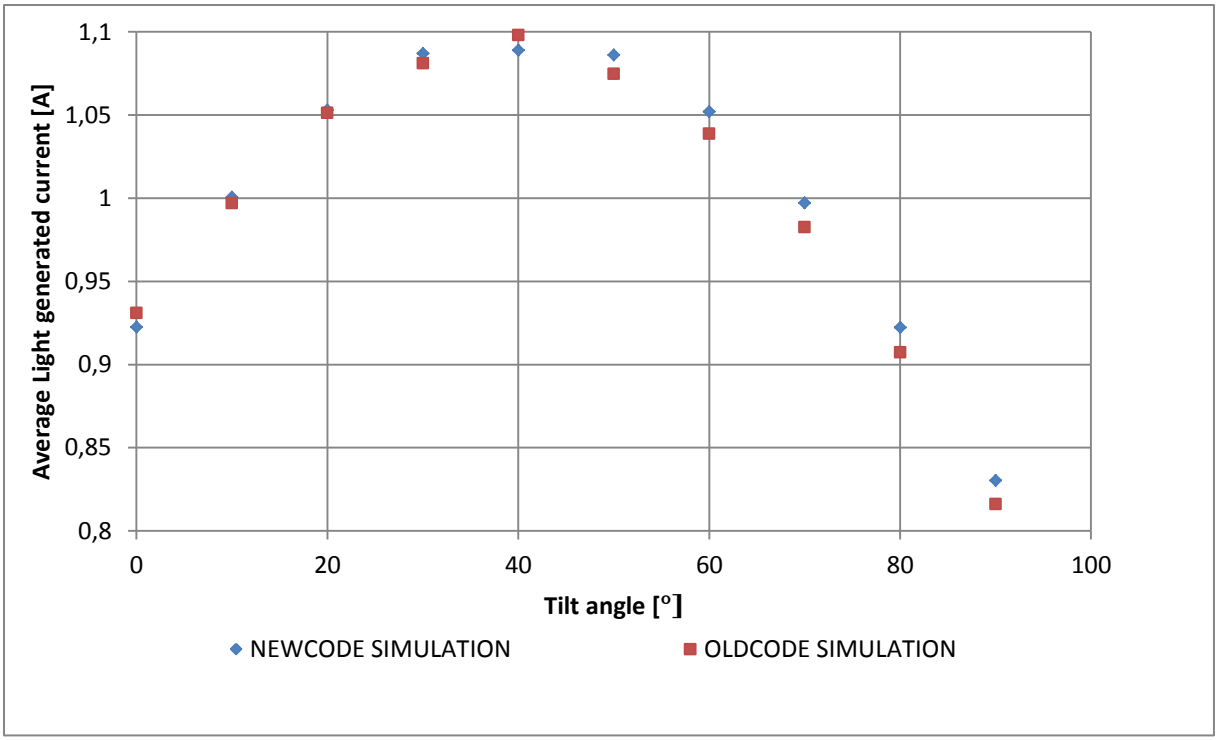

Figure 73 Yearly average light generated current vs tilt angle (Aberdeen climate).

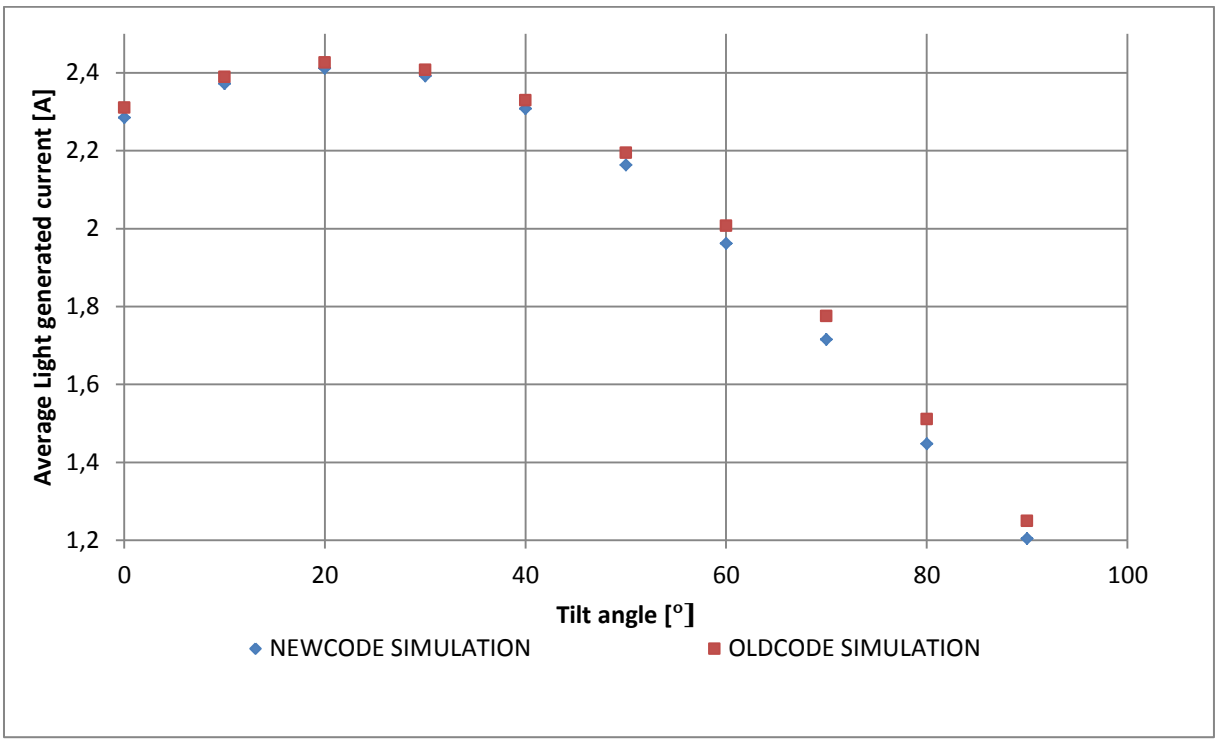

Figure 74 Yearly average light generated current vs tilt angle (Guantanamo Bay climate).